Winter 2014

Dynamics of a Tension Force-Driven Wave Energy Converter

Jason Ebner
University of New Hampshire, Durham

DYNAMICS OF A TENSION FORCE - DRIVEN WAVE ENERGY CONVERTER

BY

JASON EBNER

BSME, University of New Hampshire, 2010

THESIS

Submitted to the University of New Hampshire
In Partial Fulfillment of
The Requirements for the Degree of

Master of Science
In
Mechanical Engineering

December, 2014

This thesis has been examined and approved in partial fulfillment of the requirements for the degree of Master in Mechanical Engineering by:

Thesis Co-Director, M. Robinson Swift
Professor of Mechanical and Ocean Engineering

Thesis Co-Director, Kenneth C. Baldwin
Professor of Mechanical and Ocean Engineering
Director, Center of Ocean Engineering

Martin Wosnik
Associate Professor of Mechanical and Ocean Engineering

On December 3, 2014

Original approval signatures are on file with the University of New Hampshire Graduate School.

DEDICATION

I would like to dedicate this work to my wife, Sarah Michelle Ebner, and to my parents, Sue and Brian Ebner, for all the support and encouragement they gave me throughout the years. This would not be possible without you.

ACKNOWLEDGMENTS

I would like to acknowledge the individuals that contributed to this project as well as helped me along the way

- Dr. M.R. Swift for the advice, support and guidance during the entirety of the project. The support you provided me throughout the physical model testing and thesis writing was greatly appreciated.

- Dr. Kenneth Baldwin, for providing guidance and support especially during the two summer deployments. Your help with coordinating between teams lead to successful deployments.

- Matthew Rowell, for your leadership during the second summer deployment allowing me to focus on writing my thesis.

- Oscilla Power Inc., for supporting the efforts and providing assistance to further ensure successful deployments.

- Noel Carlson, for providing me your guidance and patience during the 2013 summer deployment. Also, thank you for always supporting me and being flexible during the deployments.

- Jud DeCew, for gradually easing me into the project from the preliminary phase. Also, thank you for teaching me the required skills to successfully perform Aqua-FE analysis.

- Gulf Challenger crew for the support and advice for the 2013 summer deployment.

- Marine Program Office along with the Mechanical Engineering Office for the support I received for any administrative needs.

TABLE OF CONTENTS

LIST OF TABLES

LIST OF FIGURES

ABSTRACT

DYNAMICS OF A TENSION FORCE - DRIVEN WAVE ENERGY CONVERTER

by

Jason Ebner

University of New Hampshire, December 2014

Two prototype wave energy buoys were designed, modeled, constructed and field tested at the University of New Hampshire's Center of Ocean Renewable Energy offshore site utilizing Oscilla Power Inc.'s power take-off (PTO) units. Oscillating wave forces are used to power the PTOs. Due to design limitations in a taut-moored buoy system having inline PTOs, a suspended heave plate system was proposed. Tension oscillations in the vertical stay from the slack-moored buoy to the heave plate were used to drive the PTOs. To verify the heave plate concept met the oscillating tension amplitudes required, dynamic tests were performed using Froude scaled wave tank physical models, vertical motion dynamic models, and numerical finite element analysis.

With successful model testing, a full scale system was deployed during the summer of 2013. The summer testing led to further refinement of the heave plate concept. Asymmetric heave plate designs were developed to reduce slack events experienced in the field study. Utilizing an asymmetrical heave plate, a new and larger system, designed by Oscilla Power Inc. in collaboration with UNH, was tested and deployed in the summer of 2014. The suspended heave plate system allowed the wave energy converter to operate efficiently and effectively with minimal anchoring requirements.

CHAPTER 1-

INTRODUCTION

1.1 Purpose:

An energy conversion using a magnetostrictive concept requires large tensions fluctuations but very small deflection changes in order to convert the wave forcing into voltage. To achieve the required parameters, mathematical modeling, wave tank experimental testing and full scale field deployments were used to develop a wave energy buoy and mooring design which was suitable for the application.

1.2 Background:

As natural resources are being exhausted at a rapid pace, the U.S government is lobbying for further renewable energy sources. One source of energy stems from renewable ocean wave energy due to its abundance. For this application, a power take off (PTO) was created and developed by Oscilla Power Inc. (OPI). The PTO converts tension fluctuations into useable power using magnetostrictive alloys. Ferromagnetic materials, of which magnetostriction is a property of, converts tension fluctuations into voltage through the changes of strain in the material resulting in changes in the material's magnetic field ("iMEC Technology," 2014). Electromagnetic induction from copper coils wound around the material, exposed to the material's varying magnetic field, creates electricity (Nair & Shendure, 2013). To achieve the required tension fluctuations, the PTOs are going to be

used with a surface buoy where wave induced buoyancy fluctuations acting on the buoy will generate the desired tension changes.

OPI's PTO compared to other wave energy converters (WEC) is that there are no moving parts. In other WEC, mechanical systems, such as rack and pinion systems, are utilized to convert motion into power which introduces more design constraints. The magnetostrictive PTO simplifies power conversion due to its small relative motion while also simplifying the WEC design constraints. In order to convert the optimum power, the WEC needs to provide large oscillation forces to the PTO within a specified range.
To create the desired tension fluctuations the PTOs require, a proper taut moored mooring system was initially configured. A taut moored mooring requires the mooring line to be in constant tension, even with the changing tidal cycle.

This mooring configuration was designed to be deployed offshore at of UNH's offshore Center for Ocean Renewable Energy (CORE) site shown in Figure 1. This site is permitted allowing for research to explore engineering, biological, environmental and operational aspects of offshore devices (Muller 2002). This site is approximately 10km off the New Hampshire coast and 2km kilometers south of the Isle of Shoals of New Hampshire in the Gulf of Maine. The approximate coordinates of the UNH CORE site are 42° 56.55' North and 70° 37.94' West. The advantage of deploying an alternative wave energy device at the CORE site is the ideal wave and current conditions during the summer. The waves at the site usually experience significant wave heights of less than 1.1 m except for the occasional storm event while the current reaches no more than 0.1 m/s.

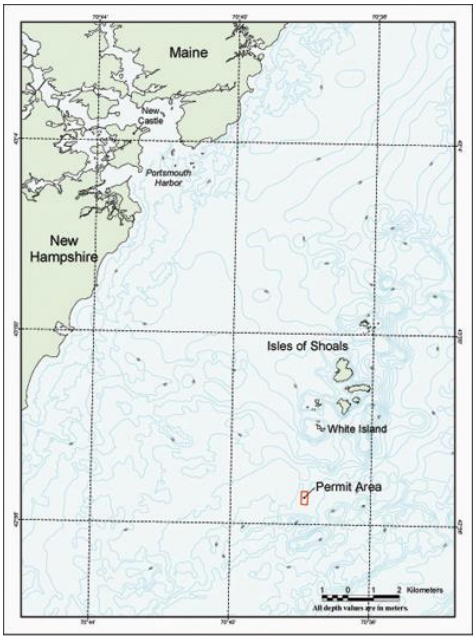

Figure 1: Location map of the UNH CORE field and permit site.

During the initial testing of the project, the original buoy and mooring system was specified to OPIs constraints of a loading force of 19 kN for a 2 m wave height. To design a system to achieve these parameters, a UNH developed finite element analysis program called Aqua-FE was used. Aqua-FE finite element analysis program was developed specifically for applications for the Open Ocean Aquaculture (OOA) projects. The software development was described by Gosz et al. (1996) and Tsukrov et al. (2000,2003). Using Aqua-FE, the buoy size and shape were specified to reach OPI's forcing goals. Aqua-FE modeling, however, indicated that the mooring lines can go slack, inducing snap loads in the mooring lines. Multiple design configurations were tested and the best of the candidate designs was chosen. The specified buoy had a diameter of 1.842m, length of 4.5m and a draft of 3m while using a taut moored system having a PTO design criteria driven force relationship of 19kN for 4m wave heights (see Figure 2). This compromise

was made to make the system smaller which includes smaller dead-weight anchors and buoy. Since slack loading was a still problem for the specified buoy, further research was needed.

An alternative approach was to design and develop a system with a heave plate. A heave plate would allow the buoy to respond slowly to wave excitation forces due to the increased inertia which, effectively, create the desired tension fluctuations in the system (Hart, 2007). The heave plate concept was applied by Ocean Power Technologies (OPT) for a wave energy converting device using a dual-absorber approach where the heave plate was used to stabilize the vertical spar allowing the follower buoy have larger vertical motion. The motion difference between the follower buoy and spar characterizes mechanical energy, which was then transformed into voltage.

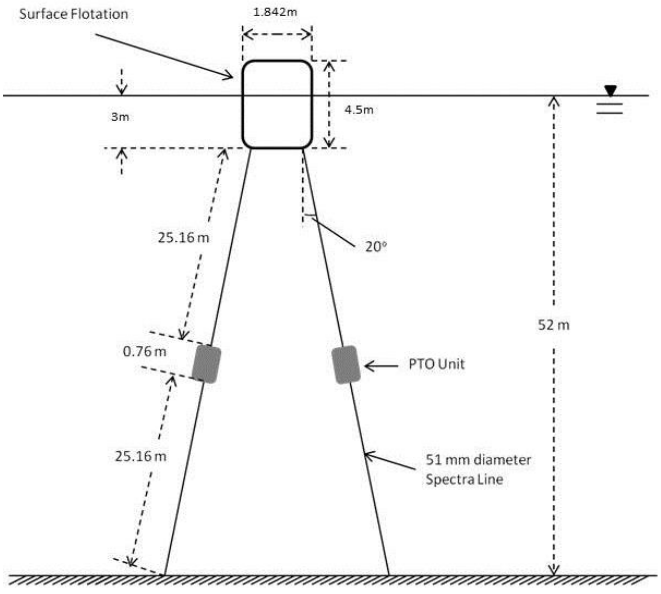

Figure 2: Preliminary taut-moored design configuration for testing at the UNH CORE site.

1.3 Objectives:

To address the challenges of converting buoy motion into energy, the following objectives were identified for the study presented here:

- Investigate/Modify the preliminary design for statistically probable wave environment and evaluate the extent of snap loads
- Specify dead-weight anchor requirements
- Develop a design alternative using a heave plate
- Conduct scale physical model testing in the wave tank
- Apply a vertical dynamic math model to evaluate heave plate concept
- Analyze complete WEC, heave plate and mooring design using Aqua-FE
- Fabricate mooring system
- Perform field testing at the CORE site for proof of concept testing during summer of 2013
- Conduct heave plate coefficient of drag testing along with added mass testing of new heave plate designs using knowledge obtained during past summer deployment for summer of 2014 testing
- Conduct scale physical model testing in the wave tank of new buoy and heave plate system
- Collaborate on mooring design and deployment procedure
- Perform field testing at the CORE site for operational use

The two deployments, summer of 2013 and 2014, acted as a trial field test and a large scale operational use respectively as design methods and knowledge of the system improved.

1.4 Approach:

The approach for developing both wave energy buoys began by defining general design criteria such as power generation requirements, deployment and operational feasibility, anchor sizing and availability as well as environmental concerns. Since preliminary work had already been performed, it was important to work out any issues that

could inhibit the success of the project. One major issue encountered in the preliminary work was snap loads. Snap loads could lead to premature failure of a component and result in a failed test. As a result of the snap loads, a design constraint was put into place where a loading force of 19 kN for a 4 m wave height would be needed for the PTO's. Another major issue in the preliminary design was the anchor sizes required for the buoy. To properly size the dead-weight anchors, surface bearing calculations were performed to ensure the anchor would be able to be recovered. Since three dead-weight anchors would be needed, another issue encountered was deployment and recovery along with the costs.

Further Aqua-FE modeling of a smaller and readily available buoy was performed to further investigate the taut moored system. This system was also proposed to be deployed during the summer of 2013 as a trial deployment. For the Aqua-FE configurations, areas of concern were tested which included effects of the tidal cycle, slack/snap loads, and tension oscillation amplitudes. To first check the effects of the tidal cycle, the buoy was simulated at multiple water depths of which include being fully submerged. The system was also tested using vertical taut moored mooring lines to see the effects of mooring line angle off the bottom of the buoy and tensions fluctuation amplitudes. The taut moored system still had slack/snap load so an alternative mooring was proposed.

Due to the cost of manufacturing, deployment and potential environmental impact of the dead-weight anchors along with the snap loads experienced in the taut moored system, another alternative mooring device, the heave plate, was proposed. The concept of the heave plate, for this application, was first tested using a Froude scaled physical model

in the Jere. A. Chase Ocean Engineering building's wave/tow tank using the preliminary buoy design.

The preliminary testing performed consisted of two rounds, a visual confirmation and a force measurement approach. During the visual confirmation testing, the buoy and heave plate was optically recorded under monochromatic waves with varying wave heights and wave periods. Also, the buoy was tested with a slack mooring system attached at multiple locations on the buoy, as well as the bottom of the heave plate, to see the effects of mooring attachment location. Various heave plate vertical stay configurations were also evaluated. Since no issues occurred during the visual observation testing, force measurement testing was performed gathering load information on the vertical stay. In addition to physical model testing, a one dimensional mathematical model was created which allowed for the comparison between the physical model testing and a simple numerical model.

It was decided, to further assess the heave plate concept, to deploy a small scale buoy during the summer of 2013 since there was a buoy readily available. A physical model of the smaller buoy was then constructed and tested using Froude scaled physical model testing. The model and Aqua-FE modeling were applied to ensure the system would work as originally intended. Using all these methods, the heave plate size was determined along with anchor sizing. The system was then constructed and deployed at the CORE site during the summer of 2013.

Based on the summer of 2013 experiment, development of a new and larger buoy was put in motion for the summer of 2014 using the heave plate mooring system. The

buoy was designed by OPI to house multiple magnetostrictive modules. UNH tow tested new heave plate designs, along with static and dynamic testing of the buoy system using Froude scaled physical models. The coefficient of drag and added mass of four heave plate models, which varied in design, were tested, and the heave plate with the best characteristics was identified. With the heave plate design selected, the buoy and heave plate system was then tested in free release tests and regular and random wave tests. From these tests, OPI made use of OrcaFlex, a commercially available package for the dynamics analysis of offshore marine systems, to analyze the system. From this modeling, the anchor sizes, mooring lines and vertical stay line were determined. The system was then assembled and deployed at the CORE site during the summer of 2014.

CHAPTER 2-

TAUT MOORING SYSTEM DESIGN ALTERNATIVE

2.1 Design and Rational

The three leg taut mooring system design shown in Figure 2 was completed as a possible mooring configuration for field testing during the summer of 2013. For this type of system to generate power, Oscilla Power's PTOs would be mounted in line with the mooring lines. As a wave passes, increase in buoyancy force would create tension in the line, and the PTOs would then convert that tension into power. It is critical to keep the mooring lines under tension at all times in order for the most tension energy to be converted to power and to avoid snap loads which could cause damage. For this system to work, multiple parameters had to be tested to ensure the system would function properly and to the expectations.

2.2 Finite Element Testing using Aqua-FE

The UNH developed, finite element analysis program Aqua-FE was used to determine the optimal mooring configuration, including buoy and mooring component sizing, as well as characterizing the motion and force the entire system experiences. During this testing, the ideal buoy and mooring size was specified using Oscilla Power's design constraint of a loading force of 19 kN for a 4 m wave height. During this testing, multiple buoy configurations were designed and tested along with varying mooring line configurations. The resulting configuration was a buoy with a diameter of 1.842 m, a height

of 4.5m and a draft of 3m. An example of the Aqua-FE model for the taut mooring can be seen in Figure 3. One of the mooring lines is facing the incident wave direction which was taken to be the worst case loading. A MathCad program for completing calculations necessary to ensure consistent input parameters to Aqua-FE is provided in Appendix I.

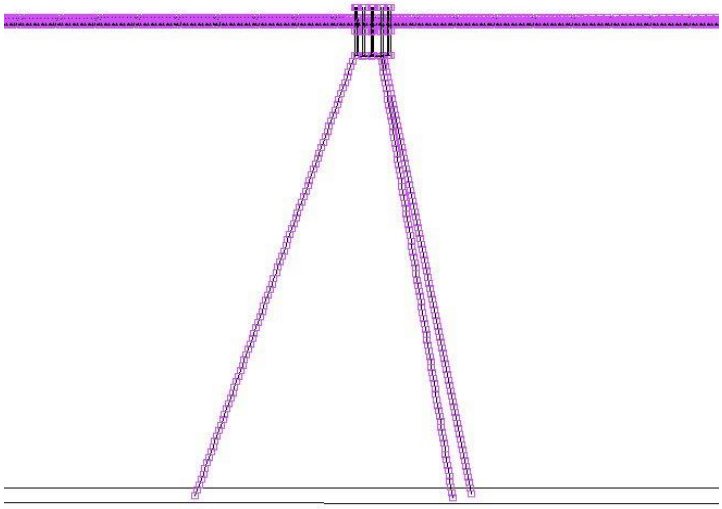

Figure 3: The three point moored system in Aqua-FE. The PTOs are located at the half-way points of the mooring lines.

2.3 Mooring Line Specification

The Aqua-FE simulations provided predictions of the mooring line tensions which the system would experience as can be seen in Figure 4. Shown by the results using a JONSWAP spectrum with a significant wave of 2.8 m, an ocean swell period of 10 s, and local wind driven waves with a period of 5.34 s, there are multiple slack events in the mooring line. A storm event of this magnitude has a likelihood of less than 1% of happening based off of wave statics of the UNH CORE site seen in Table 1.

Table 1: Wave statistics of the UNH site by month from 2000-2009.

Month	# Records	# Records Hs > 1.5 m	# Records Hs > 2.8 m	Max Hs
April	5640	2364 (41.9%)	453 (8.0%)	8.49 m
May	5356	1148 (21%)	227 (4.3%)	5.59 m
June	6335	1815 (12.8%)	94 (1.5%)	5.06 m
July	5901	501 (8.5%)	4 (0.06%)	3.86 m
August	5665	416 (7.4%)	25 (0.4%)	3.85 m
September	5526	1347 (24.4%)	54 (1.0%)	4.73 m
October	5380	2254 (41.8%)	540 (10.0%)	7.42 m

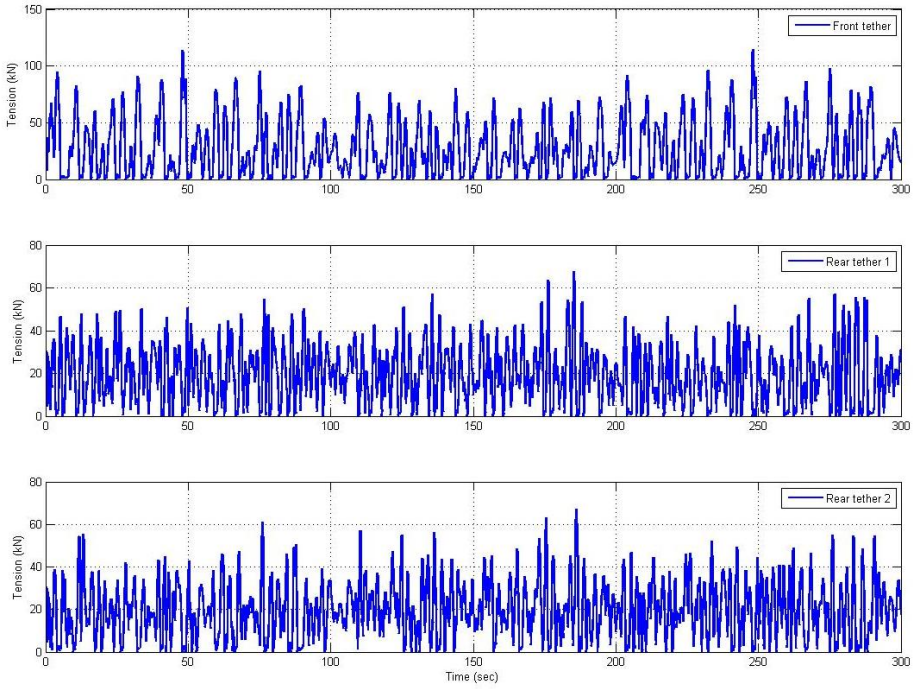

Figure 4: Aqua-FE results of preliminary buoy testing utilizing a JONSWAP spectrum with a significant wave height of 2.8m, an ocean swell period of 10s, and local wind driven waves with a period of 5.34s.

To help eliminate both snap events experienced by both the mooring line and PTOs, 19 kN for a 4m increase in surface elevation target force oscillation on all three mooring lines was put in place by OPI. Also, the maximum mooring line tension of 114 kN and a mean tension of 96 kN was found and used to estimate the minimum mooring requirements. Yale Cordage provided multiple suggestions for line meeting the design criteria as well as useful data on line physical properties. Then comparing the spring constants of the recommended mooring lines for the system, the optimal line was determined to be 1.15in diameter Unitrex XS Max Wear. From the properties of the Unitrex XS Max Wear, the 1.15in diameter line has a 4:1 working load to minimum breaking strength with a working load of 139.15 kN. Allowing the minimum breaking strength to be four times larger allows for a built in factor of safety in the line.

2.4 Bearing Surface Calculations

Since mooring tensions and large upward components and reliability was crucial, dead-weight anchors were incorporated. For this case, three deadweight anchors would be designed and constructed using readily available materials for a low cost solution along with a relatively quick turnaround time. No compromise was made regarding anchor sizes since the anchors would be used for both the summer 2013 deployment and a larger scale summer 2014 deployment. Since the maximum force the buoy will exert was 114 kN, or 107 kN vertically, each anchor had to be designed to hold that loading.

Since cost is a big factor, especially given the tensions these anchors are going to have to restrain, it was important to select a common material to act as the dead-weight. While having a block of lead would be the best functional solution due to its high specific

gravity which results in the best correlation between dry weight and wet weight, it is economically unfeasible. The best material in this situation that is readily available, along with being easily formed, is concrete. However, concrete has a low specific gravity so that the weight minus buoyancy force in water is 57% of its dry weight. Thus anchor sizes effectively have to double in size to account for buoyancy. A concrete mass of 20800 kg was selected which has a weight of 204 kN, a weight minus buoyancy force of 116 kN, for a factor of safety just over unity. Another issue with concrete is that concrete is very weak under tension. This is a very big issue considering upward tension of the mooring line means the anchor will be under constant tension and changes in tension.

In addition, there is always a concern for the environment. Since the overall goal was to create an eco-friendly energy device, it was important for this system to be friendly to the environment. This meant that the anchors had to be easily recoverable. Given the mass of the anchors, this would not be an easy task, especially since it was unknown whether the sea floor could support a structure this size without letting it sink into the sediment. To optimize the shape of the anchors, along with ensuring the sea floor has enough bearing capacity, sea floor bearing capacity calculations for cohesionless and cohesive soils were performed following the Handbook for Marine Geotechnical Engineering examples and parameters outlined by Rocker (1985).

To obtain a safe and practical solution, the most extreme parameters in the surface bearing calculations were used to assure that the anchors would be able to be recovered. To do this, it was important to know the surface conditions at the CORE site which

consists of a relatively flat sandy and silt seabed. From there, the proper soil friction coefficient, drained friction angle, factor of safety, among other parameters, were specified, and example calculations could be found in the handbook. The end result was that a dead-weight anchor of 2.8 m x 2.8 m x 1.3 m would be the ideal size and would work in both cohesionless and cohesive soils. These calculations are provided in Appendix II for cohesionless soils and Appendix III for cohesive soils.

2.5 Anchor Frame Testing

Once the anchor dimensions were determined from the surface bearing calculations, an internal frame was designed to support the concrete and withstand the mooring line loading during the deployment, installation and removal. A sample frame design can be seen in Figure 5. Without an internal frame, excessive tensile stresses would be applied to the concrete which could result in premature failure. It is important that this internal frame can support the forcing entirely without relying on the concrete to act as support. To do this, SolidWorks Simulation software, along with Marc Mentat finite element analysis software, was used to analyze three different frame designs. These designs consisted of a full frame constructed of 50 mm square bar acting as the mooring line connection, while also transferring load from to various bottom support frames.

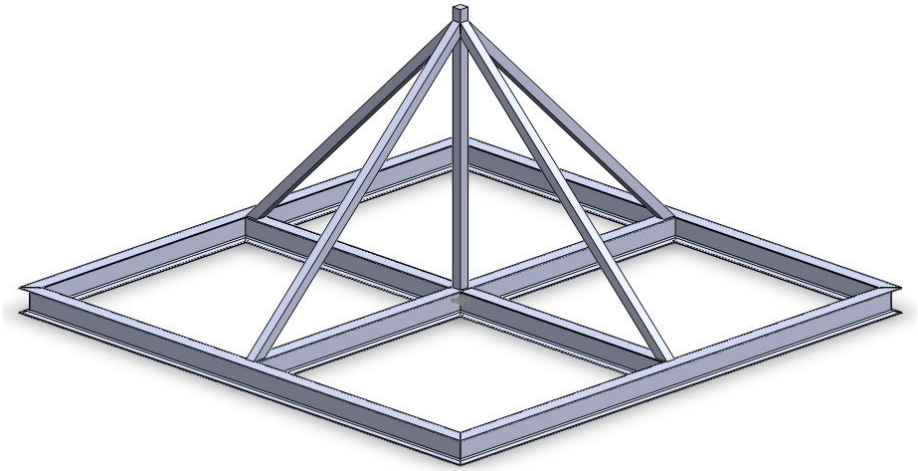

Figure 5: Example of an anchor frame to be used as internal loading support in the concrete dead-weight anchor.

Using different analysis approaches, both the SolidWorks Simulation and Marc Mentat software provided similar results. The mooring loading location on the top of the anchor frame had a 114kN force applied while the bottom support beams were fixed in location. This force was predicted by Aqua-FE as the worst case loading during the 2.8 m significant wave height storm with a 10 second ocean swell period and local wind driven waves with a period of 5.34s. In Figure 6, a sample of the results can be seen. Also, in Table 2, a list of results is provided. The von Mises stress results were then compared to the yield strength of 345 MPa for ASTM A992 steel to ensure there is no loading failure. Since the von Mises stresses from the testing is significantly lower than the yield strength of ASTM A992, the design is safe for the extreme wave loading condition.

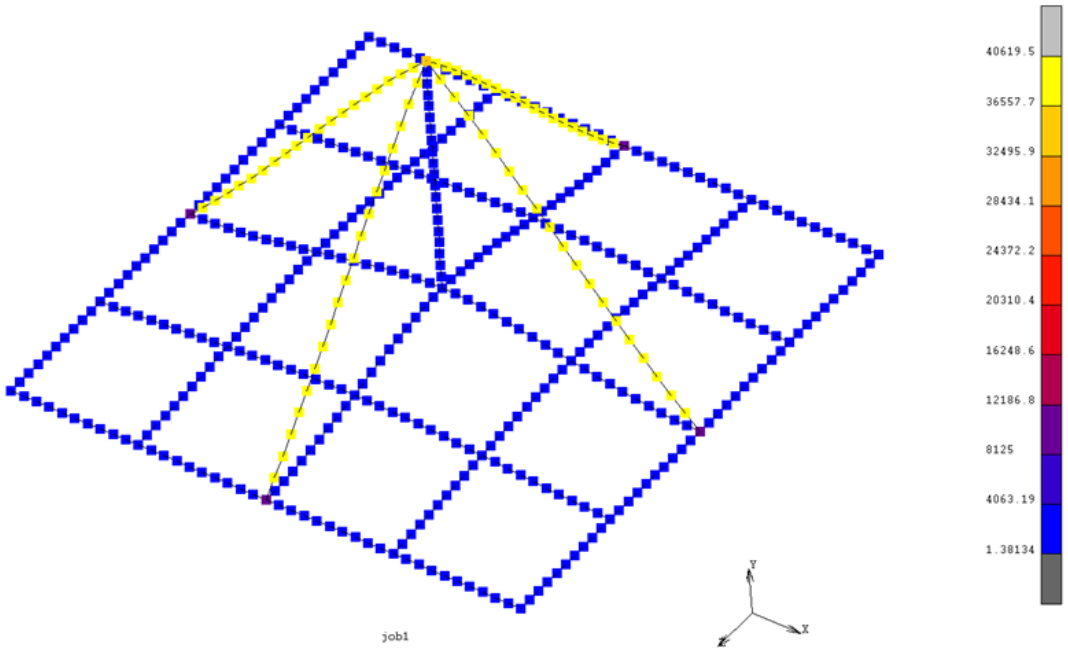

Figure 6: Sample results of von Mises stress from Marc Mentat finite element analysis testing performed on the anchor frames.

Table 2: Table of results from finite element analysis on the internal anchor frames in the dead-weight anchors.

Frame Configuration	SolidWorks Max von Mises Stress (N/m^2)	Marc Mentat Max von Mises Stress (N/m^2)	Percent Difference (%)
5x10 S-Section Bottom Section	40148.5	40840	1.7
4x7.7 S-Section Bottom Section	39570	40840	3.16
50mm Solid Square Bar Bottom Section	40573	40620	0.115

2.6 Design Assessment

Multiple issues arise when using a taut moored system to generate power using Oscilla Power's PTOs. The first and most important issue is that the system will only operate at its peak performance approximately twice a day due to tidal elevation change. The buoy would have to be set into location during low tide such that the system would be under constant tension. When it is high tide, the buoy would be fully submerged and it will not be able to ride the waves as intended. The slack-snap load phenomenon could not entirely be eliminated and still provide the tension oscillation required by the PTOs. Another issue with the taut moored system is deployment of the anchors. Due to their size and mass, the anchors would require a larger vessel to deploy them. While out at the site, the anchors would have to be dropped within a few meters of the desired GPS coordinate. If the anchors are too far off, the mooring line will no longer be in tension and the PTOs will not be able to generate the optimal power. Because of these deficiencies, the heave plate concept was investigated.

CHAPTER 3-

HEAVE PLATE GENERAL DESIGN

3.1 Design Rational

The changing water level problem was addressed using a slack mooring as shown in Figure 7 where the PTO's are located along the vertical stay to the heave plate. Oscillating buoyancy forces on the buoy are restricted by the plate creating the tension changes needed by the PTO's.

3.2 Design Configuration

A heave plate is a horizontal plate located beneath the buoy that resists vertical motion of the buoy (see Figure 7). As the buoy responds to wave-induced fluctuations in buoyancy force, tension changes are created in the stay. PTO's located along the stay use the tension oscillation to generate voltage. Usually, however, heave plates are fixed rigidly to the buoy components. For the OPT WEC, for example, the heave plate is attached directly to the base of a central spar. Thus, the use of stays required a careful development plan to ensure that the concept was feasible.

Since the best operating position of the heave plate is below the region of wave motion, the stay was designed to be as long as possible with no chance of hitting bottom. For the CORE site, a plate depth of 37 m below the waterline was a reasonable compromise. The buoy would use a slack line mooring configuration to keep the system in a general location while minimizing interference with the buoy-heave plate dynamics. These mooring lines do not have to be under any tension, resulting in smaller anchors and

line. Due to the slack mooring, the system will operate throughout the tidal cycle and will accommodate mean water level changes from other sources, such as storm surge.

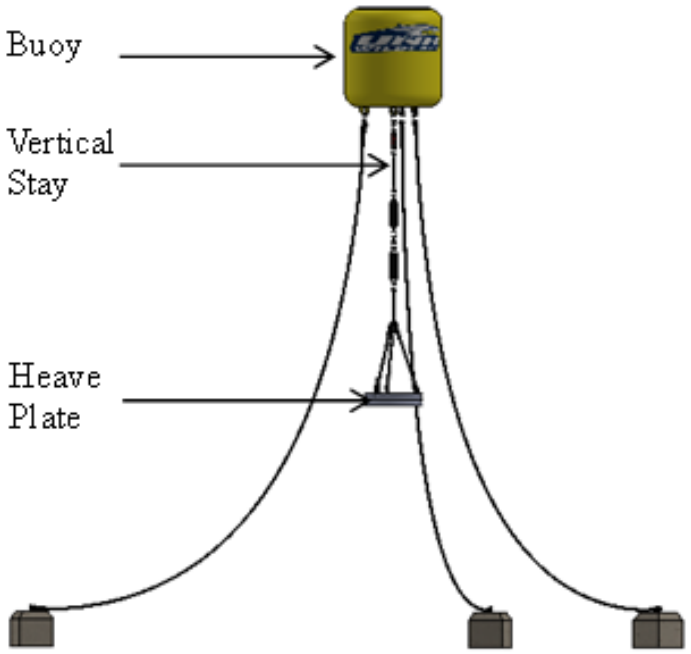

Figure 7: The buoy, PTO, heave plate system held in position using a three-point, slack-moored anchoring configuration.

Since there was no prior research available regarding heave plates used in this way, a wave tank test program was initiated to determine whether the heave plate would function properly using one or more stays. Of particular concern were entanglements, tensions oscillation amplitudes, gliding induced by lateral currents, and slack/snap events.

CHAPTER 4-

HEAVE PLATE – INITIAL TESTING

4.1 Purpose

While the heave plate concept appeared to have great potential, it was very important to properly test the design to ensure the system would function properly in a real environment. To verify that the heave plate system would in fact work, a scale model of the preliminary design buoy was built. The dimensions of this cylindrical buoy consisted of a mass of 2451 kg, a diameter of 1.842 m and a height of 4.5 m. A freeboard of 1.5 m was assumed adequate which corresponds to a draft of 3 m. At this draft, an excess buoyancy force of 56.3 kN was available to support a heave plate. Using these dimensions, a 1:20 Froude scaled model was built resulting in a model buoy with a diameter of 9.21 cm and height of 22.5 cm. At a scaled draft of 15cm, a mass of 999g was displaced (in fresh water). For heave plates of negligible volume, the 999g mass would be the sum of buoy mass plus heave plate mass.

4.2 Froude Scaling

In all tank experiments, Froude scaling was used to relate model scale experimental parameters and measurements to full scale counterparts. Froude number, velocity scale divided by the square root of gravitational constant times length scale, characterizes the ratio of inertia to gravitational forces. Since these are the dominant processes associated with wave motion, dynamic similitude is achieved by matching Froude number at model

scale to that at full scale. Geometric similitude is achieved by maintaining the same shape, and the length scale ratio is the ratio of a full scale dimension to that at model scale. As a result, the full scale to model scale ratio of velocities and time scales is the square root of the length scale ratio. Approximating equal fluid densities, the ratio of volumes, masses, weights and forces are equal to the scale ratio cubed. A sample of the effects of Froude scaling is shown in Table 3. A full discussion of Froude scaling as it relates to wave tank testing is presented by Chakrabarti (1994).

Table 3: Sample ratios (full scale/model scale) for the two tank tested physical models.

	Prototype 1	**Prototype 2**
Length	20:1	10:1
Time	4.47:1	3.2:1
Velocity	4.47:1	3.2:1
Force	8000:1	1000:1
Power	35777:1	3162:1

4.3 Physical Model Construction

The physical model buoy was fabricated of closed cell Dupont Styrofoam as shown in Figure 8. It was intentionally built light (approximately 100g) and to use ballast so that designs of different buoy to heave plate mass ratios could be tested. Knowing the model had to be very light and waterproof, previously purchased closed cell foam boards were used. Since the foam boards were 3 inches thick, 3 square sections were cut to the rough dimensions required. The foam was then cut to the outer diameter of 9.21 cm using a band saw. The centers of the circles were drilled forming a 2 inch diameter hole to allow room for ballast. Only two of these disks were drilled out fully, while the third disk was only

drilled out approximately 1.5 inches. The third disk would be used for the bottom where the vertical tethers would attach. Prior to assembly, the third disk was reduced in thickness to acquire the proper height of the buoy using a belt sander. To assemble the three layers, Liquid Nails glue was used. However, for future reference, a foam epoxy similar to Epsilon® EPS Foam Coating Epoxy would have been better as the Liquid Nails melted the foam slightly.

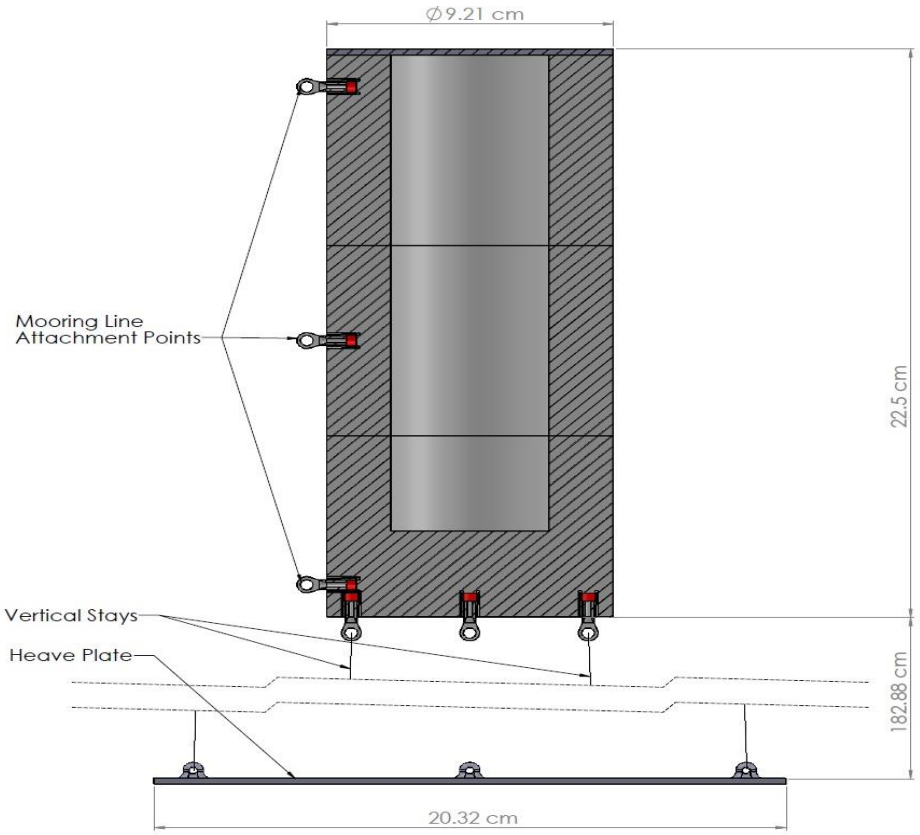

Figure 8: Physical model schematic of preliminary buoy design.

Once the glue was dry, approximately 24 hours, an outer shell was added for rigidity and some additional strength. To do this, automotive filler called Bondo® was used. The filler was applied and then smoothed to create a smooth outer surface. Mooring

line eyes were made using ring vinyl 22-18 AWG electrical connectors. These connectors provide excellent strength and are rust resistant which is ideal for this application. To use the electrical connectors, four 0.25 inch holes were drilled approximately 0.375 inch into the bottom disk in a square pattern, three inches on edges, centered on the buoy's bottom. A fifth hole was drilled in the center of the bottom for a central vertical stay line. The holes were then filled with Liquid Nails, and the electrical connectors were pushed in. In addition to the vertical stay attachment points, three connectors were added to the side of the buoy at the bottom, middle, and top. These connectors allowed slack moored mooring point location tests to be performed. Once the assembly was dry, three layers of white paint were applied followed by four layers of water sealant. The final mass of the buoy shell was 103g.

Construction of the heave plate was less complex. A single piece of 8 inch by 8 inch by 0.093 inch thick clear Lexan was used. Lexan is a very tough plastic that was chosen to resist shattering due to cyclic inertial and fluid dynamic loads. To mount the vertical stays to the heave plate, four holes were drilled in the corners, 0.5 inches from adjacent edges. An additional hole was drilled in the center of the plate. Cotter pins were then used for mounting points. To ensure the cotter pins did not move or fall out, Loctite Marine Epoxy was used. To provide sufficient mass, square pieces of lead flashing were cut up and added. To ensure the heave plate had an even weight distribution, a string was temporarily attached to the center of the plate allowing a visual check of levelness. The final dry mass of the heave plate was 1062 g while displacing 85 g of fresh water, while the overall system mass was 1165 g. The total displacement, at a design draft of 15 cm, was

999 g plus 85 g, adding to 1084 g. Thus the combination floated slightly low. The heave plate was painted white for better visibility under water. Once the paint was dried, four vertical tether lines were connected to the bottom of the buoy and the heave plate using 50 lb (breaking strength) Polar Ice braided ice fishing line.

4.4 Physical Model Testing: Qualitative Testing

Once the buoy and heave plate model construction was finished, wave tank visual experiments testing were performed to get a qualitative understanding on how and if the system works. The model was first put into the tank to verify that the proper draft was achieved. After this was done, a slack moored mooring line was connected to the buoy. This mooring line was located near the wave maker paddle so that the mooring line ran parallel with the wave direction. The purpose of the slack mooring was to hold the buoy in a region while not interfering with the buoy motion. The system was then tested using two different heave plate tether lengths subject to different wave heights with varying wave periods. Using two different tether lengths would indicate the effects of the wave motion below the water surface.

To determine the two different vertical tether lengths, water wave mechanics was applied. As a wave passes by the buoy, wave motion decreases vertically downwards through the water column creating varying water particle trajectories which are dependent on the relative water depths. To characterize the vertical structure of wave motion, the dispersion relationship,

$$\sigma^2 = g * k * tanh(k * h)\,, \tag{1}$$

was used to find wave length. In this relation, $\sigma = 2\pi/T$, $k = 2\pi/L$, T is the wave period, L is the wave length, g is gravity and h is the water depth (Dean & Dalrymple 1984). Since the offshore site water depth was 52 m, and the wave tank depth is 2.44 m, a scale factor of 1:20 was selected so that the scaled vertical structure of the waves is replicated in the tank. In the tank, as well as the offshore site, the ratio of depth to wavelength, h/L, indicated that waves ranged from deep water to intermediate. The two vertical stay lengths were 18.3 m and 37 m full scale. The 37 m length was chosen to be the longest possible without interacting with the bottom. At this length, the heave plate would be below wave motion for the widest range of wave periods. If the long length led to entanglement or other practical problems and the length had to be shortened, the 18.3 m tether length tests would indicate whether improvement was possible and what the decrease in heave plate function would be.

The first testing scenario involved the full scale tether length of 37 m. The first important visual observation was that the heave plate system resisted the buoy's vertical motion while remaining stationary as intended. The other noted observation was as the wave period increased to about 8 seconds (full scale), the heave plate provided less vertical motion resistance. For the longer wave periods, the wave motion caused the heave plate to move in more of an elliptical motion instead of staying stationary. Another important observation was that there were no slack events. This was important because slack events would result in snap loads which could be detrimental to the system. The next testing scenario was done using the 18.3 m (full scale) vertical tether length. As expected, the heave plate provided less resistance at shorter wave periods than the previous 37 m vertical

tether length. Since no dynamic instability or entanglement issues arose using the longer tether, it was decided that the 37 m vertical tether would work best for the full scale deployment.

Since the heave plate configuration was still a new concept, the effects of current were also tested in the tank utilizing the tow carriage to simulate three different currents for both tether lengths. These full scale currents were 0.1 m/s, 0.5 m/s, and 1 m/s. It was found that current had very little effect on the system. Once these qualitative tests were performed, it was concluded that the heave plate system would work leading to more testing.

Since the model buoy was designed to be adjustable, different weight distributions were tested along with different mooring line attachment locations. The first experiment was to see the effects of mounting the mooring line to the bottom of the heave plate. Using the same testing parameters as the prior tests, the mooring line location on the bottom of the heave plate showed very little effect of the heave plate motion. Since there was no improvement and sub-surface mooring attachment points have inherent practical difficulties, this concept was not developed further. Another test that was performed was to alter the mass distribution of the system to approximately a 50/50 distribution. During the tests of this distribution, the model buoy had a mass of 647 g and the heave plate had a mass of 549 g. For this test configuration, only the 37 m (full scale) vertical tether was tested. It was observed that the buoy had less upright stability than when the heave plate had the majority of the mass. This test was important to better understand the effects of the mass distribution on the system. This completed the visual tests and design development.

Next it was important to measure tether tension oscillations to see if they were adequate to drive the PTOs.

4.5 Physical Model Testing: Quantitative Testing

The next important step, after visually verifying the system would operate as intended, was to ensure that the system would generate the required tether tensions for the PTOs to work efficiently. To do this, a single 10 lb capacity submersible Futek load cell was placed in line with the heave plate tether located on the down wave corner. The buoy and heave plate model was configured with the full scale tether length of 37 m and with a model buoy mass of 647 g and model heave plate mass of 549 g. Full scale wave periods (Froude scaled) of 4 s, 5 s, 6 s, 7 s, 8 s, and 10 s were tested. For each of these wave periods, full scale wave heights of 0.4 m, 0.8 m, 1.2 m, 1.6 m, 2 m, and 2.4 m were used. In Figures 9 and 10, samples of load cell data are shown where the top plot is the model scale total load time series and the bottom plot is the model scale wave loading time series with the mean removed. The mean force was removed because it is the force oscillations about the mean that drive the PTOs. Oscillation amplitudes about the mean were arranged, and the overall results of these tests are shown in Figure 11.

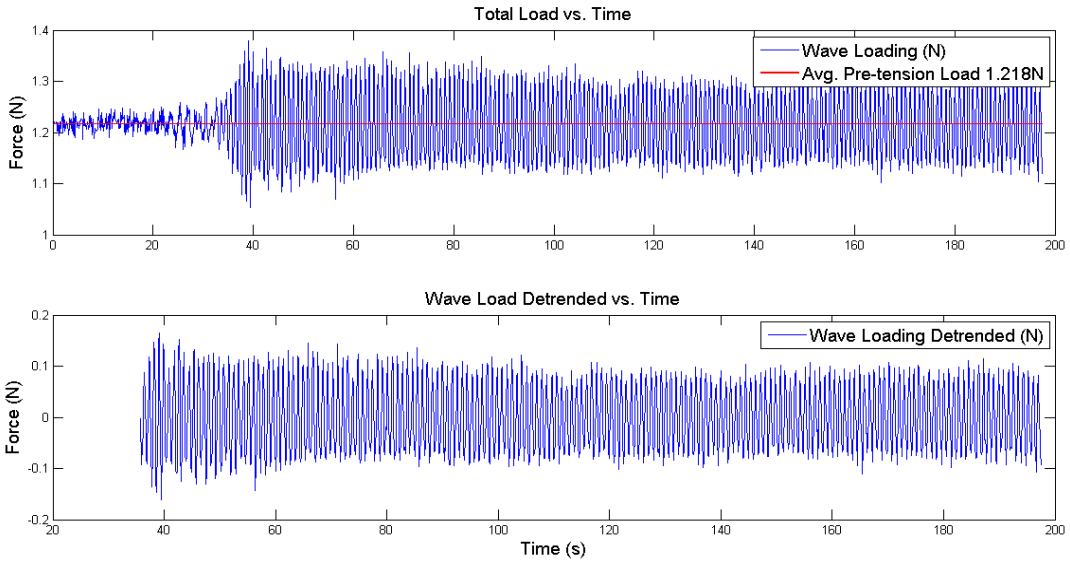

Figure 9: Model scale testing results for full scale wave period of 4s and wave amplitude of 0.2m. The full scale results concluded with tether line tension amplitude of 988.66N.

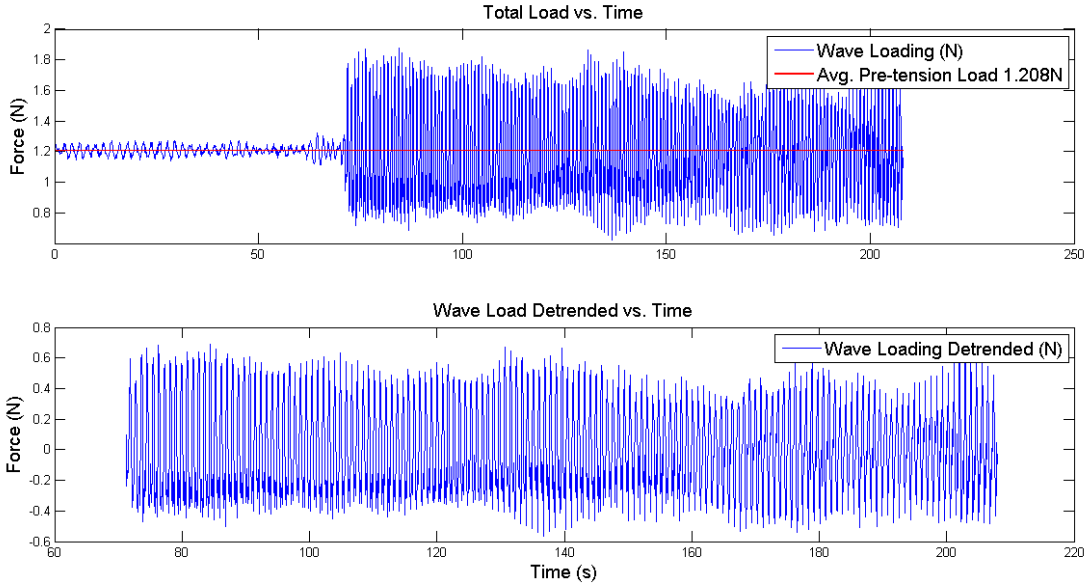

Figure 10: Model scale testing results for full scale wave period of 4s and wave amplitude of 1.2m. The full scale results concluded with tether line tension amplitude of 4880.6N.

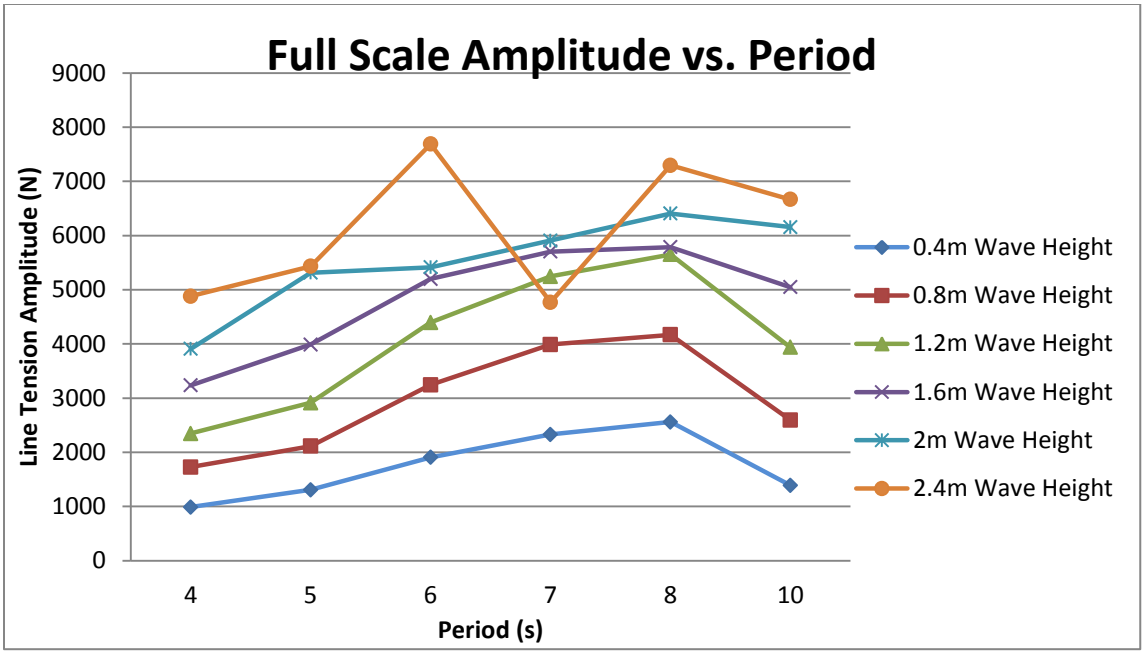

Figure 11: Full scale measured heave plate tension oscillation amplitudes as a function of period for different wave heights. Tension amplitude in a single stay, one of four, is plotted for the preliminary design buoy with heave plate.

As seen in Figure 11, with increasing wave period, the line tensions increase up until a wave period of 8 s. At wave periods of greater than 8 s, the wave vertical structure transitions from a deep water case to an intermediate wave case. Due to this transition, the heave plate is no longer in a region of no vertical wave motion. Also seen in Figure 11, as the wave height increases, the line tension amplitudes increase linearly. There is a dip in data at the 7s wave period for the highest wave of 2.4 m height. This is due to the system's natural heave period causing the buoy to lose vertical stability. As the wave crest passes by, the buoy will rise up, but as the wave trough passes by the buoy, the buoy will lose vertical stability in the water, causing the buoy to essentially fall laterally into the water until the next wave peak comes. To overcome this issue, the buoy size and mass would have to be adjusted to further increase or decrease the natural period.

4.6 Vertical Motion Dynamic Model

A vertical (heave) motion mathematical model was developed to serve as a design tool. This analytical, one-dimensional dynamic model is based on application of Newton's second law in the vertical direction to the buoy-heave plate system. Buoy added mass, wave radiation damping, buoy buoyancy force, plate added mass, plate damping, wave buoyancy force, wave vertical velocity force and wave acceleration force are included. The reduction in wave forces with depth was taken into account. The stay tension force was then isolated by analyzing the heave plate dynamics undergoing the heave motion predicted for the combination. The model was validated by comparing predictions to the tension measurement data shown in Figure 11. The model was then used to provide an initial estimate of stay tension amplitude as a function of buoy and heave plate mass and dimensions, wave period, and wave height.

The vertical (heave) equation of motion, based on the approach described by Berteaux (1991) is

$$m_v\ddot{x} + b\dot{x} + cx = (c\eta + d\dot{\eta} + m''\ddot{\eta})e^{-kD} \quad (2)$$

where

m_v	Mass and added mass of both the buoy and heave plate
b	Damping coefficient of both the buoy and the heave plate
c	$\rho g S$ where S is cross sectional area of the buoy
d	Wave drag coefficient
x	Heave displacement dependent variable
m''	Wave acceleration forcing coefficient
k	$2\pi/L$ where L is the wave length
D	Buoy draft.

For single frequency wave forcing,

$$\eta = a\cos\sigma t\ , \tag{3}$$

where a is the wave amplitude, σ is 2π over wave period, and t is time, the vertical (heave) displacement can be expressed in the form

$$x = aReal[H(\sigma)e^{i\sigma t}] \tag{4}$$

for which the normalized complex frequency response, or transfer function is

$$H = \ e^{-kD}\left[\frac{(c - m''\sigma^2) + i\sigma d}{(c - m_v\sigma^2) + i\sigma d}\right]. \tag{5}$$

Vertical displacement amplitude normalized by wave amplitude is termed the Response Amplitude Operator (RAO) and is given by

$$RAO = \ |H| = e^{-kD}\left[\frac{(c - m''\sigma^2)^2 + (d\sigma)^2}{(c - m_v\sigma^2)^2 + (b\sigma)^2}\right]^{1/2}\ . \tag{6}$$

Applying the equation of motion to the heave plate alone yields a dynamic equation for (total) tether tension,

$$T = W_p + m_t\ddot{x} + b_p\dot{x}\ . \tag{7}$$

Amplitudes of tension fluctuation from mean tension can then be evaluated as

$$(\Delta T)_{amplitude} = (T - W_p)_{amplitude} = a|H|\{[(m_p + m_{ap})\sigma^2]^2 + [b_p\sigma]^2\}^{1/2} \tag{8}$$

where

W_p	Weight of heave plate
b_p	Damping coefficient of the heave plate
m_p	Mass of heave plate
m_{ap}	Added mass of heave plate
m_t	$m_p + m_{ap}$.

Buoy added mass and damping ratios were estimated using free-release scale model results obtained by Turmelle (2007) for a similarly shaped aquaculture feed buoy so that

$$\frac{m_{ab}}{m_b} = 0.52 \tag{9}$$

and

$$\zeta = \frac{b_b}{2\omega_o(m_b + m_{ab)}} = 0.089\,, \tag{10}$$

where

$$\omega_o = \left[\frac{\rho g S}{(m_b + m_{ab}}\right]^{1/2} \tag{11}$$

with variables defined as

m_b	Mass of buoy
m_{ab}	Added mass of buoy
b_b	Damping coefficient of buoy
ρ	Density of fluid
S	Cross sectional area of buoy.

Previous tank tests of similar buoys indicated that wave forcing coefficients can be approximated by taking

$$d = b_b\ , \tag{12}$$

and

$$m'' = 1.1 m_{ab}\ . \tag{13}$$

The plate added mass was obtained using the formula for a circular plate of the same area,

$$m_{ap} = \frac{8}{3}\rho r^3 \tag{14}$$

and the plate damping coefficient was related to its drag coefficient using an equivalent integration approach,

$$b_p = \frac{4}{3\pi} c_d |aH| \tag{15}$$

in which $|aH|$ was approximated by a, and a plate drag coefficient c_d of 1.12 was used.

The vertical motion dynamic model was applied to the preliminary buoy design with heave plate, and the predictions compared with the tank test measurements are shown in Figure 12 and 13. The mathematical model predictions agree well with the measurements at short and long periods and for all periods at low wave heights. The model does not, however, replicate the lack of vertical stability at high wave heights near heave resonance. (Those predictions can be interpreted as the tension amplitudes that would have been obtained had buoy shape been shorter and wider to eliminate buoy toppling in the wave troughs.) With this understanding, the mathematical model was judged suitable to make initial estimates of tether tension amplitudes for design purposes.

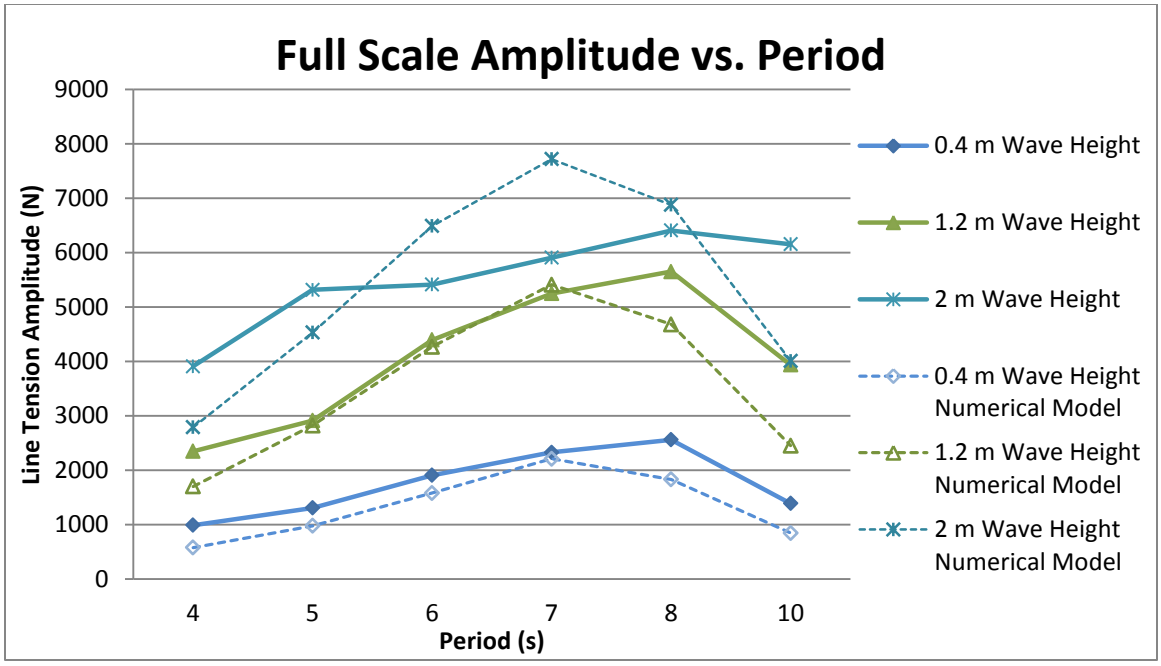

Figure 12: Vertical motion dynamic model results compared to physical model testing results for 0.4 m, 1.2 m and 2 m wave heights.

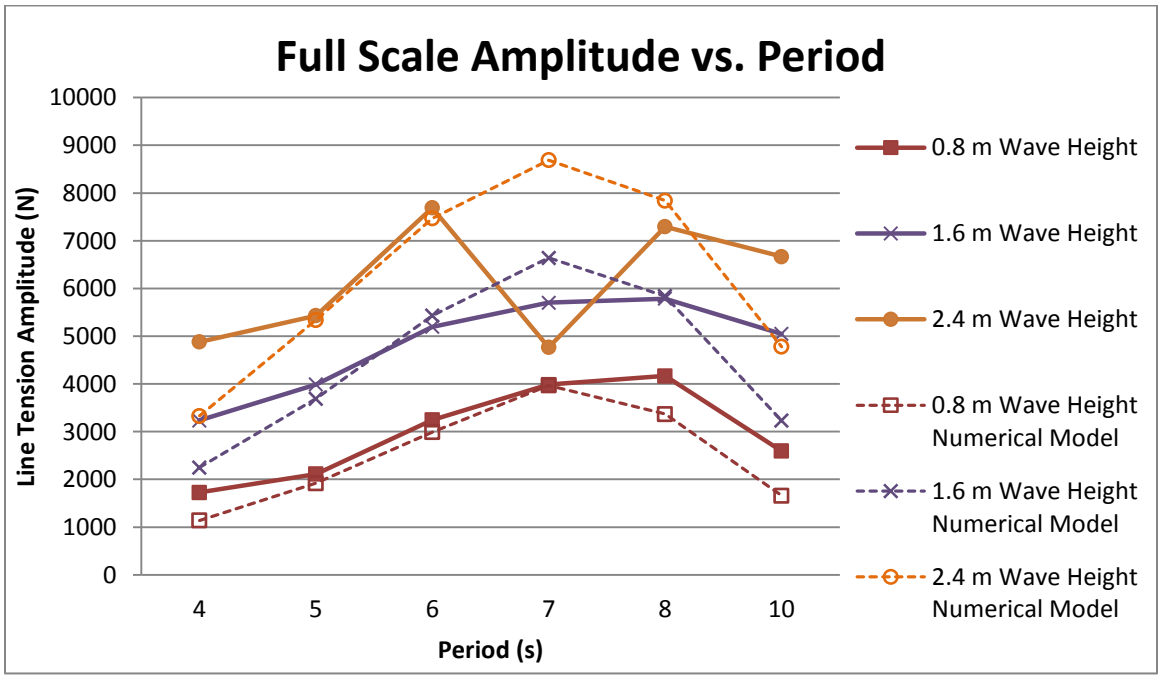

Figure 13: Vertical motion dynamic model results compared to physical model testing results for 0.8 m, 1.6 m and 2.4 m wave heights.

CHAPTER 5-

SUMMER 2013 MODEL TESTING

5.1 Overview of Summer 2013 Deployment

A trial deployment at the CORE site was performed during the summer of 2013 in preparation for a larger scale deployment the following summer. This deployment gave both Oscilla Power and UNH the basis for developing a detailed plan for the 2014 deployment, along with experiencing the difficulties of deploying an energy capturing buoy into the ocean. It was determined at this point to use the heave plate concept because of the favorable tank tests and vertical dynamics mathematical model results (see previous chapter).

For the 2013 system, a previously purchased buoy would be used in the deployment, so it was imperative to design the system around that specific buoy's capabilities which were different from the preliminary buoy design. This buoy had been tested in Lake Washington (LW) where sea states were normally less than a half meter. Subsequently, the LW buoy was tested in the large, outdoor Ohmsett wave tank while taut-moored to the tank bottom. While LW buoy was not as large as the preliminary buoy, scaled model tank testing with heave plate, along with Aqua-FE tests, were performed to ensure a successful deployment.

5.2 Physical Model Testing: Tank Testing

Once it was determined to use the LW buoy, it was important to tank test the buoy-heave plate configuration. The buoy, a Urethane Product Corporation SSSB-7000, has a diameter of 1.67 m, a height of 1.67 m and a mass of 567 kg. To reduce cost, the heave plate consisted of the bottom sinker structure used for testing at Ohmsett. The frame had full scale dimensions of 1.67 m by 1.67 m resulting in a 1:1 ratio of buoy width to heave plate width. Using scale model construction similar to the preliminary model buoy, a 1:20 scale model of the SSSB-7000 was constructed. The buoy model diameter and height were 84 mm, and the mass was 0.071 kg. Additional mass was added to the model to imitate the mass of the PTOs along with the data acquisition system. The overall mass of the buoy with the PTOs/instrumentation was 0.109 kg (877.6 kg full scale). The heave plate had a mass of 0.184 kg to get the desired full scale draft of 0.835 m. From previous physical model testing, a full scale 37m long vertical stay was used. This time, however, instead of having 4 vertical tethers mounting to the bottom of the buoy and the heave plate, a single vertical stay connected the heave plate and buoy.

To determine how to connect the vertical stay to both the buoy and the heave plate, physical models tests were performed. The two types of terminations tested were (1) a single bridle attached to the heave plate only and (2) bridles attached to both the heave plate and the buoy (see Figure 14). The bridles were intended to (1) prevent tipping of the heave plate and (2) minimizing both buoy and heave plate tipping. Due to the limited amount of time prior to deployment, only these two test cases were performed, and only measurements of tether tension were compared.

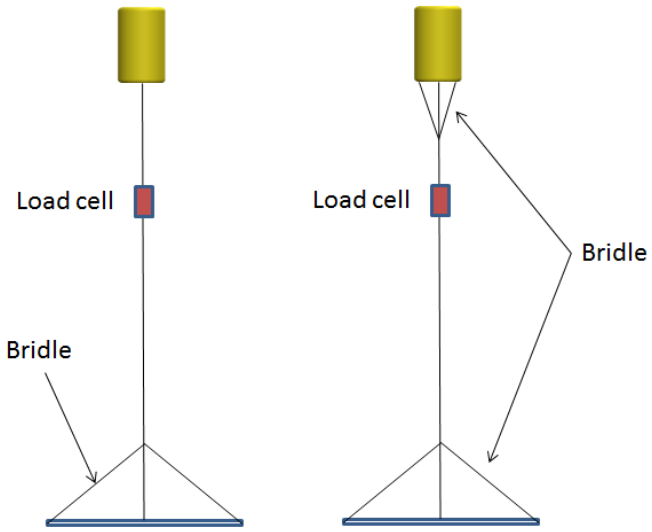

Figure 14: The two different vertical stay mounting configurations tested with the physical model.

The first scenario tested was the single bridle on the heave plate and the tether connecting to the bottom center of the buoy with a 10 lb capacity submersible Futek load cell mounted in line with the vertical stay. The model was run under the same regular wave regimes as the preliminary model to have a direct correlation between the two systems. These wave regimes consisted of 0.4 m, 0.8 m, 1.2 m, 1.6 m, 2 m, and 2.4 m full scale wave heights and full scale periods of 4 s, 5 s, 6 s, 7 s, 8 s, and 10 s. For the single bridle case, the buoy was visually less stable under short period waves, and also the heave plate moved more with increasing wave period. The reason for this is because the natural period of this system was approximately 3 seconds (full scale). Stay tension amplitude results are shown in Figure 15.

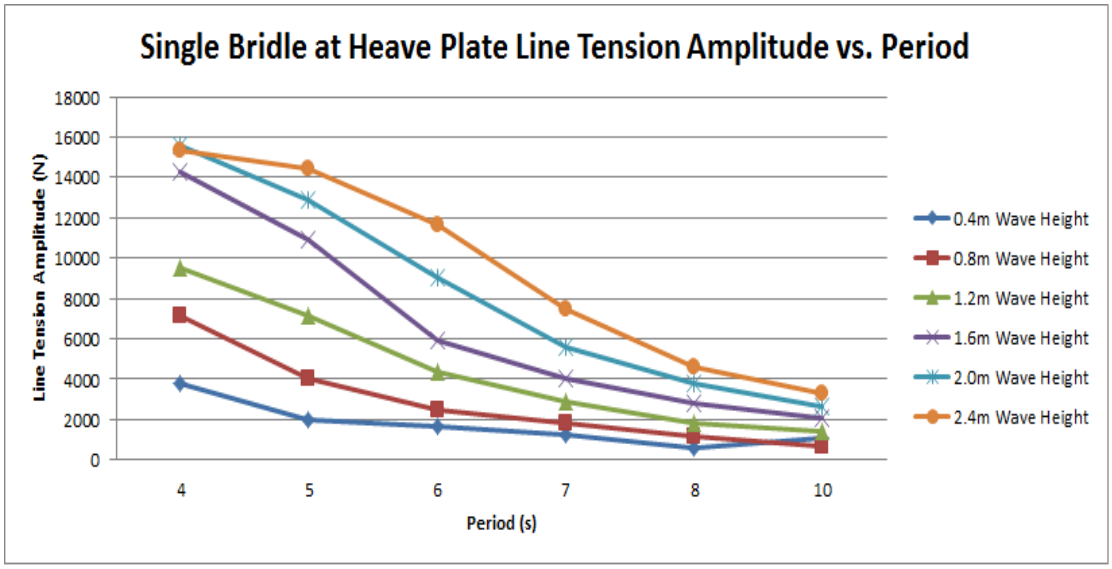

Figure 15: Summer 2013 tank testing model with a single bridle mounted on the heave plate with the vertical tether mounting directly to the middle of the bottom of the buoy.

The next testing scenario was with the double bridle system. Initial visual observations indicated that the buoy was more stable with less bobbing motion. The reduced motion should result in higher tension amplitude in the vertical tether. All other observations were similar to with the single bridle system tests. Tension amplitude results of the double bridle testing are shown in Figure 16.

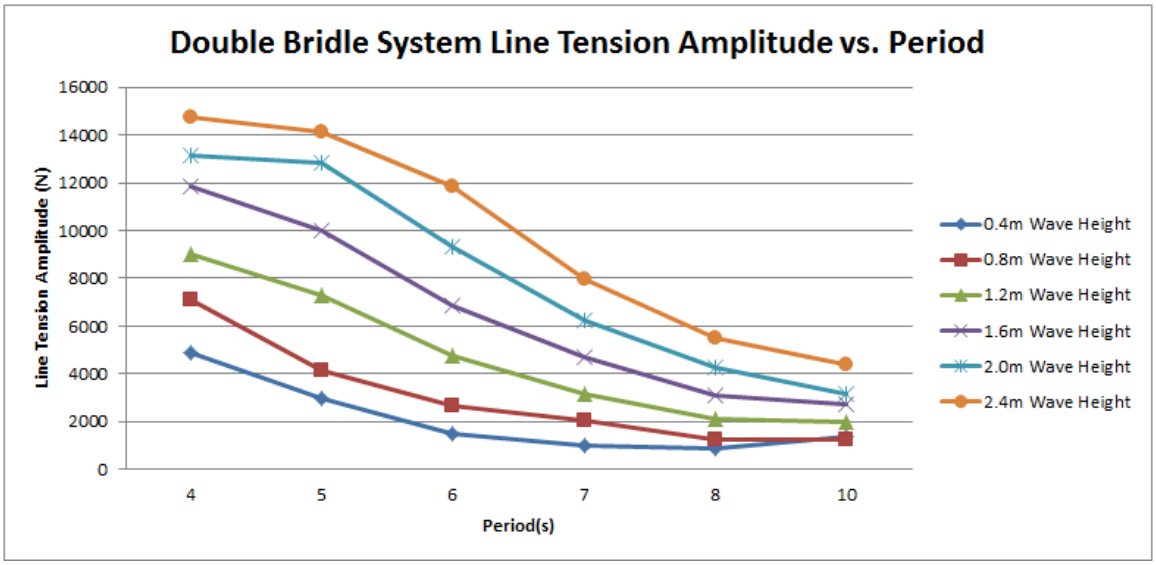

Figure 16: Summer 2013 tank testing model with a bridle mounted on the heave plate and a bridle connecting to the bottom of the buoy.

The single bridle system and the double bridle system tension amplitudes are compared in Figures 17 and 18. It can be seen that for shorter wave periods, the line tension amplitude is higher for the double bridle system. For longer wave periods, there is little difference. Though the double bridle system had slightly larger maximum tension amplitudes, a more complicated deployment plan would be needed. Since the tension benefits were small, the single bridle system was chosen for practical considerations of easier field deployment.

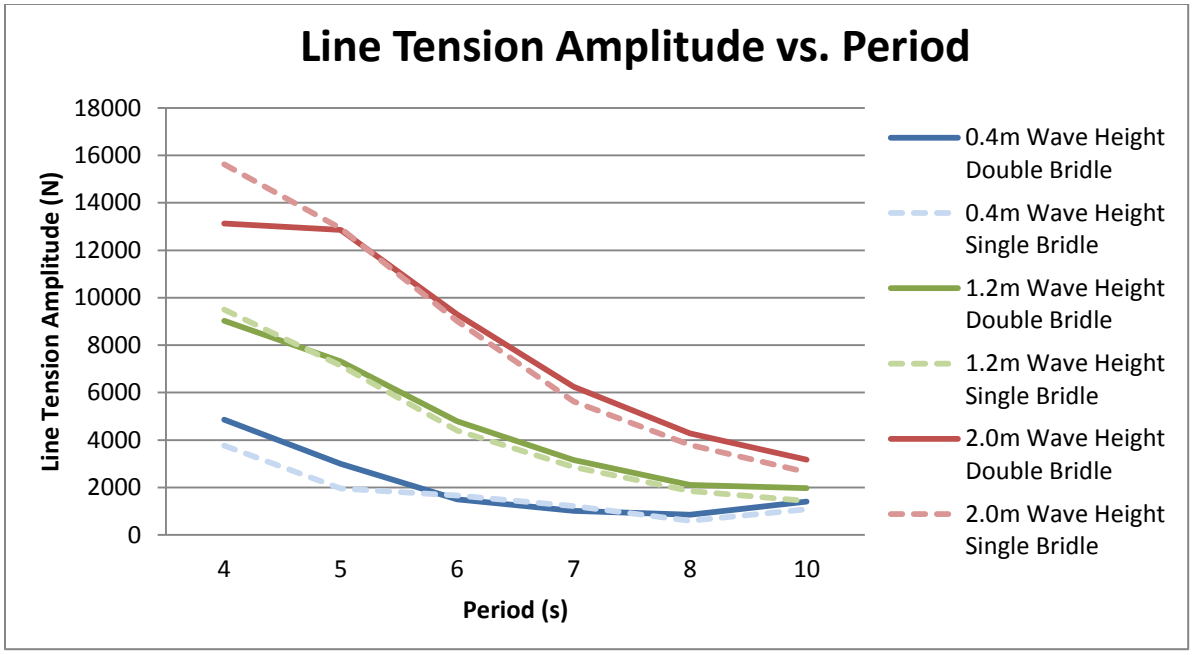

Figure 17: Single bridle system compared to the double bridle system for the wave heights of 0.4 m, 1.2 m, and 2.0 m.

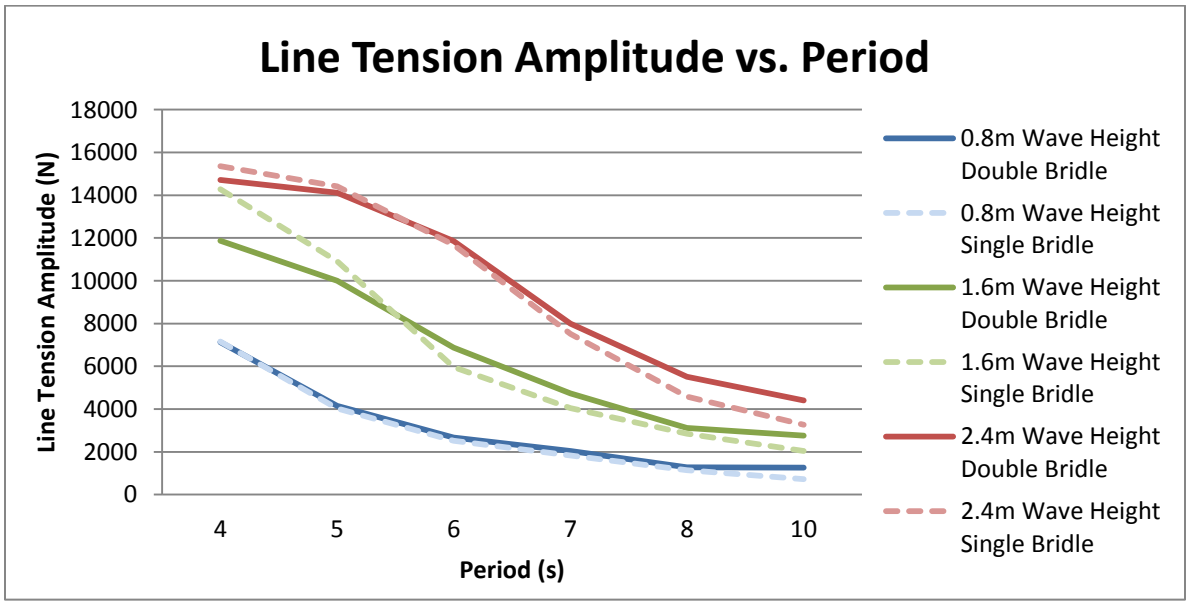

Figure 18: Single bridle system compared to the double bridle system for the wave heights of 0.8 m, 1.6 m, and 2.4 m.

5.3 Vertical Dynamics Modeling

The vertical motion dynamic mathematical model (described in section 4.5) was applied to the LW buoy-heave plate combination. Dimensions and masses given in the previous section were used. To evaluate the model for this application, predications were compared to wave tank data as seen in Figure 19. Comparison at wave periods in the range of 4-10 seconds indicated that the model is sufficiently adequate for initial design purposes. Note that the mathematical model indicates a peak in tension response at a period of 3 seconds which was out of the range of the wave tank periods. Full scale buoy mass of 877.6 kg and heave plate mass of 1472 kg were regarded as the "design" values to be used as fabrication objectives.

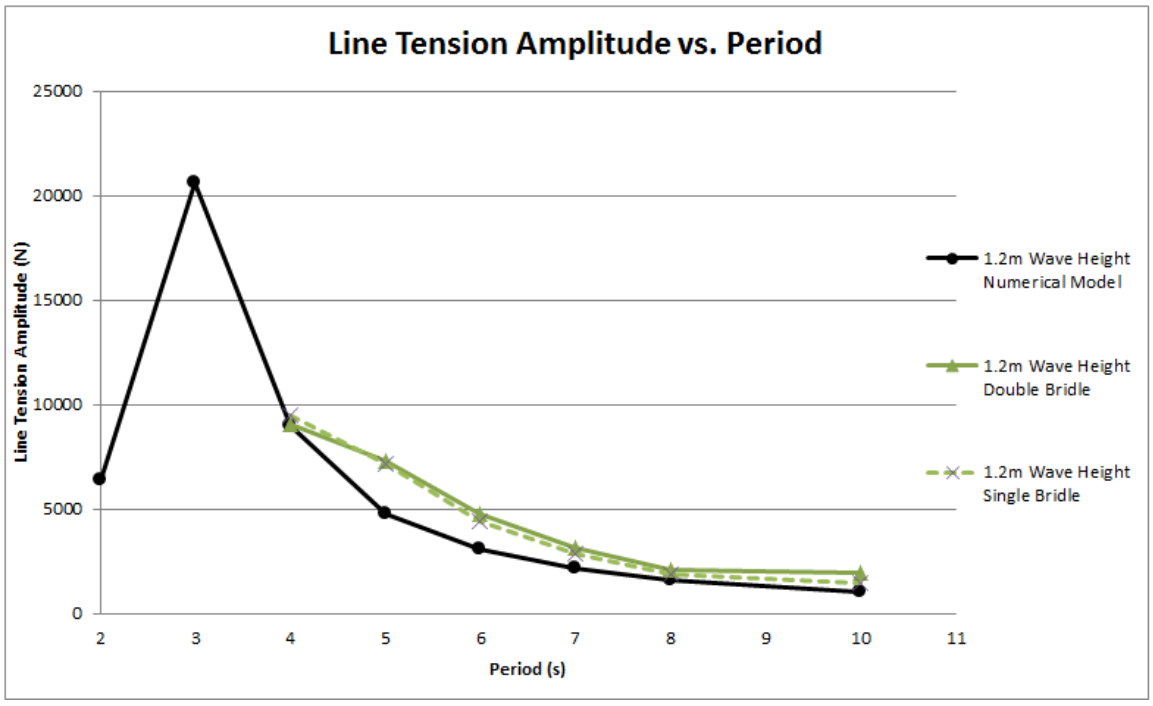

Figure 19: Vertical dynamic model results compared to physical model testing of a single bridle and double bridle.

5.4 Finite Element Testing: Heave Plate

Once the tank testing was performed, which finalized the deployment design, Aqua-FE was applied and used to determine the required anchor sizes. Since Aqua-FE requires the buoy to be created using multiple cylinders to acquire the proper drag and buoyancy, a MathCAD sheet was used to calculate the correct cylinder sizes. This MathCAD sheet program uses prescribed overall submerged volume, mass distribution and design configuration to compute the proper densities so that the correct hydrostatic balance was achieved. An example of this MathCAD program can be seen in Appendix I. Once the buoy finite element model was configured, it was run under a few test cases where the static mooring line tensions were examined and compared to the expected results from the MathCAD program. Once all results were matched, the Aqua-FE model was then run under regular and random wave scenarios.

For the Aqua-FE model, a single mooring line, having a 3 to 1 scope (line length to water depth) and in line with the wave motion, was used to determine the maximum tension the mooring lines should experience. To ensure the Aqua-FE model was accurate, the tank test vertical tether measurements, Froude scaled to full size, were compared to the Aqua-FE predications as shown in Figure 20. The predictions are somewhat high, but this conservative result indicated additional safety when using Aqua-FE for specifying mooring components.

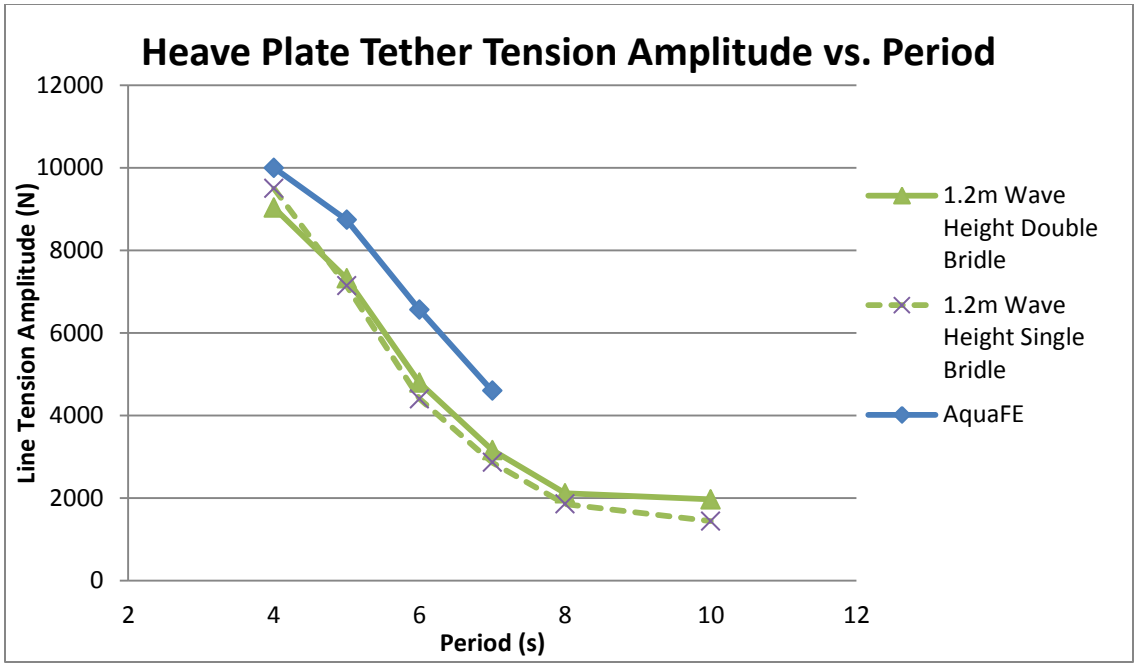

Figure 20: Comparison between Aqua-FE and physical model testing in the wave tank.

To use Aqua-FE to predict mooring line tension design purposes, a wind event generating a random sea was assumed. The random wave scenario tested had a significant wave height of 1.5 m and period of 5.34 s. The resulting mooring line tensions can be seen in the top two plots (of Figure 21), where the top plot shows the tension of the mooring line attached to the buoy and the middle plot shows the tension of the mooring line attached near the anchor. The vertical stay tension amplitude is shown on the bottom plot in Figure 21. The maximum tension experienced was 13.62 kN while the mean mooring line tension was 1.06 kN. To further test the system, currents were also simulated. The two currents tested, under the same random wave loading, were 0.1 m/s and 0.5 m/s. The resulting loads on the mooring line can be seen in Figure 22 for the 0.1 m/s current and Figure 23 for the 0.5 m/s current. For the 0.1 m/s current, the maximum mooring line tension was 15.23 kN

while the mean mooring line tension was 1.31 kN. For the 0.5 m/s current, the maximum mooring line tension was 37.7 kN and the mean mooring line tension was 3.31 kN. From this data, the available anchors at the UNH facility, (2) 500 lb Danforth anchors and (1) 100 lb Bruce anchor, were considered for the current system configuration. The 500 lb Danforth anchors, while embedded, provides approximately 25 times its mass in holding power in hard soils. The Bruce anchor provides approximately 60 times its mass in holding power for hard soils, however, only provide approximately 5 times its mass in holding power in soft soils. To ensure the Bruce anchor would be subjected to less loading, it would be deployed on the west mooring line which is protected from weather coming off the coast. These anchors were selected for the summer system based on the holding strength and availability.

For completeness and to have design values available for comparison, the LW buoy employing a taut-moored system was analyzed. Aqua-FE predications for this configuration (not used) are presented in Appendix IV.

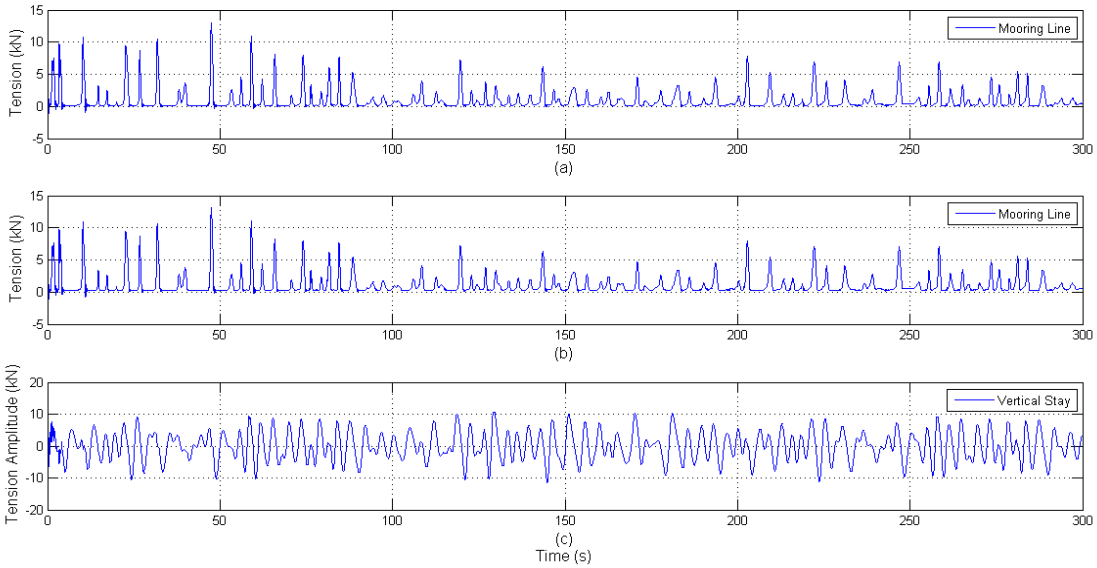

Figure 21: Aqua-FE model of the 2013 summer deployment buoy to determine maximum mooring line tensions. The wave regime this plot shows is a random sea with a significant wave height of 1.5m and a period of 5.34s. In the above figure, (a) is the mooring line tension at the buoy, (b) is the mooring line tension near the anchor, and (c) is the tension amplitudes on the vertical stay.

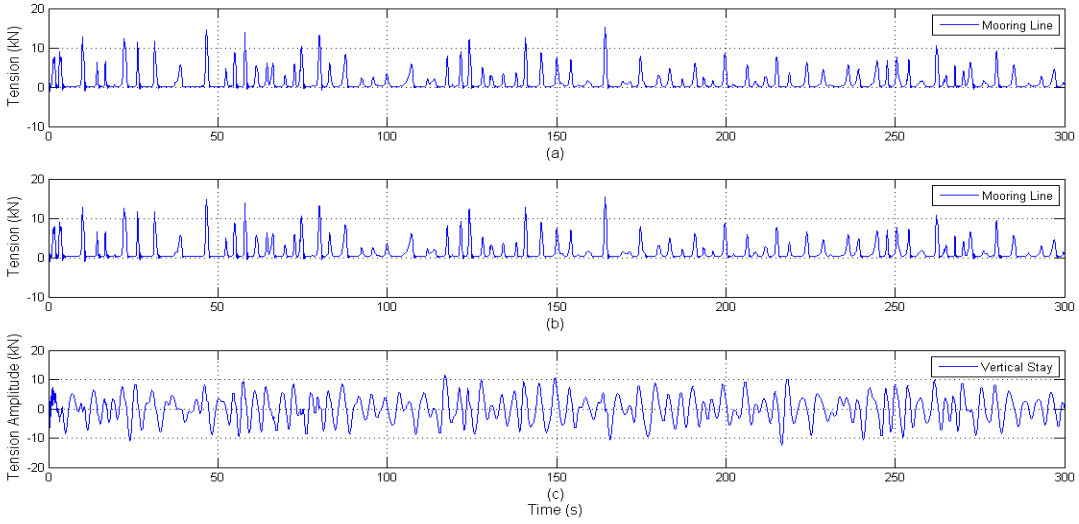

Figure 22: Aqua-FE model of the 2013 summer deployment buoy to determine maximum mooring line tensions. The wave regime this plot shows is a random sea with a significant wave height of 1.5m and a period of 5.34s with a current of 0.1m/s. In the above figure, (a) is the mooring line tension at the buoy, (b) is the mooring line tension near the anchor, and (c) is the tension amplitudes on the vertical stay.

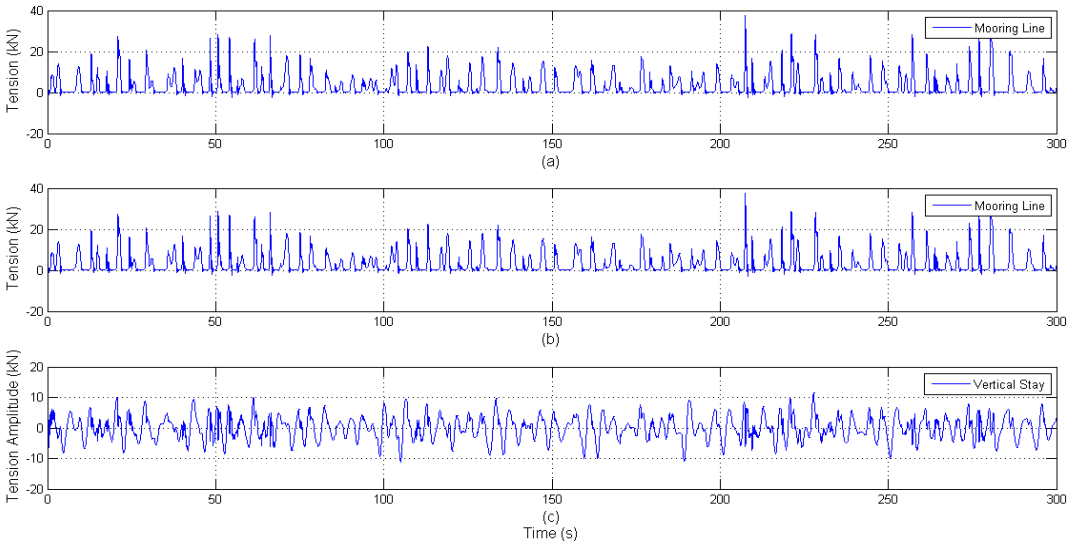

Figure 23: Aqua-FE model of the 2013 summer deployment buoy to determine maximum mooring line tensions. The wave regime this plot shows is a random sea with a significant wave height of 1.5m and a period of 5.34s with a current of 0.5m/s. In the above figure, (a) is the mooring line tension at the buoy, (b) is the mooring line tension near the anchor, and (c) is the tension amplitudes on the vertical stay.

CHAPTER 6-

SUMMER 2013 DEPLOYMENT: CONSTRUCTION AND PREPRATION

6.1 Overview

In preparation for the deployment of the buoy and heave plate assembly during the summer of 2103, every component used in the system had to be specified, purchased, and assembled. To stay within budget, most of the materials used were recycled from previous deployments and projects. It was also important that the equipment met a working load minimum of 20,000 lb set by Oscilla Power. This was to ensure that the system could survive any extreme event like snap loading or large storms. A preliminary system meeting these requirements was configured preliminarily using SolidWorks to verify component compatibility and assembly. The final system configuration in SolidWorks is shown in Figure 24.

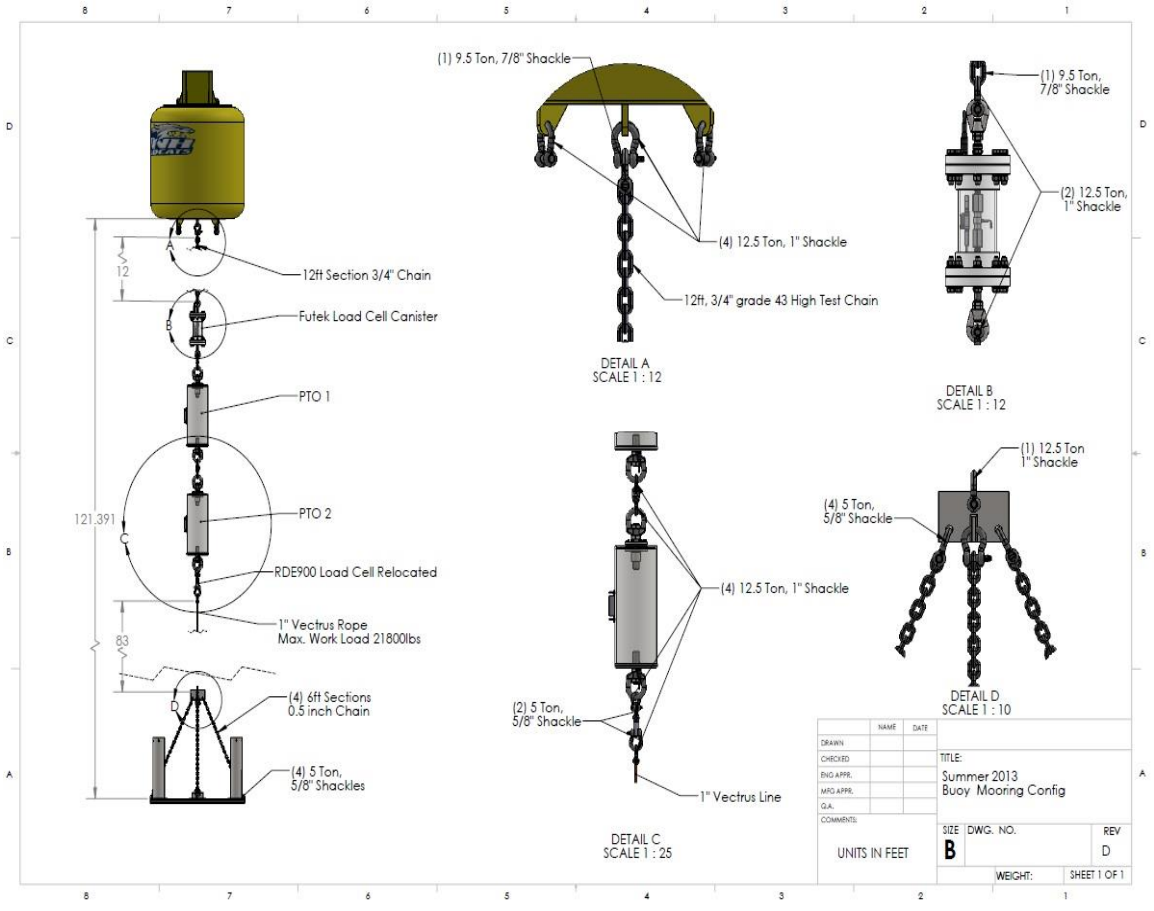

Figure 24: Buoy and vertical stay final configuration for summer 2013 deployment.

6.2 Buoy and Mooring Preparation

A slack, 3-legged mooring system was used to minimize buoy response to waves. For each mooring line, 1.5 inch 3 strand Polysteel line was used because 1380ft of surplus line was available at no cost, and this particular line surpassed the working load limit with a tensile strength of 47,560 lbs. To achieve a scope of approximately 3 to 1 line to water depth (approximately 150ft), the available line was divided into thirds making each mooring line 460 ft long. After the mooring lines were cut, an additional 10 ft of line was cut off each. These 10 ft sections would be used as a connecting segment to the mooring

eyes at to the bottom of the buoy allowing connection to and release of the mooring lines to be done above water.

Mooring lines were connected to the anchors using 1 inch shackles. To ensure the anchors were recoverable, crown lines were installed on the anchors using lines long enough to attach surface floats. For the crown lines, ¾ inch nylon line was used having a working load of 1070 lbs which should be ample for dead lifting the anchors for recovery and repositioning. A 600 ft spool of line was bought and divided equally between the three crown lines so that each line was approximately 200 ft long. To minimize chaffing, a ¾" thimble was spliced into the lower end of the line which connects to the anchor. The upper end of the line did not have a thimble so that the float could be easily tied. The float would later be attached to the line while the anchor was being deployed.

To ensure that the majority of the force at the anchor would be parallel with the seafloor to maximize embedment anchor capacity, a shot (90ft) of chain was used. This chain had to meet the required 20,000lb working load while also being no larger than ¾ inch due to shackle size limitations. The resulting chain was ¾ inch Grade 43 high test chain from ALP Industries. The chain has a working load limit of 20200 lbs which met the required loading restrictions. This chain was directly attached to the anchor and the mooring line was attached to the opposite end. A 12 ft section of this chain was also used in the vertical stay to make installation and recovery easier.

Once all the mooring lines and anchors were assembled, the instrumentation and vertical tether holding the heave plate were assembled. It was imperative to protect the data recording instrumentation using a iM2750 Pelican case located on top of the buoy.

Inside the Pelican case, a DT80 data system would record the data while being powered by a 12 v battery that weighed 112 lbs. This pelican case was mounted in the center of the buoy top, right above the center pad eye, in order to keep an even mass distribution to help offset the weight of the battery. To mount it in the center, a frame was constructed out of ¼ inch angle steel to raise the Pelican case over the central pad eye. The Pelican case would then mount to this frame via 3 bolts. The frame then connects to the buoy using a fiberglass grating which was secured in place using the buoy's built-in mounting plate.

With all this vulnerable equipment, which was essential for data gathering and transmitting, it was concluded that the Pelican case would need to be protected from over topping waves. To do this, an external cover was designed and built out of fiberglass with guidance from local boat builder Cabot Trott of Salty Boats of Maine. Drawn in SolidWorks, the external cover would enclose the Pelican case and also mount to the buoy. The final design drawing, used for fabrication, is shown in Figure 25.

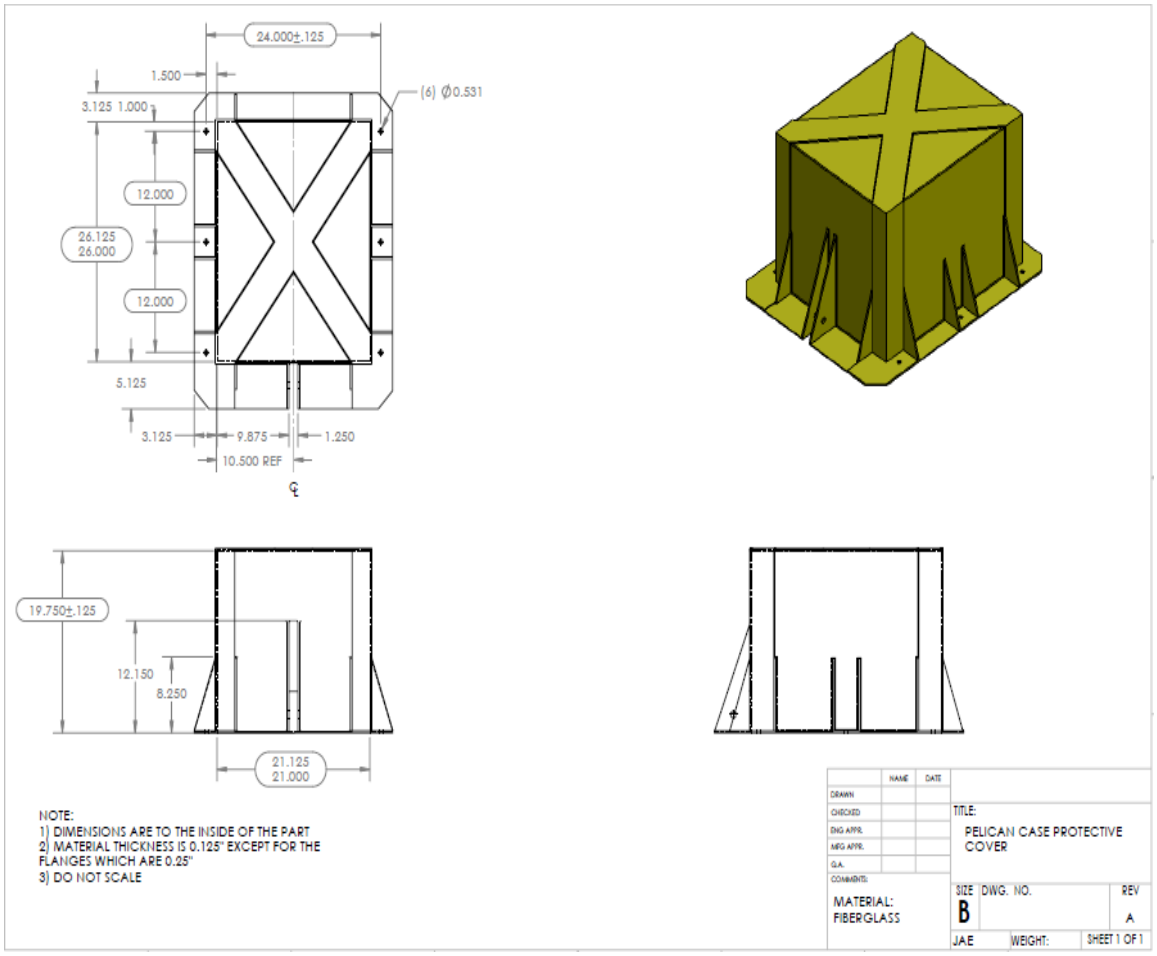

Figure 25: Pelican case cover finalized design modeled in SolidWorks.

It was suggested by Cabot that the case be built using flat fiberglass panels which would connect to an internal frame for strength. To create the flat panels, it was recommended that two different thicknesses of fiberglass be used. The two thickness used were a 1.5 oz mat and a strength adding 24 oz mat be used. A flat table was built where the fiberglass could be laid and wetted. A sheet of 4 ft by 8 foot 0.090 FRP wall board was placed smooth surface up on a flat piece of plywood for rigidity. This assembly was then

put on two saw horses to make laying the fiberglass easier. To further increase the rigidity of the table, 2 inch byb4 inch pieces of wood were run lengthwise between the saw horses.

The first step in constructing the fiberglass panels was to put 6 layers of mold release wax on the table to prevent the fiberglass from sticking. The fiberglass rolls were then cut into pieces to prepare them to be layered. Then, a layer of polyester resin was applied to the table top.

The construction process would consist of 2 layers 1.5 oz mat, 1 layer of 24 oz, 1 layer of 1.5 oz, 1 layer of 24 oz, and 2 layers of 1.5 oz. In between each layer, a generous amount of polyester resin was applied to thoroughly wet the fiberglass. After the final layer was placed down, a bubble remover roller was applied to eliminate the bubbles in the layup. Once all the panels were cured, they were cut to size then glued to a frame using West Systems epoxy resin with 406 colloidal silica adhesive filler.

Once the fiberglass composite was cured, the pieces were trimmed to size so the internal frame could be constructed. Available ¼ inch fiberglass angle was used for the frame. The angle was cut to the shape and sizes needed and then sanded down so that the adhesive would have a surface to adhere to. To further promote adhesion, acetone was used to clean the surfaces of the fiberglass angle. The frame was then assembled and glued together using the epoxy resin adhesive. The flat panels were then sanded, cleaned and glued to the completed frame. Once everything was glued, and for extra assurance against breakage, all the seams were filled with 3M Marine Adhesive Sealant Fast Cure 5200. When the whole case was cured, two coats of yellow paint were applied to match the buoy color resulting in the final product seen in Figure 26.

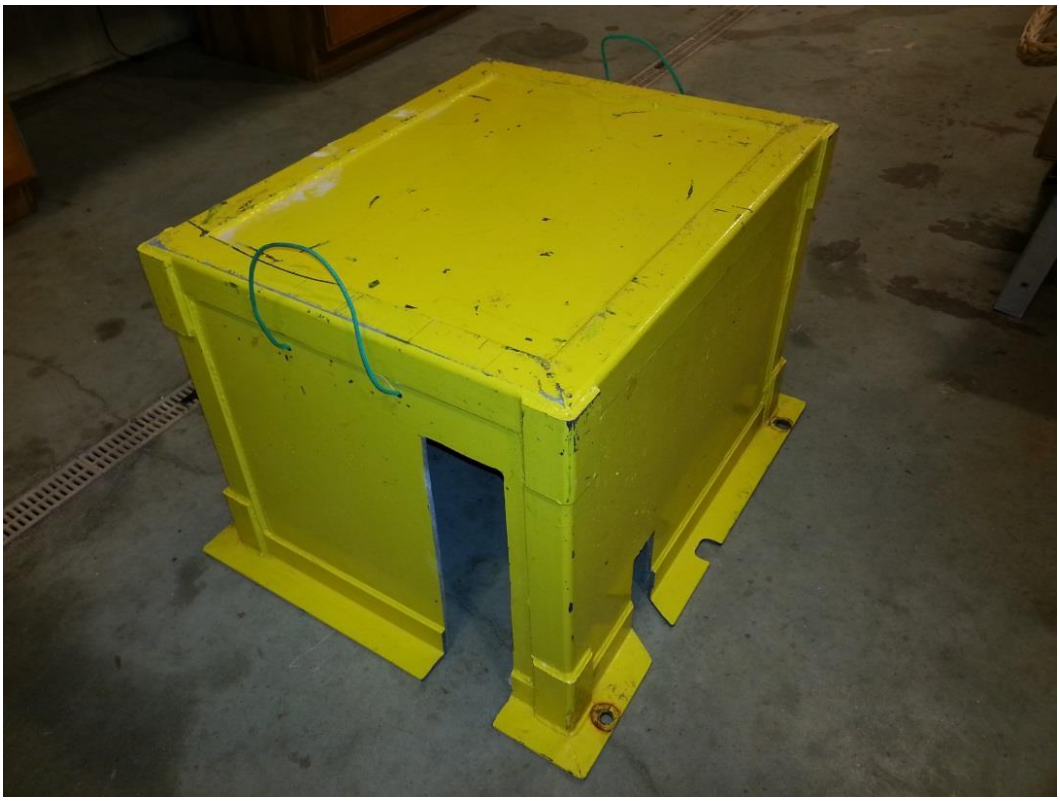

Figure 26: Final result of pelican case cover fabrication.

To attach the Pelican case cover to the top of the buoy, 4 of the bolts holding down the fiberglass grating were removed and replaced with ½ inch-13 threaded studs. These four studs would protrude out of the buoy, and the case would line up and slide over the studs via through-holes in the cover. Once the cover was over the studs, 4 washers were used to protect the fiberglass through-hole while being secured using 8, ½ inch-13 nuts, where 4 of the nuts were used as jam nuts. To prevent the nuts and studs from seizing in sea water, AquaShield lubricant was applied.

6.3 Vertical Tether and Equipment Preparation

For the vertical tether line, it was imperative that nothing fail because all the instruments and PTOs were incorporated into this single line. Also, this line was to have little stretch to ensure that the maximum tension loading was acting on the PTOs and not being diminished by line compliance. The ideal material to use in this case would be chain or metal line which has minimal stretch. However, metal cable was not used was because it would be very difficult to deploy and recover using the UNH research vessel Gulf Challenger. This is because metal cable, unlike line, could not be gripped on the capstan. For this reason, a long section of line was used between the bottom of the last load cell and the heave plate. A one inch Vectrus line from Yale Cordage was determined to be the best for this application. Yale Cordage is also local which meant for quicker delivery time. To save time, Yale Cordage also spliced two thimbles into the line. To make the 37 m water depth mark for the heave plate, it was determined that a 25 m line section would be required eye to eye.

Abiding by the minimum working load limit of 20,000 lbs put in place by Oscilla Power, the shackles were properly sized but not oversized to the point where the pin could not fit in the respective equipment. To do this, accurate measurements were taken of the mooring equipment and instrumentation. Then, using McMaster Carr's online catalog, shackle sizes were determined following the stated criteria. The resulting shackle breakdown for the vertical stay is shown in Figure 27.

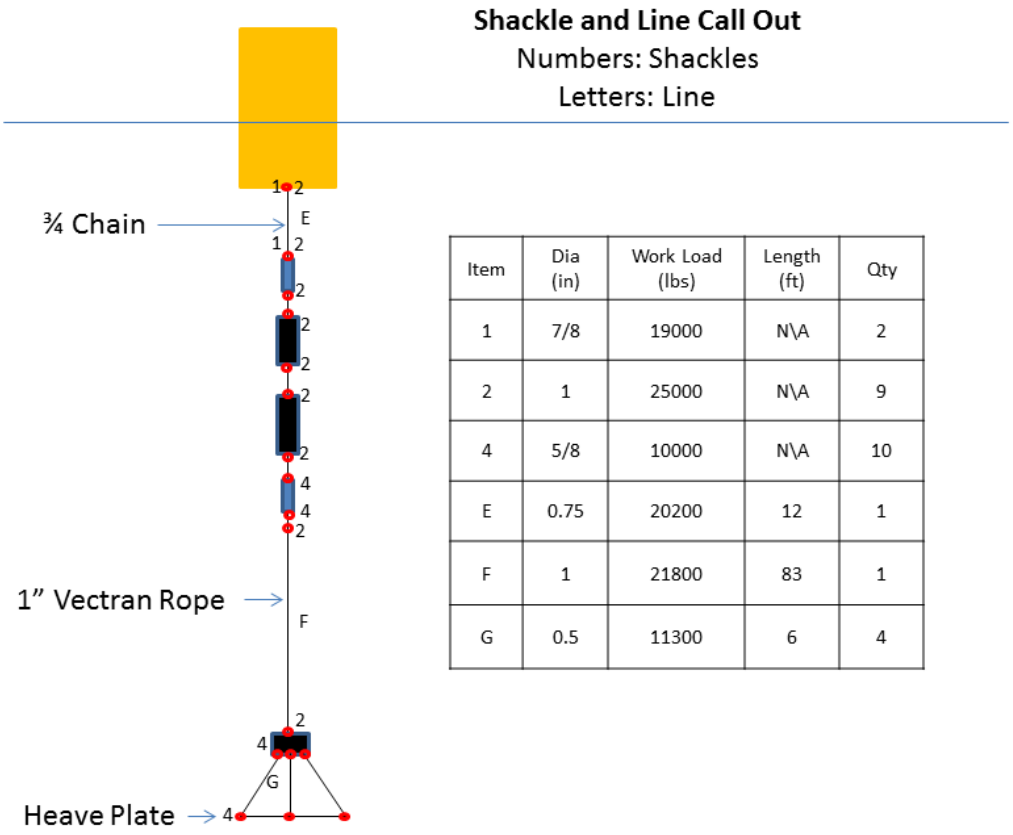

Item	Dia (in)	Work Load (lbs)	Length (ft)	Qty
1	7/8	19000	N\A	2
2	1	25000	N\A	9
4	5/8	10000	N\A	10
E	0.75	20200	12	1
F	1	21800	83	1
G	0.5	11300	6	4

Figure 27: Final configuration of vertical stay showing line choice and shackle breakdown.

Upon arrival, the PTOs were constructed with a plain steel outer case which would deteriorate when placed in the water. To help protect them, a rust preventative was applied along with a top coat to help prevent marine life from growing on them. This was important for OPI because they would be using the PTOs for further testing after the 2013 deployment. In preparation for painting the PTOs, electrical connections were taped. The first two coats of paint consisted of a rust preventative called Petit Metal Primer which is supposed to prevent rust while also protecting base metal. To further protect the PTOs, two top coats of Petit Unepoxy Antifouling paint were applied. This antifouling paint was to

prevent marine life while also providing an aesthetically appealing surface. The final result can be seen in Figure 28.

Figure 28: Final result of preventative paint coatings.

CHAPTER 7-

SUMMER 2013 DEPLOYMENT: FIELD TRIAL AND RECOVERY

7.1 Buoy and Mooring Deployment

Full scale trials of the LW buoy-heave plate combination were conducted at UNH's CORE site south of the Isle of Shoals. Due to various practical and fabrication changes, the buoy, PTO and instrumentation mass increased from a design value of 877 kg to an as-deployed value of 1540 kg. The design mass of the heave plate, on the other hand, decreased from 1472 kg to 408 kg.

The full scale deployment happened in two stages. The first stage was to deploy the three anchors (see Figure 7) while the second stage was to deploy the buoy and heave plate assembly (shown in Figure 24). The main reason for a two stage deployment was having adequate time during a working day to deploy the heave plate system. Deploying the anchors in a separate trip also freed up a lot of deck space; as it would be found out later, there was not much of it after loading the buoy and heave plate assembly.

The weather delayed the initial deployment date a couple of times, so after much anticipation, on the afternoon of July 9,2013, the UNH Gulf Challenger proceeded to the first anchor location where the Bruce anchor was set (see Figure 29). Anchor positions were specified in GPS coordinates obtained using an Excel spread sheet program. The Bruce anchor was deployed first because it was the lightest of the anchors, and its deployment was good practice prior to the larger anchors being deployed. The two larger Danforth anchors were then lowered into the specified GPS locations. The mooring lines

were connected, during the installation of the anchors, to a central float so that three mooring lines were terminated at a single point. This allowed the buoy and heave plate to be later installed and secured without divers.

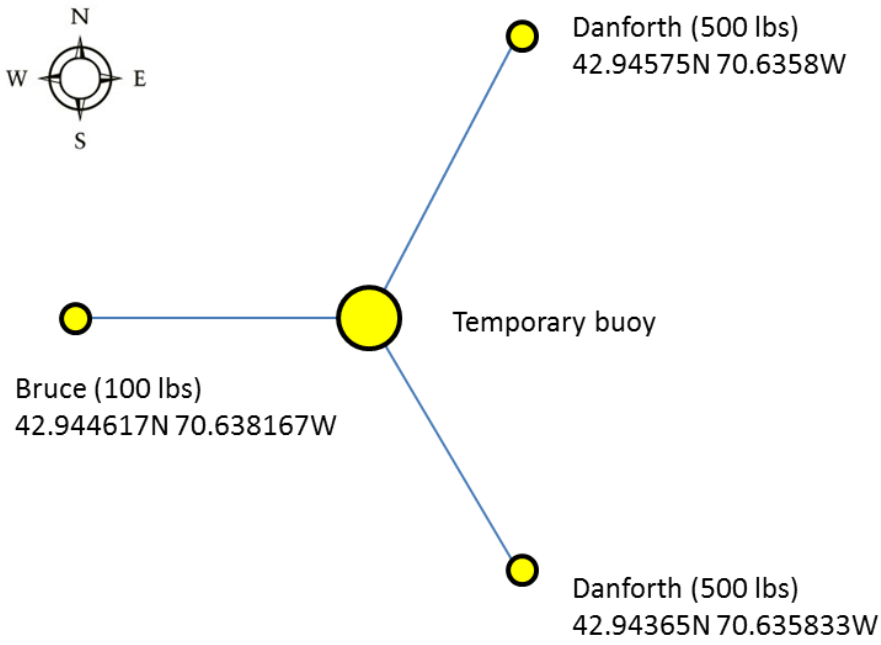

Figure 29: Anchor placement with coordinates determined by Excel spreadsheet program.

The following day, the boat was loaded with the buoy and the heave plate assembly in the morning and departed the dock around 11am. Once arriving at the site, the float that the mooring lines were attached to was removed from the water allowing the Gulf Challenger to use the anchors to keep the boat moored while deploying the buoy-heave plate assembly. The heave plate was deployed first, and everything followed in succession ending with the installation of the buoy. To lower the heave plate into the water, a secondary line of ¼ inch Amsteel was used that was released slowly from an on-deck reel winch. The reason for this secondary line was that the 1 inch Vectrus was too large in

diameter to wrap around the winch reel. While the heave plate was being lowered, the Amsteel line was being attached to the Vectrus line because this same line would be used during recovery. Once the end of the Vectrus line was in sight, the PTO closest to the heave plate, PTO2, was raised up on the A-arm of the boat. Then, the load of the heave plate was transferred to PTO2. This same process of transferring loads was performed throughout the rest of the deployment. While the loads were being transferred from one element to another, the instrumentation cabling was installed from each instrument to the top of the buoy. Installing the cabling proved to be difficult due to the length of cable, as well as providing the proper strain relief. To ensure the strain relief of the cable, it was attached via zip ties to the chain and instrumentation while including a generous amount of cable slack between the zip ties. Once all of the vertical stay line was lowered in the water, it was time to install the buoy.

Installing the buoy did not go according to plan, however, due to the worsening sea state. Wave height was increasing, and with all the weight of the heave plate and vertical stay in the water, the connection of the mooring lines to the buoy was rushed. Once the vertical stay was attached to the buoy, two of the mooring lines were connected to the buoy directly, while the third line was attached to one of the other mooring lines. Due to the sea state, the 10 ft sections of mooring line were not attached to the bottom of the buoy. While the buoy-heave plate was in the water and secured to the three mooring lines, entanglement was possible and tension could not be put on the mooring lines. Since sea state prevented correction at that time, the Gulf Challenger left the site returning to the UNH Pier. The

instrumentation case had not been installed, and therefore no data would be collected until the weather cooperated.

On July 16, 2013, the Gulf Challenger returned to the buoy to adjust the mooring line that was not connected to the buoy and also reset the anchors. To fix the Bruce anchor mooring line connection to the buoy, the buoy end of the mooring was mounted to the side of the buoy at an above water attachment point. Then, a temporary line of approximately 15ft was run between the north Danforth mooring line and the Bruce mooring line to help distribute mooring line tension. An image of this assembly can be seen in Figure 30. The next step was to reset the anchors so that the mooring lines were in tension. Tensioning the mooring lines would reduce chances of entanglement with the heave plate, as well as pull in the floating mooring lines underwater. To put tension in the system, the south Danforth anchor was lifted off the seafloor using its crown line and the boat moved south until tension was visibly seen on the buoy. Once the system was tensioned, the Gulf Challenger did one final visual check of the system prior to returning to the UNH Pier.

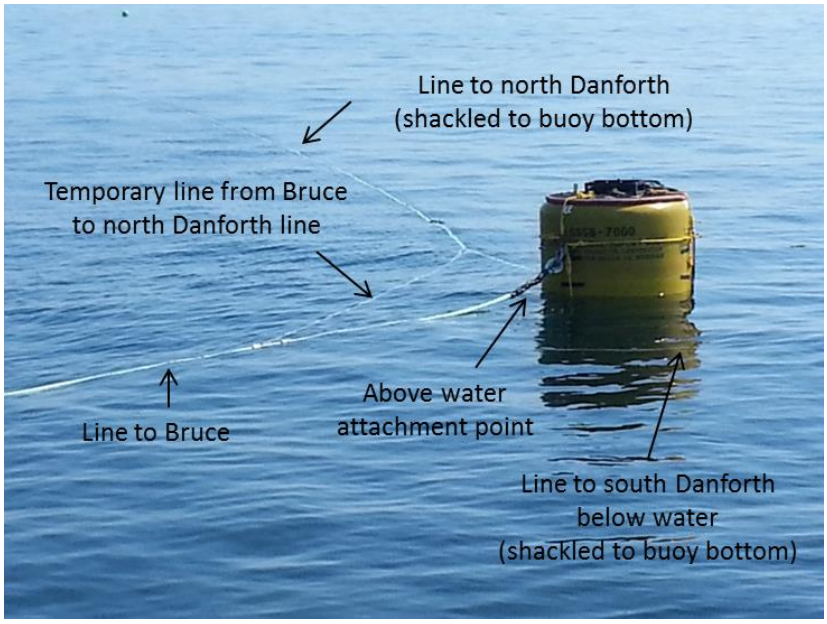

Figure 30: Temporary line connecting the north mooring line to the east mooring line.

Once the Gulf Challenger reached the pier, UNH's smaller vessel, the Galen J, was loaded up with the Pelican case, battery, and Pelican case cover to head back out to the site and install the equipment. The instrumentation installation went fairly smoothly, partially because of the calm sea state. During this installation, the DT80 data acquisition system was not reading any of the instrumentation. After running some tests over the internet from Salt Lake City, the system worked correctly. One load cell, the top mounted Futek (see Figure 24), did not work properly after this fix. It was assumed that water had penetrated its protective case, but this could not be confirmed. However, just prior to leaving, the buoy navigation light stopped working. The reason for this was one of the fuses had blown. So a quick jumper wire was made as a temporary fix to make the system fully operational. A final visual inspection was performed prior to leaving the site and, in Figure 31, the final system can be seen.

Figure 31: The final assembly of the buoy and heave plate system on July 16, 2013.

7.2 Modified Heave Plate Mass

Weekly buoy checks along with battery changes were performed. However, from the heave plate tether load cell data, slack events were being recorded. As stated earlier, slack events could result in a system failure due to the snap loads that are incurred after the slack. To reduce this, it was concluded that more mass would need to be added to the heave plate. Fortunately, there were a dozen railroad wheels at the pier to use for this project. A single wheel had a weight of 680 lbs, and weight minus buoyancy force of 590 lb which added significantly to the heave plate mass. As plans for installing the added weight were under way, a large storm passed through having 7 ft significant wave heights causing damage to the instrumentation wiring. This damage was repaired while the buoy and heave plate were out of the water to add the railroad wheel.

To add the railroad wheel, Riverside and Pickering Marine was hired to lift the buoy out of the water so the required fixes could be made. Riverside and Pickering Marine's crane was used to raise the buoy, vertical stay, and heave plate all in one step. Once it was out of the water, the railroad wheel could be added to the heave plate along with the necessary repairs done to the instrumentation cables. At this point, it was determined that the Futek load cell would not be able to be fixed, so it was completely removed from the vertical stay. Also, while the buoy was out of the water, the wiring from the data acquisition system on top of the buoy to the sensors mounted below the buoy along the heave plate tether had a protective sleeve added to prevent any chafing that may occur in future storms. Once all the repairs were made, the 10 ft mooring line tails were incorporated between attachment points on the buoy bottom and the mooring lines as originally intended. After the system was lowered back into the water, the crane picked up an anchor and re-tensioned the system.

7.3 Field Results

To obtain data, OPI installed multiple instruments which connected to a data acquisition system. To record the tensions on the vertical stay, there were two load cells mounted in line, as shown in Figure 24. Due to the Futek load cell failing only the Stellar Tech RDE900 load cell was obtaining tension data at a frequency of 4.5 Hz. The frequency was limited due to the DT80 data acquisition sampling speed while multiple channels were being recorded. This data acquisition system would automatically transfer data via satellite to OPI's office in Seattle. As a fail-safe, the data were also recorded to a USB flash drive.

The recorded data for the PTOs consisted of voltage and dynamics (3-axis acceleration, and 3-axis orientation). The voltage was the main priority of this deployment for proof of concept so it was important this data was recorded. From the recorded data and corresponding tether load cell data, tensions correlated well with PTO voltage. The voltage output for both PTOs was nearly identical as well. A 3-axis accelerometer was used to see the accelerations in the x-, y-, and z-axis of a PTO to better understand the motion of the tether and the PTOs. Two 2-axis gyroscopes were used to record the angles of a PTO. The angles and accelerations of the PTOs data allowed for slack events to be observed.

The final instrumentation included was mounted on the buoy to understand some of the buoy's dynamics. A 3-axis accelerometer was mounted in the Pelican case on top of the buoy to obtain the x-, y-, z-axis accelerations of the buoy. Additionally, a pressure sensor was mounted on the buoy to record pressure changes. Having buoy accelerations and tether tensions, response amplitude operators could be determined for wave height to tether tensions.

Overall, the system performed as designed. Under storm events with 6.5ft to 7ft, significant wave heights, and loading measured at 14,000 lbs, the data recorded slack events, however, all mooring and vertical stay equipment and hardware performed as intended. This weather along with the deployment gave OPI an opportunity to get at sea data sufficient to evaluate their WEC concept.

7.4 Deployment Obstacles

On August 9, 2013, the buoy was once again hit with a large storm event having significant wave heights of 6.5 ft. This time, the battery tie-down broke and allowed the 112 lb battery to move around in the Pelican case. This ultimately broke the seal of the Pelican case allowing water to get into the box. This movement also dislodged some equipment and almost the dislodged the Pelican case from the frame that attached it to the buoy. Luckily, the system still worked after a few on the spot repairs. A new battery tie down was made out of spare materials carried on the Galen J. The rest of the system just needed to be dried, cleaned, and tested. The buoy, however, was still in place; mooring lines were not broken; the heave plate was still attached, and data were still being collected.

On the August 21, 2013, the buoy and system were disconnected from the mooring lines by another vessel. Two of the mooring lines were cleanly cut by what appears to be a knife, while the third mooring line was cut with a great deal of fraying, possibly caused by a prop. This event left the buoy to drift 3-4 miles west, southwest. Fortunately, a local fisherman reported the buoy to the Coast Guard providing coordinates of the buoy. The UNH team investigated using the Galen J. Upon arriving at the buoy, there was a tail of approximately 100-150 ft of the 1.5 inch Polysteel line floating from the buoy, as seen in Figure 32. The buoy and heave plate assembly was also very close to running itself "ashore". There was close to 37 m of equipment hanging directly below the buoy, and the water depth at the original test site is only 52 m. Where the buoy was found, the water depth was very close to the 37 m mark.

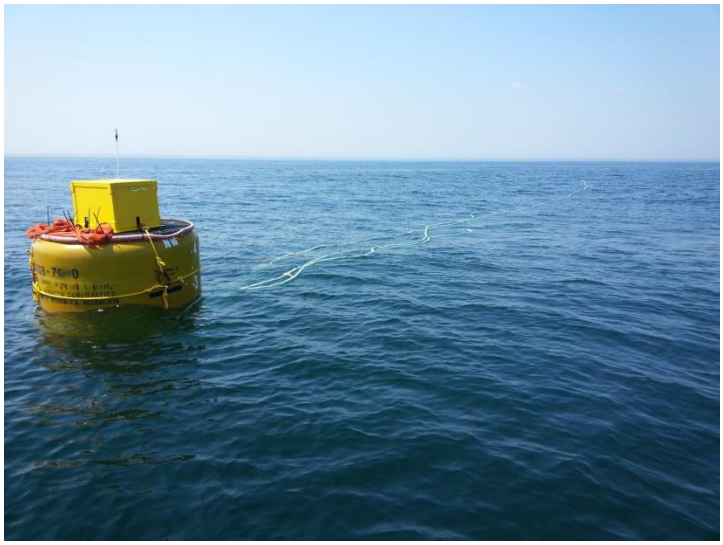

Figure 32: Buoy floating away from the site with the mooring lines trailing behind it.

There was no way to stop the buoy from drifting with the Galen J, so Riverside and Pickering Marine came to the provided coordinates and anchored the buoy in place. In the meantime, the trailing mooring lines were removed from the mooring line tails. The 10 ft mooring line tails were then attached to the bridle on the side of the buoy to keep them out of the way. Finally, the Galen J went to the original anchor site where the remaining mooring line was floating. This line was coiled up and tied to the crown line so that the majority of the line was in a specific location. Doing this would also help with the anchor recovering because both crown line and mooring line could be used to recover the anchor.

7.5 Buoy Recovery

Riverside and Pickering Marine was chosen to recover the buoy because they had the ability to quickly remove the system using a crane and barge. Using the Riverside and Pickering Marine crane, however, is weather sensitive. The barge and crane could only be operated in still water conditions, and due to this, the recovery was delayed a couple weeks

longer than anticipated. Upon arriving at the buoy all the equipment was removed, and a crane hook was attached to the top of the buoy. The crane then simply lifted the buoy out of the water. Once the crane reached its maximum range of lifting the buoy, the vertical stay was tied off to the barge and then repacked. The entire removal process took approximately 15 minutes. The buoy and heave plate being lifted out of the water can be seen in Figure 33.

Figure 33: Buoy and heave plate being removed from the summer deployment.

CHAPTER 8-

GENERAL DESIGN FOR SUMMER 2014 DEPLOYMENT

8.1 Design and Rational

With the summer of 2013 deployment experience, a new buoy and heave plate system was to be designed utilizing the knowledge acquired during the first deployment. To better meet the requirements of the specific PTO's to be tested, OPI completed the detailed design and oversaw the construction of the buoy and heave plate. UNH's role was to collaborate on the design concept, provide proof of concept testing, physical model testing and assistance with the deployment.

One of the major issues that was encountered in the previous deployment was slack events experienced in the vertical stay. To help eliminate this, asymmetric heave plates were designed and tank tested. In this approach, the heave plate was streamlined for downwards motion while having larger drag and added mass for upwards motion. The tow test program included measuring the coefficients of drag and added mass of four newly designed heave plate concepts. The drag coefficients of the asymmetric heave plates are important to understand because they characterize how the heave plates fall faster or rise slower in the water column in response to the buoy motion. The asymmetric added mass will further reduce the buoy's upward vertical motion compared to downwards motion while increasing tension amplitude in the vertical stay and decreasing the likelihood of slack events. Tank testing provided the basic data for selecting the best of the four designs.

OPI also integrated a larger scale PTO system that was mounted inside of the buoy. This allowed for easier access to the PTO system while ensuring that no cables running up the vertical stay are damaged which was experienced during the previous deployment. Also, in terms of long term reliability, the PTOs could be monitored more easily to ensure proper operation. This new PTO system, however, had to be incorporated inside the buoy which effectively made the buoy volume eight times larger than that of the LW buoy.

Since the buoy-heave plate system was changed significantly, it was important that physical model testing be performed. The physical model testing included free release experiments of the buoy only, free release testing of the buoy and heave plate, as well as regular and random wave loading, along with tow testing. These results were used to evaluate the system design directly, as well as provide empirical coefficients required by the numerical model OrcaFlex. OrcaFlex, the commercially available equivalent of Aqua-FE, was used by OPI to model the system for a wide range of possible wave environments.

CHAPTER 9-

2014 PHYSICAL MODEL TESTING: HEAVE PLATE DYNAMICS

9.1 Design and Rational

From the summer 2013 deployment, it was concluded that the snap loads experienced in the vertical stay should be reduced. To minimize snap loads, a series of asymmetrical heave plate designs were generated for which resistance in the upwards direction was greater than for downwards motion. The drag coefficient and added mass of these heave plate designs were tested in both directions. The tests examined the effects of orientation both in a maximum drag orientation (upwards) and minimum drag orientation (downwards). Testing was done by towing scale models of heave plates and measuring the tow force using a submersible load cell. Tows were done at constant velocity to find drag coefficient and while accelerating to determine added mass. After the tests, the best design was selected for the full scale deployment during the summer of 2014.

Four heave plate designs were investigated – three were variations of the shape shown in Figure 34, while one was circular with an upward curving lip. These designs were asymmetrical for the main purpose of lessening slack events while also increasing the oscillating load experienced on the vertical stay. A list of heave plate dimensions are provided in Table 4.

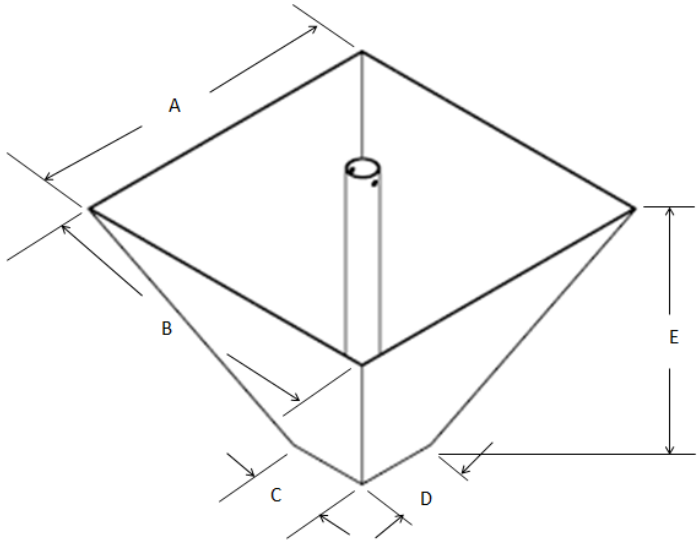

Figure 34. The tapered, rectangular cross-section concept used for three of the heave plate designs. Dimensions are provided in Table 4.

Table 4. Full scale dimensions for heave plate designs proposed for testing. For the tapered, rectangular cross-section concept shown in Figure 34, the design name refers to full scale dimensions in feet.

Heave Plate Design Name	Dimension A (m)	Dimension B (m)	Dimension C (m)	Dimension D (m)	Dimension E (m)
8x8x6	2.44	2.44	0.61	0.61	1.83
10x10x7	3.05	3.05	0.61	0.61	2.13
10x10x4	3.05	3.05	0.61	0.61	1.22
Circular	3.439 diameter				0.203 edge

The drag coefficient and added mass of the heave plates were investigated because they play a significant role in the vertical dynamics of the buoy-heave plate system, and the best of the candidate designs needed to be selected. The drag coefficient, C_d, is a dimensionless quantity, defined by

$$C_d = \frac{F}{0.5\rho A v^2}, \tag{16}$$

in which F is the drag force, ρ is the water density, A is a reference area (usually the projected area) and *v* is the incident velocity. The drag coefficient quantifies the resistance of an object in a fluid environment, or in this case, the ocean water (see, for example, Berteaux, 1991). For the heave plate, the drag when the buoy is moving upward is intended to be larger and, therefore, creates more tension in the vertical stay. The exact opposite case of lower drag when the buoy is moving downward is also desired. The lower drag allows the heave plate to drop faster in the water column in an effort to reduce or eliminate slack events in the vertical stay.

The effect of added mass on the system is also significant to help minimize the vertical motion of the buoy and increase vertical stay tension. Added mass is the inertia added to the system due to the volume of fluid deflected by an object accelerating or decelerating through it (see, for example, Berteux, 1991). Added mass can incorporated into the equation of motion according to

$$F = (m + m_{added})a, \tag{17}$$

where *F* is the force, *m* is the mass of the object, *a* is the acceleration and m_{added} is the added mass of the system. Virtual mass is the combined actual mass plus added mass. Once again, the goal for the heave plate was to have a high added mass value when the buoy moves upward and have a low added mass value while the buoy is moving downward.

9.2 Heave Plate Model Construction

To construct the heave plate models, the full scale dimensions had to be Froude scaled to model scale by a ratio of 1:10. Upon doing this calculation, the side thickness of the heave plate became a concern due the scaled wall thickness (0.04 inches). It is important to simulate the edge thickness in this application because the flow separation around the edges may determine the most suitable heave plate design. Material substitutions were considered to build an underweight model. Ballast would then be added to achieve the design mass which was subject to change at the time of model fabrication. One alternative was to create the models out of fiberglass. Creating the models out of fiberglass would make fabricating the models' intricate design an easier process, however, the desired thickness would not resist bending enough to work properly. The other choice was to use 0.04 inch aluminum sheet metal. Since the aluminum sheet metal was stiffer, it was chosen as the primary material. To create the circular model, fiberglass was used due to the simplicity of fabricating it out of fiberglass as opposed to sheet metal.

Multiple quotes were sent out to fabricate the models and, of the returned quotes, the price per model was approximately $300 with a week lead time. Due to the cost, it was decided to produce the heave plates using the available UNH machine shop. In order to do this, 3 sheets of 24 inch by 24 inch 0.04 inch thick aluminum, along with a cartridge of Loctite H3151 epoxy for adhering the pieces together, was ordered through McMaster Carr. Once the materials arrived, an outline was sketched on the metal, and using a shear, the pieces were cut out. Once all the pieces were sheared to size, the pieces were checked to ensure the proper dimensions were achieved. To prepare the pieces to be epoxied

together, the edges were all sanded to create a rough surface for the epoxy to adhere to. The final step in the preparation was to clean surfaces with acetone which removed all the grease and dirt that may have been left on the surface. The pieces were then assembled using a fixture tacking them in place using short beads of hot gluing. Then, in between the hot glue beads, Loctite H3151 was applied ensuring that the gaps were filled. After the full cure time of 24 hours, the hot glue was removed, and more Loctite H3151 was applied in the gaps. Once the epoxy was fully cured for the whole model, additional sheet lead ballast weight was added to achieve the desired model mass of 1 kg. The sheet lead was epoxied flat to the inside of the aluminum walls near the apex. The constructed models without sheet lead ballast can be seen in Figure 35.

Figure 35: Model heave plates to be used in tank testing. The 10x10x4 model is shown in top left; the 10x10x7 is shown in top right; the 8x8x6 is shown in bottom left, and the circular model is shown in bottom right.

9.3 Testing Fixture Configuration

To perform the drag coefficient and added mass measurements, the physical models were tested utilizing the Jere Chase Ocean Engineering Lab's tow carriage. While others have tested asymmetrical shapes while oscillating vertically, in these experiments, the tow carriage was used to generate horizontal velocities and accelerations which were uniform over a short time interval. To properly use the tow carriage, a fixture had to be created which would allow the heave plate to be tested in both orientations, allow the heave plate to move while minimizing extra drag load to the load cell, and be quick to install and remove.

To keep the fixtures from interfering with the flow during testing, a symmetrical NACA airfoil was mounted in the front of the carriage (see Figure 36). This airfoil was designed to be as streamlined as possible as not to interfere with the flow by the heave plate. On the bottom of the airfoil, a Sentran ZB4 500 lb capacity submersible load cell was used. To capture the loads and simulate the vertical stay, a steel cable was run from the load cell to a bridle which connected to the four corners of a frame (see Figure 36). This 14 inch by 14 inch frame was constructed out of aluminum and was designed to mount the heave plates so the tow force would be measured by the load cell while being held in position relative to the carriage motion shown in Figure 36. Additionally, two vertical 80-20 extruded aluminum struts were attached to the carriage on either side of the mounting frame (see Figure 37). Horizontal steel cables from each strut to the mounting frame provided lateral stability. The aluminum struts were mounted on the outer most points of the carriage to not interfere with the water flow. Additionally, load cell force

measurements were done with no heave plate in place so fixture resistance could be subtracted leaving heave plate only fluid forcing.

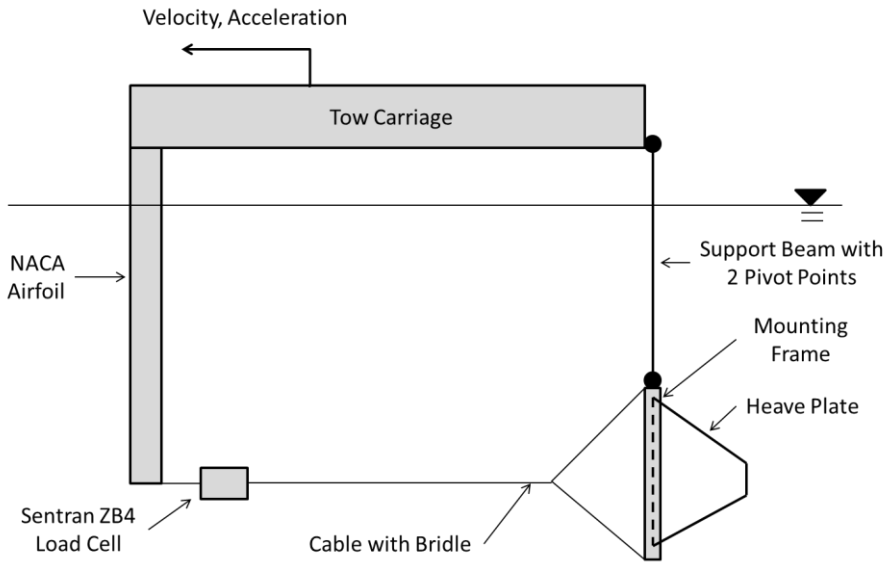

Figure 36: Side view of testing fixture. The tow carriage is shown with the fixture mounted to the front and rear. The heave plate is attached to a mounting frame which is connected to the Sentran ZB4 load cell.

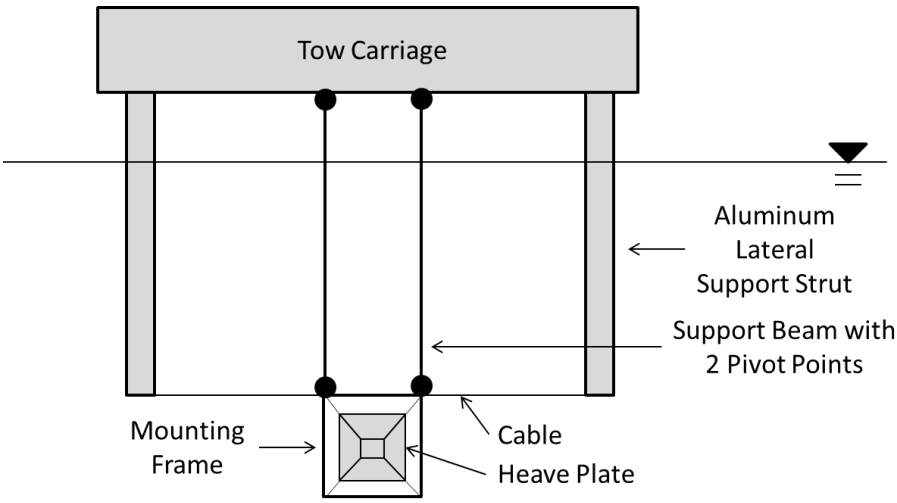

Figure 37: Rear view of testing fixture. The lateral support struts are shown along with the steel cable that provides lateral support to the heave plate.

9.4 Drag Coefficient: SolidWorks Flow Simulation

To obtain an initial estimate of the drag coefficients that would be expected, SolidWorks Flow Simulation analysis was performed for the model scale test conditions. To help with the configuration of the model, the Flow Simulation Wizard was used. Since the flow was an external flow in water, an external flow in a fluid with density of 1000 kg/m^3 was applied. A laminar flow scenario was input for an initial condition along with no wall roughness and adiabatic wall conditions. Having these parameters enabled a reduced calculation time. As shown in Figure 38, incident fluid flow was to be in the positive or negative y direction, corresponding to minimum or maximum drag, respectively. To ensure the edge of the heave plate was simulated with accuracy, a local initial mesh was created. Once this mesh was created, the final meshing was optimized in a 3D computational domain to capture the full effects of fluid motion on the heave plate.

To find the net drag force, "surface goals" were set up on the upstream and downstream surfaces of the heave plate. From these surface goals (SG), the net contribution to drag force was calculated and summed. Using the resultant force, the drag coefficient of the heave plate was calculated. According to

$$Drag\ Coefficient = (SGForce\ Y1 + SGForceY\ 2)/(0.5 * \rho_{water} * velocity^2 * area) \quad (18)$$

where SG Normal Force 1 is the normal force of outer surface and SG Normal Force 2 is the inner surface of the heave plate. When adding the equation goal, it was important to ensure that the units are set to unitless because the coefficient of drag is a unitless coefficient.

The models were run for velocities ranging in 0.25 m/s increments from 0.5 m/s to 2 m/s using initial mesh settings of level 4. This mesh level is a predefined parameter on a scale of 1 being worst meshing and 8 being the best and longest calculation mesh level. Once the minimum drag orientation was simulated, the same velocities were run using the maximum drag orientation to obtain the drag coefficient in the opposite direction. This setup was kept consistent throughout the simulations for the four models.

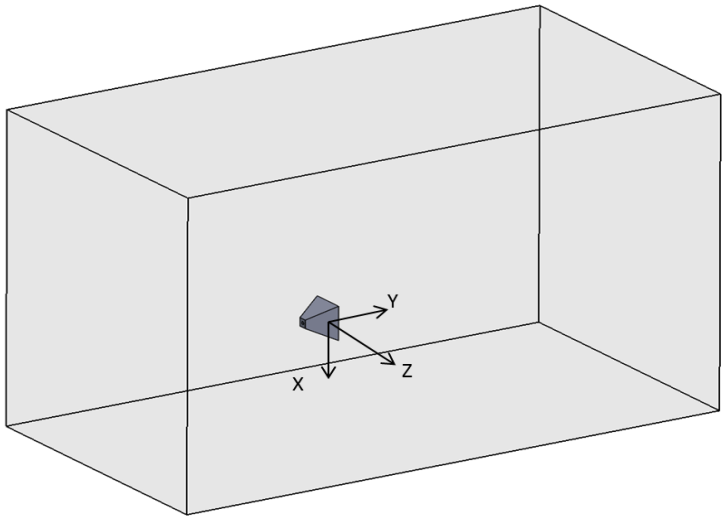

Figure 38: Image of modeling configuration using SolidWorks Flow Simulation.

Figures 39 and Figure 40 provide drag coefficient predictions for the minimum drag orientation and maximum drag orientation, respectively. As shown, the results for both drag orientations were constant despite the increase in velocity. A predicted drag coefficient of approximately 1.3 was obtained for all shapes at the maximum drag orientation, while at the minimum drag orientation, approximate values of 0.6 and 0.8 were generated. This initial study data set was compared with the physical model testing to provide an independent evaluation of tank measurements.

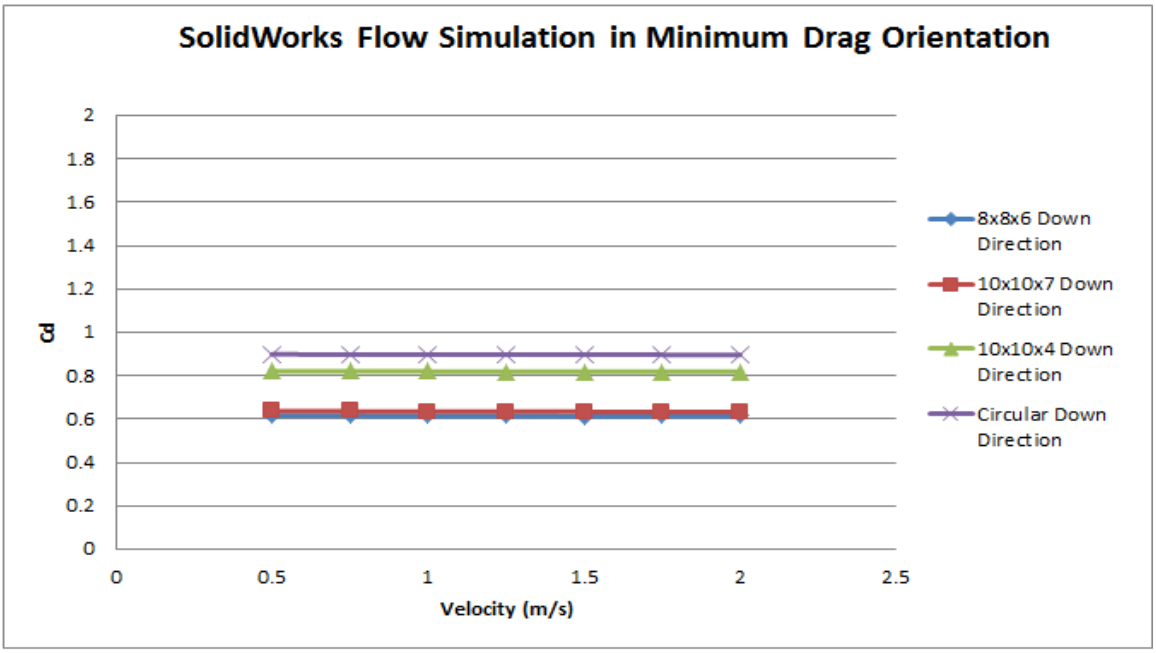

Figure 39: SolidWorks Flow Simulation results for the minimum drag orientation of the heave plates. Velocities are in model scale.

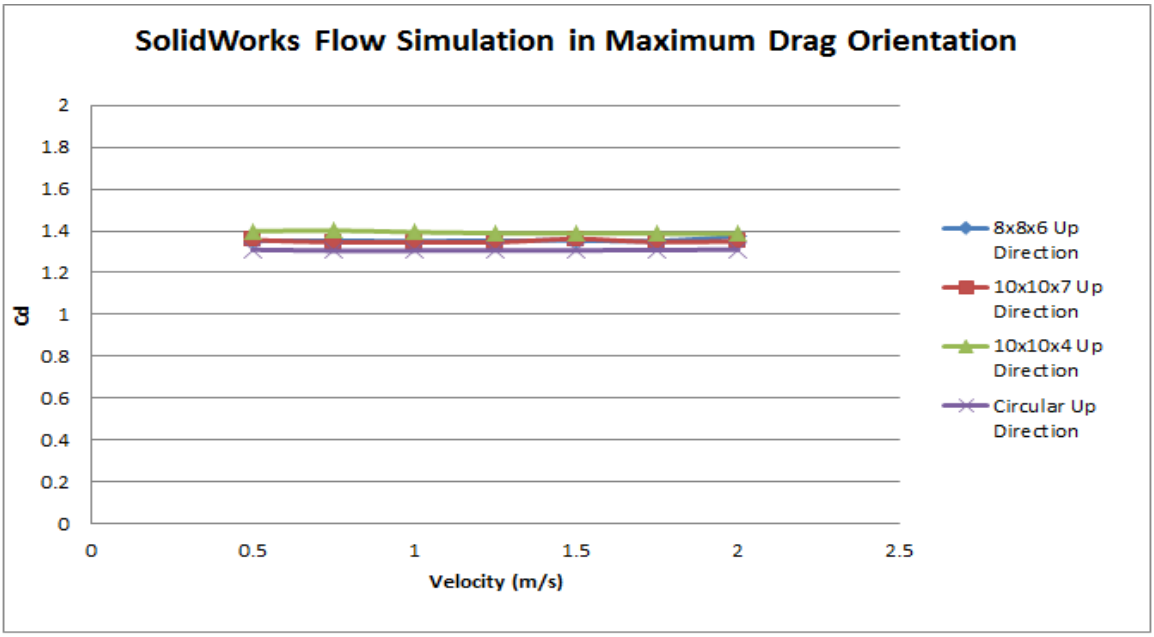

Figure 40: SolidWorks Flow Simulation results for the maximum drag orientation of the heave plates. Velocities are in model scale.

9.5 Drag Coefficient: Physical Model Testing

The drag coefficient testing performed in the tank was done using procedures similar to the SolidWorks testing. Tank testing velocities, however, were modified from the SolidWorks simulations due to flow instability induced, lateral oscillations of the model heave plate at higher velocities. For the tank testing, the velocities were 0.3 m/s to 0.7 m/s in 0.1 m/s increments for both the minimum drag and maximum drag orientations.

To ensure the Froude scaled physical tank test models will experience similar flow characteristics as the full scale heave plate, Reynolds number comparisons were performed. The Reynolds number, according to

$$Re = \frac{\rho \mathrm{v} L}{\mu} \ , \tag{19}$$

is the ratio of inertial forces to viscous forces where ρ is the fluid density, v is the velocity, L is the characteristic linear dimension and μ is the dynamic viscosity. In depth discussion of the Reynolds number is presented by Fox, Pritchard and McDonald (2009).

In order to calculate the expected velocity for the full scale heave plate, Airy wave theory was used. Assuming the buoy and heave plate were rigidly connected and that the buoy motion was not damped during wave loading, the vertical velocity of the heave plate was calculated. The resulting velocity was 0.39 m/s in a fair weather wave event with a period of 6 s and wave height of 0.75 m. Using this velocity, the Reynolds number for the full scale system was 909541. The Reynolds number for the Froude scaled physical tank test model resulted in 146107 using a velocity of 0.6 m/s. The Reynolds numbers for both the tank test Froude scaled models and for the full scale heave plate fall in the turbulent

regime. This allows for applying results from the Froude scaled physical tank test models to the full scale heave plate.

Since a frame was used to mount the heave plate, the frame only drag was measured as well at each velocity. Doing this allowed the frame drag to be subtracted from the total measured drag giving the heave plate drag force. The general drag force definition, Equation (16), modified for this application, is

$$C_{d_{physical\,model}} = \frac{2 * (F_{total} - F_{frame})}{v^2 * \rho_{water} * A_{reference}}. \quad (20)$$

In this expression F_{total} is the measured force of the heave plate and frame; F_{frame} is the force from the frame only experiments for the same velocity of the F_{total} trial; v is velocity; ρ_{water} is the density of water, and $A_{reference}$ is the reference area of the heave plate.

Three runs were performed for each velocity so that the average Cd could be acquired. Taking the average Cd helped reduce error from the experiment. The average standard deviations, normalized by average value, was 2.26%. The final results are shown in Figure 41 for the minimum drag orientation and Figure 42 for the maximum drag orientation along. Overall results are provided in Table 5.

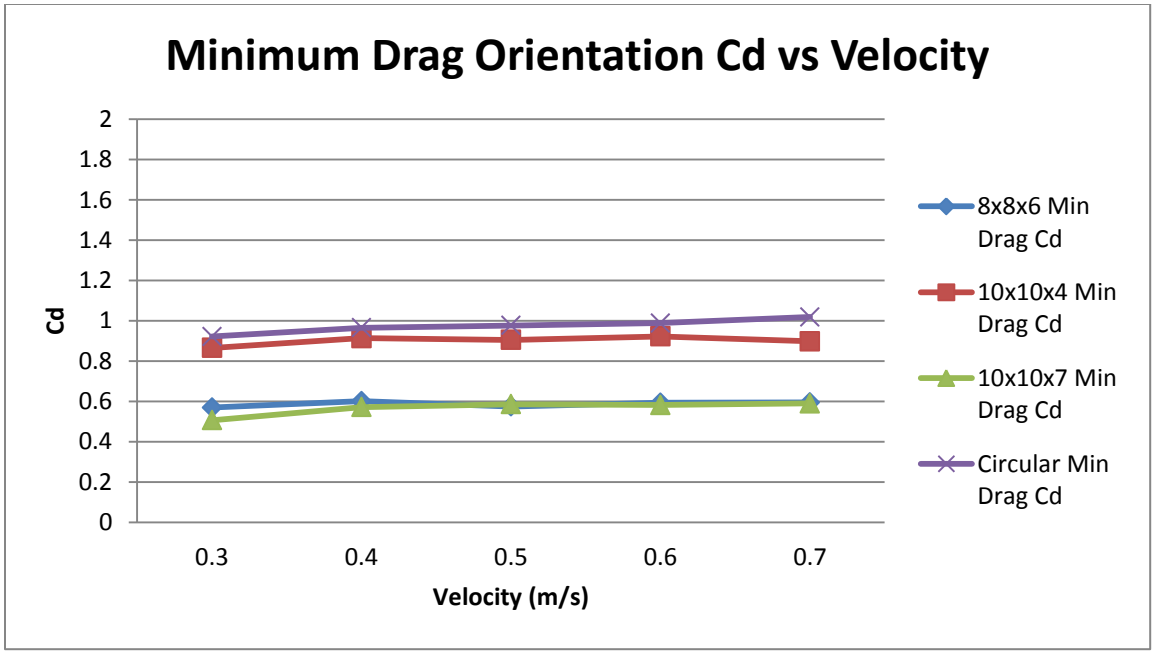

Figure 41: Tank testing results of the drag coefficient in the minimum drag orientation. Velocities are model scale.

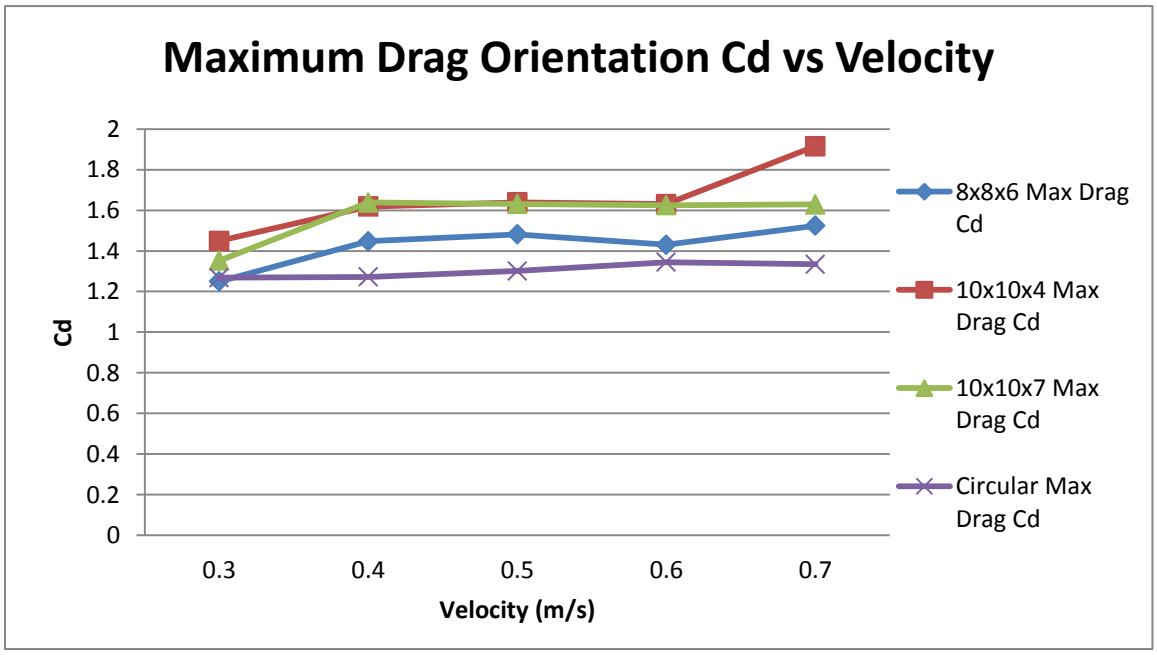

Figure 42: Tank testing results of the drag coefficient in the maximum drag orientation. Velocities are model scale.

Table 5: Table of Cd Results from Tank Testing and SolidWorks.

Model	Orientation	Average Cd Tank Testing	Average Cd SolidWorks Flow Simulation	Percent Difference (%)
8x8x6	Maximum Drag	1.47	1.35	8.51
10x10x4	Maximum Drag	1.65	1.39	17.11
10x10x7	Maximum Drag	1.63	1.35	18.79
Circular	Maximum Drag	1.30	1.30	0
8x8x6	Minimum Drag	0.587	0.614	4.50
10x10x4	Minimum Drag	0.901	0.819	9.53
10x10x7	Minimum Drag	0.583	0.634	8.38
Circular	Minimum Drag	0.975	0.897	8.33

The SolidWorks Flow Simulation and physical model testing results were fairly close indicating no major errors in test procedures. This margin of error is expected due to the refinement of meshing used in the SolidWorks model, while during testing the model was not perfectly stable requiring time averaging to reduce effects of slight oscillations in the loads. In comparing heave plate designs, it should be noted that the 8x8x6 and 10x10x7 designs were among the highest in maximum drag and had the lowest minimum drag. From the drag standpoint, these are the most desirable asymmetric characteristics.

9.6 Added Mass Testing

Since the buoy and heave plate system was intended to create the most tension oscillation in the vertical stay, the heave plate design had to be optimized to achieve the most added mass in the upward direction. The added mass is defined by Equation (17) and represents the effects of inertia of the surrounding fluid. For testing the heave plate, it was expected that the added mass would remain constant with varying accelerations. To verify

this, physical model testing was performed for two different acceleration values, 0.25 $\mathrm{m/s^2}$ and 0.50 $\mathrm{m/s^2}$.

To perform the physical model testing, the same fixture used for the drag coefficient was used because the tow carriage acceleration and velocity could be controlled. Since the added mass can only be calculated during acceleration, a carriage control code was specifically created to accelerate the tow carriage at a desired acceleration to a desired maximum velocity. To ensure that the system was stable prior to the acceleration phase, the tow carriage was first brought to a steady velocity of 0.25 m/s. From this initial velocity, the tow carriage was then accelerated to the final velocity and then decelerated to zero. Setting the desired maximum velocity reached was essential because the acceleration portion of the trial needed to be easily distinguishable during data processing. Once the speed control code was created, trials were performed to help identify testing parameters. From these trials it was determined that the system would always start at an initial velocity of 0.25 m/s and accelerate at either 0.25 $\mathrm{m/s^2}$ or 0.5 $\mathrm{m/s^2}$ to a final velocity of 1.5 m/s.

During the testing, each model was run in both orientations for a minimum of 3 times so that an average could be calculated to help reduce error. Also, added mass tests were performed for the frame only so that frame added mass could be subtracted. Heave plate added mass was calculated according to

$$m_{added_{hp}} = \frac{F_{total} - F_{d_{heave\ plate}} - F_{d_{frame}}}{a} - m_{frame} - m_{heave\ plate} - m_{added_{frame}}, \qquad (21)$$

where $m_{added_{hp}}$ is the added mass of the heave plate; F_{total} is the total force during acceleration; $F_{d_{heave\ plate}}$ is the drag force of the heave plate; $F_{d_{frame}}$ is the drag force of

the frame; m_{frame} is the mass of the frame; $m_{heave\ plate}$ is the mass of the heave plate; $m_{added_{frame}}$ is the added mass of the frame only, and a is the acceleration of the carriage. To subtract the added mass of the frame during the acceleration, frame drag and heave plate drag had to be calculated for each total force measurement. Figures 43 and 44 show measurement time series of the added mass testing at an acceleration of 0.5 $\mathrm{m/s^2}$ for the 8x8x6 heave plate in both the maximum and minimum drag orientation respectively. Note that the frame only time series had to be shifted to match the start of the acceleration phase.

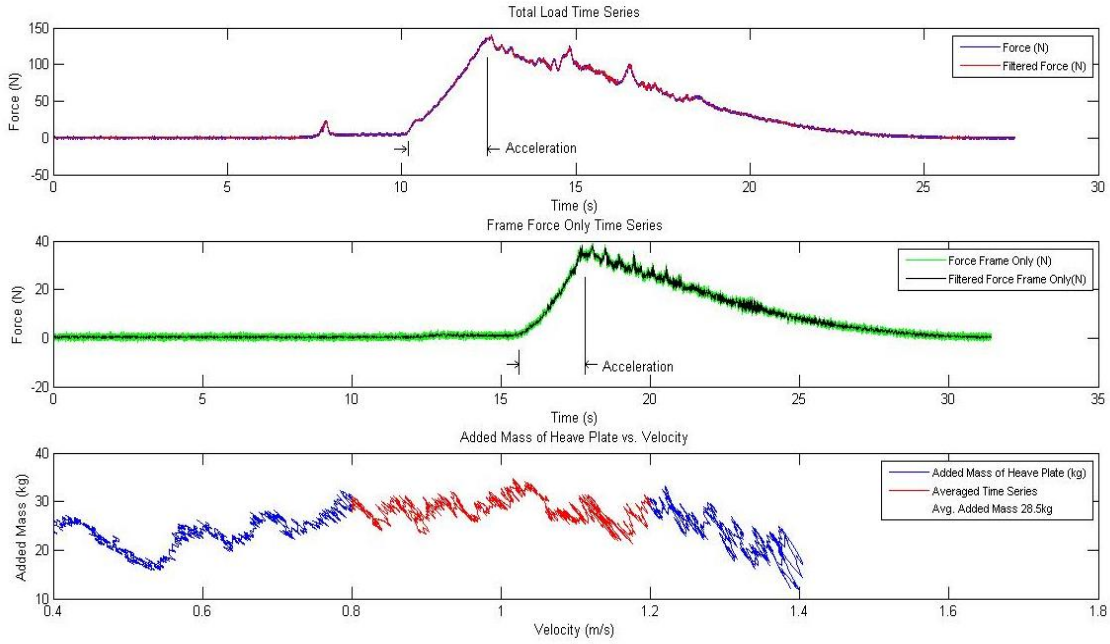

Figure 43: 8x8x6 maximum drag orientation added mass results for acceleration at 0.5 $\mathrm{m/s^2}$.

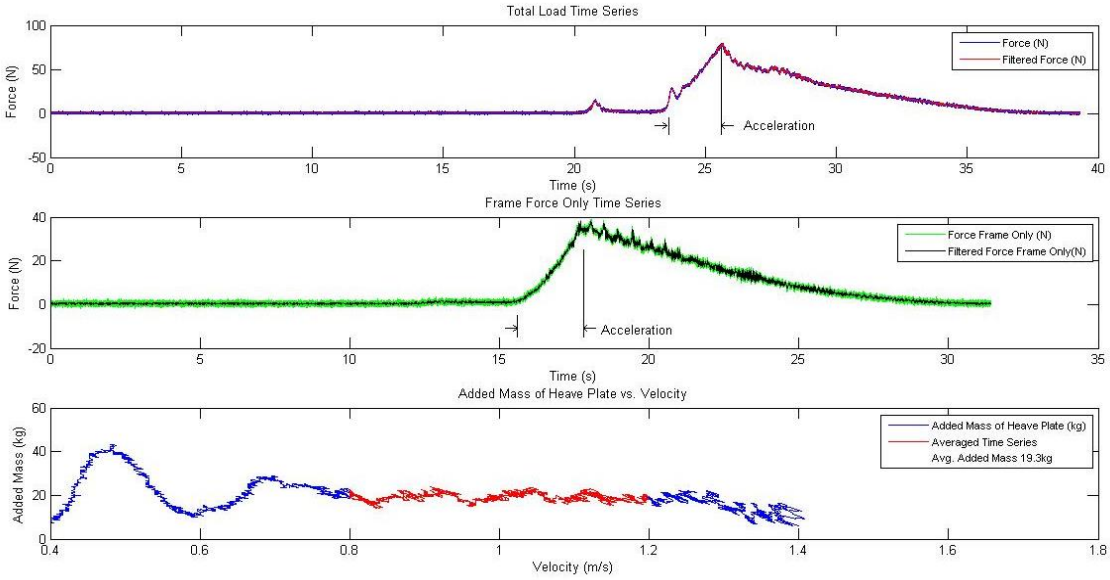

Figure 44: 8x8x6 minimum drag orientation added mass results for acceleration at 0.5 m/s^2.

The 8x8x6 design had the smallest added mass during descent (minimum drag orientation) of all the designs and was, therefore, the least likely to cause line slackness followed by snap. Since its asymmetrical drag characteristics were also good, this design was selected for further development and buoy testing. The final results of this testing are summarized in Table 6.

Table 6: Results of added mass testing.

Model	Orientation	Added Mass (kg) 0.5m/s/s	Added Mass (kg) 0.25m/s/s	Percent Difference (%)
10x10x4	Maximum Drag	42.145	40.349	4.35
10x10x7	Maximum Drag	47.4378	47.0067	0.913
8x8x6	Maximum Drag	28.807	31.5523	9.095
Circular	Maximum Drag	60.759	67.4	10.37
10x10x4	Minimum Drag	37.11	38.99	4.94
10x10x7	Minimum Drag	37.4	43.14	14.25
8x8x6	Minimum Drag	19.5	23.4	18.13
Circular	Minimum Drag	41.82	46.99	11.65

CHAPTER 10-

2014 PHYSICAL MODEL TESTING: BUOY DYNAMICS

10.1 Overview

Once the full scale buoy design was finalized by OPI, a 1:10 scale model buoy (see Figure 45) was constructed by OPI and sent to UNH for tank testing in the Jere A. Chase Ocean Engineering Laboratory's wave tank. This model had a diameter of 36.5 cm, height of 40 cm, an anticipated draft of 27 cm, and a mass of 17.85 kg. Buoy and heave plate experiments were done using the 8x8x6 heave plate design model.

Figure 45: Froude scaled model buoy of full scale design constructed by Oscilla Power and used for physical model testing.

The tank testing included pitch and heave free release tests of the buoy and heave free release tests of the buoy and heave plate. The buoy and heave plate combination was also tested under regular and random waves with a 25 lb load cell mounted in line with the vertical stay to record stay tension. The load cell was used to determine if there were any snap or slack loads so that further work could be done to reduce or eliminate these. Buoy motion was measured optically and wave surface elevation was measured both optically and by use of a wave staff.

10.2 Free Release Tests

Free release tests, done without waves, consisted of raising the buoy slightly (heave testing) or rotating the buoy slightly (pitch testing) and releasing from rest. The resulting decaying oscillation was recorded. The observed motions were fitted to a damped harmonic oscillator model to infer added mass or mass moment of inertia and damping ratio. These data, as well as heave and pitch time series, were also provided to OPI to support their separate modeling effort.

To measure pitch and heave of the buoy and of the buoy and heave plate system, a program called OPIE, or optical positioning instrumentation and evaluation system, was implemented. OPIE, as described by Michelin and Stott (1996) is an optical system that consists of a progressive scan digital video camera that records images at a user set frame rate. To process the video recorded by the camera, a dedicated computer with a frame grabber and processing software was implemented using Matlab. Small black target dots attached to the models were tracked using the OPIE software. To calibrate the video recordings, a known diameter circle was measured in pixels by OPIE prior to the

experiment. Then OPIE would use this information to convert distances on images in pixels to conventional distance units. By knowing the distance and time, OPIE could then calculate the distances, velocities and accelerations in the vertical and horizontal direction.

For the heave free release testing, the buoy was placed approximately in the middle of the tank in front of the tank's observation window. This distance was chosen to help eliminate wave reflections off the tank walls along with ensuring the buoy would fit within the viewing range of the camera. Also, since the buoy alone did not have the correct mass distribution, an additional 1.842 kg mass was added directly to the bottom of the buoy. This added mass corrected the mass distribution allowing it to float upright. The buoy was then lifted approximately 5 cm while ensuring the same cross sectional surface area was maintained in the water, and then it was released. The buoy oscillated in a damped vertical motion, as expected, for approximately 5 seconds. The same procedure was repeated using the buoy and heave plate system. For the testing with the heave plate attached, the additional mass added to the bottom of the buoy was removed because it was no longer required. A typical result can be seen in Figure 46.

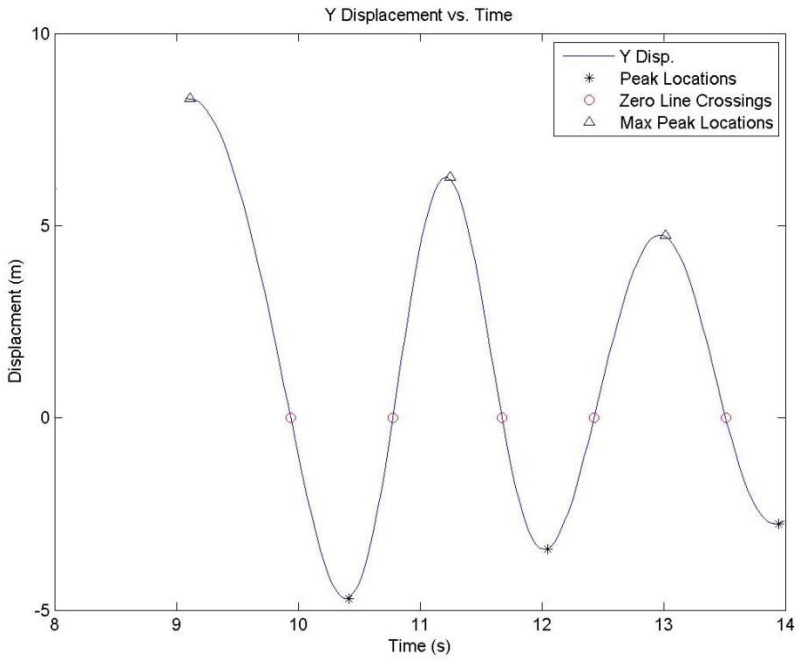

Figure 46: Heave decay test result for buoy and heave plate system.

Pitch decay tests for the buoy-only system were performed similarly to the heave decay tests. For the pitch tests, however, the buoy was rotated about a horizontal axis (perpendicular to the observation window) and released from rest. Figure 47, shows a typical pitch time series for the buoy-only system. The reason for pitch testing the buoy only, and not the buoy and heave plate system, was because the inferred virtual mass moment of inertia and damping ratio could clearly be attributed to the buoy itself.

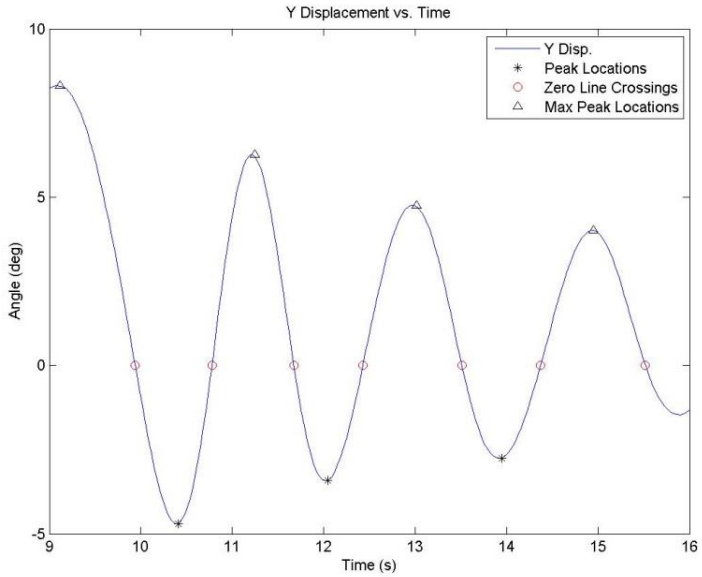

Figure 47: Pitch decay test result for the buoy-only system.

For analyzing the results of both the heave and pitch decay testing, it was assumed motion could be represented by the following linear, second order, damped harmonic oscillator equation,

$$\ddot{x} + 2\zeta\omega_o\dot{x} + {\omega_o}^2 x = 0\ . \tag{22}$$

In this equation, x is the generic dependent variable, either pitch angle or heave displacement; ζ is the damping ratio, and ω_o is the undamped natural frequency. The undamped natural frequency can be expressed for heave and pitch, respectively, by the following equations,

$$(\omega_o)_{heave,pitch} = \sqrt{\frac{\rho g S}{m_v}}, \sqrt{\frac{B * gm}{I_v}}\ . \tag{23}$$

In equation (23), ρ is the density of the fluid; g is the gravitational constant; S is the water-plane area where the testing was performed; m_v is the virtual mass defined as the sum of

actual mass of the buoy and the added mass; B is the equilibrium buoyancy force; gm is the metacentric height, and I_v is the virtual mass moment of inertia. The undamped natural frequency ω_o is related to the damped natural frequency ω_d according to

$$\omega_d = \frac{2\pi}{T_d} = \frac{2\pi}{\omega_o\sqrt{(1-\zeta^2)}}\ , \tag{24}$$

where T_d is the damped natural period. The damped natural period was determined as time between zero crossings in the free release time series. Following the linear model, the damping of the response over one period follows the model of

$$\frac{x(t)}{x(t+T_d)} = \exp(\zeta\omega_o T_d)\ . \tag{25}$$

The ratio of response over one period $\frac{x(t)}{x(t+T_d)}$ was then averaged using a minimum of 3 peaks to ensure accuracy in the final result while also assuring the proper damped response it maintained. Knowing the response ratio and T_d, the damping ratio ζ and undamped natural frequency ω_o could be calculated using equations (24) and (25). Once the undamped natural frequency was known, the virtual mass m_v, or virtual mass moment of inertia I_v, could then be calculated using equation (23). The tests were performed at least three times and then averaged to achieve the final results. Note that application and interpretation of this model for the buoy and heave plate system was approximate. The model assumed symmetric behavior in the up and down directions, while this system was asymmetric.

For the buoy-only free release testing, the full scale heave damped natural period T_d was determined to be 2.95 seconds. This period is slightly less than the typical wave period

range expected at the site (3-10 seconds) so that the buoy was expected to contour the waves for vertical heave a majority of the time. The damping ratio was also determined to be 0.065 indicating that the heave damping was small. The resulting virtual mass m_v from the testing was 22768 kg resulting in the added mass of the buoy being 4918.5 kg. For the buoy and heave plate system, the full scale damped natural period T_d was determined to be 3.76 seconds. For the pitch decay testing, it was determined that the damped natural period T_d was 5.385 seconds and the damping ratio was 0.0618. This puts the pitch resonance in the middle of the wave energy range and also indicates that the buoy has light pitch damping.

10.3 Wave Testing: Regular Waves

The buoy and heave plate model was slack-moored in the wave tank and forced using regular (single frequency) waves. Buoy motion, wave surface elevation and stay tension were recorded.

A 25 lb capacity submersible Futek load cell was mounted in line with the vertical stay. Buoy motion was tracked using the OPIE system. Using OPIE to track the buoy demonstrated what type of motions the buoy would experience during the full scale deployment. A single slack mooring line positioned the buoy opposite the observation window. To Froude scale line compliance, an elastic element with a spring constant of 24.69 N/m was used. Test results were used by OPI to calibrate and validate their OrcaFlex numerical model. OPI then applied OrcaFlex to both fair weather and storm scenarios at the UNH test site. Standard procession to yield basic seakeeping characterizations was done at UNH.

The initial round of testing consisted of full scale regular wave periods ranging from 2.5 seconds to 8 seconds along with wave heights varying between 0.2 m to 0.5 m. These ranges were typical of wave spectra seen at the test site. This testing range also intentionally placed the buoy/heave plate natural period of approximately 3.8 s between two different wave periods so that the buoy's extreme motion and stay tension amplitude would be bracketed. A summary of the results is provided in Table 7.

Table 7: Regular wave testing results for buoy with 8x8x6 heave plate attached. Values have been Froude scaled to full scale.

Wave Period (s)	Wave Amplitude (m)	Line Pre-Tension(kN)	Line Tension Amplitude (kN)	Heave Amplitude (m)	Pitch Amplitude (deg)
2.5	0.2	38.22	1.796	0.0739	2.0271
3	0.2	38.21	5.78	0.2254	6.9615
3.5	0.2	38.18	6.53	0.2493	4.1056
4	0.3	38.15	13.4	0.6081	8.338
5	0.3	38.14	6.76	0.5089	3.121
6	0.5	38.15	7.11	0.6795	5.5331
7	0.5	38.06	5.08	0.5936	4.0664
8	0.5	38.20	3.06	0.6898	4.2597

Assuming stay tension amplitude is a linear function of wave height, tension amplitude for a 1m high wave was calculated and is plotted as a function of frequency in Figure 48.

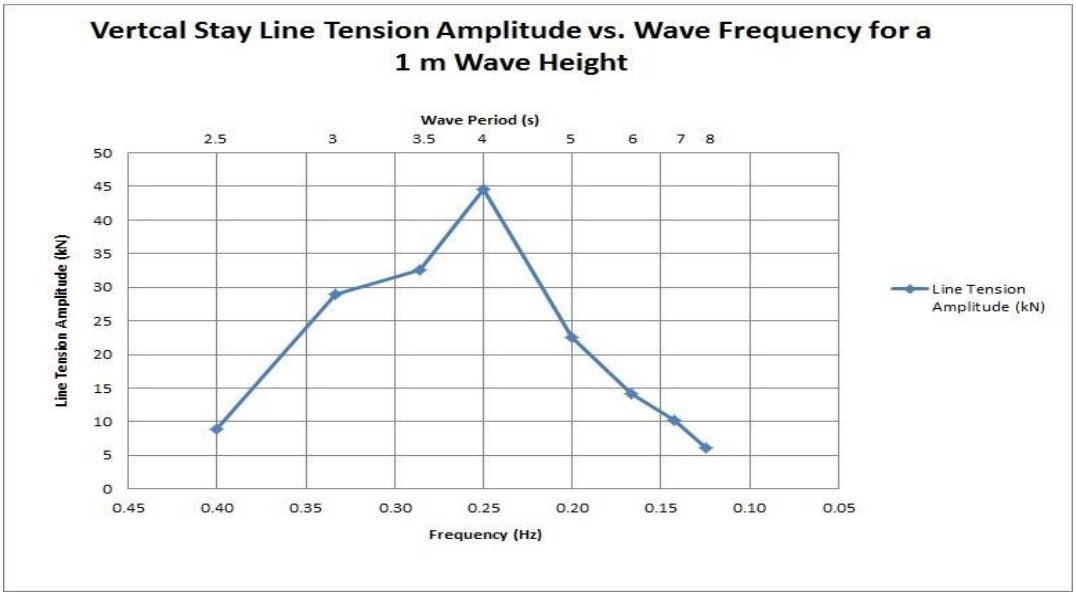

Figure 48: Stay tension amplitude as a function of frequency (cycles/s) for a 1 m wave height.

The heave response amplitude operator (heave amplitude normalized by wave amplitude) was calculated and plotted in Figure 49.

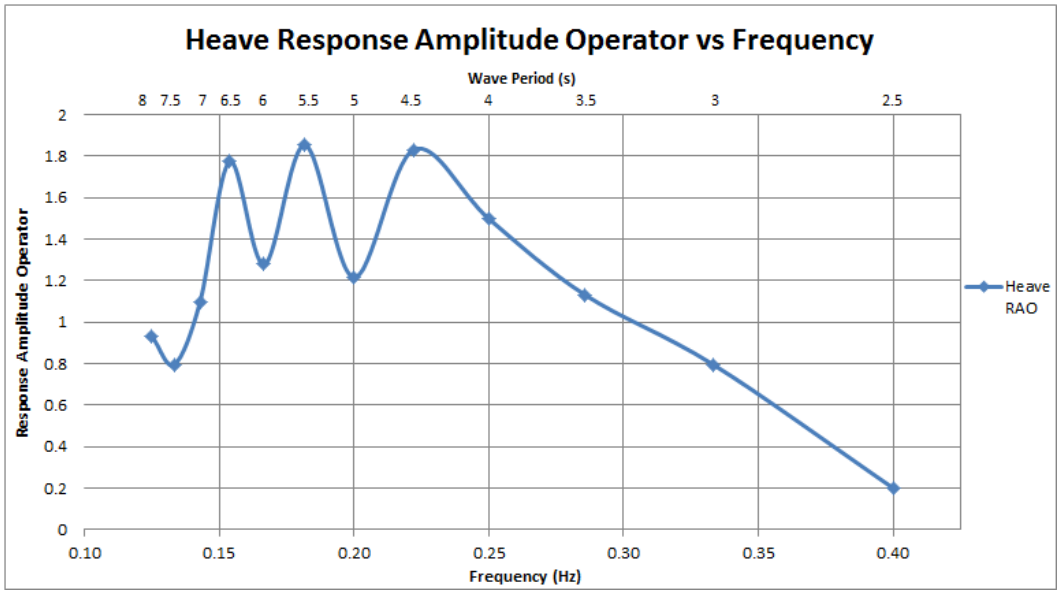

Figure 49: Heave response amplitude operator (heave amplitude normalized by wave amplitude) for the buoy and heave plate system.

As shown in Figure 48, the vertical stay experiences the maximum tension amplitude at 4 second wave periods for a 1 m wave height. After the 4 second wave periods, the tension amplitudes on the vertical stay taper off rapidly. This could be due to the heave response amplitude of the buoy and heave plate system (shown in Figure 49). From Figure 49, the damped natural period can be determined as approximately 5.5 s where the data oscillates showing the instability of the system. This natural period is different from the natural period from free release tests performed in section 10.2. This variation could be due to the over simplification of the calculations performed for the free release testing. During the free release testing, it was assumed that the buoy and heave plate interaction was symmetric in the up and down direction where this is not the case as shown in Figure 49. Further testing would have to be performed to better understand the buoy and heave plate interaction and its effects on damped natural period.

10.4 Wave Testing: Random Waves

As in the regular wave experiments, buoy heave, wave surface elevation and stay tension were measured. Particular attention was focused on the extremes in tension which are imparted directly to the PTOs. Measurement time series were provided to OPI to support their OrcaFlex modeling effort, while basic stay tension statistics were determined at UNH.

Once the regular waves were tested, it was time to see how the system responded to a random sea scenario. To perform this random sea scenario, a Bretschneider spectrum was defined with specified user inputs of significant wave height H_s and peak period on the wave tank software interface. Also, the same testing configuration used in the regular wave

testing was implemented to ensure a correct comparison between the two tests could be made.

Upon performing the first round of testing, it was found that the wavemaker generated waves did not match the control system input parameters. This presented a problem, but due to time restrictions, the testing proceeded. The wave staff data was later used to determine the actual significant wave height and peak period occurring during each test run.

The testing indicated that in most instances slack events on the vertical stay were nonexistent except for one of the larger significant wave heights of 1.785 m full scale with a dominant period of 6 s. Stay tension time series having events is shown in Figure 50 where the top plot shows the load cell tension force at model scale and the bottom plot shows the wave surface elevation at model scale. The slack events can be seen where the loading approaches 0 N on the top plot. This plot shows that the system is not working ideally, however, this sea state will only be experienced during storms which might occur 2-3 times during the summer. This is an area for further development for future full scale deployments in harsher wave environments. For all tests, the typical mean load was approximately 38 kN, which is the weight of the heave plate. Sea state parameters and corresponding extremes in stay tension are provided in Table 8.

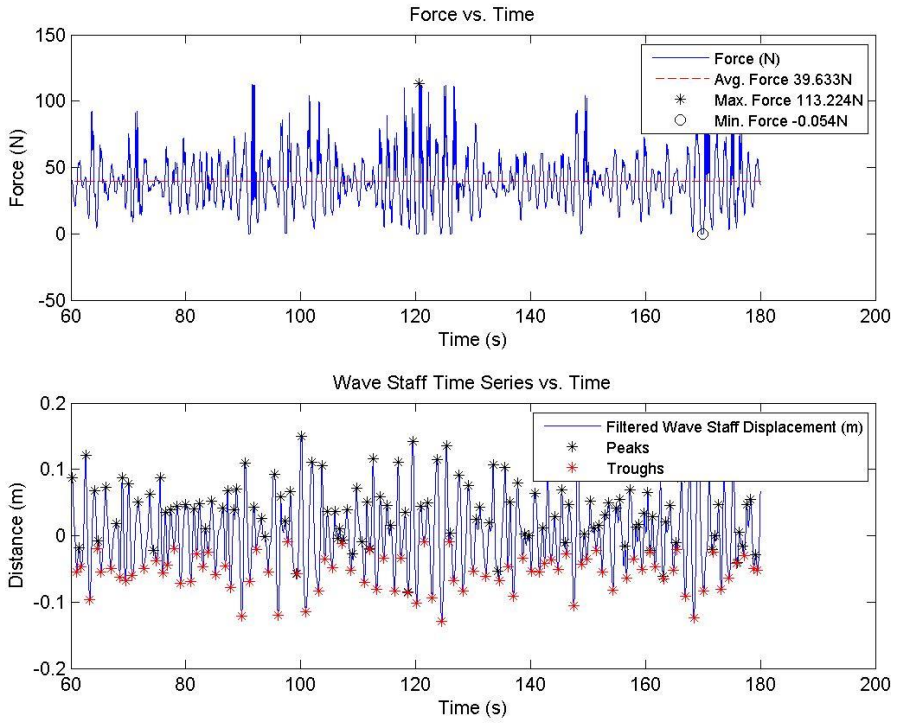

Figure 50: Random wave physical model testing load cell tension force and surface elevation time series for a random sea with a full scale significant wave height of 1.785 m and a dominant period of 6 s.

Table 8: Random wave testing full scale results.

Wave Period (s)	Hs (m)	Max Load (kN)	Min Load (kN)
4	0.275	51.601	23.328
4	0.845	66.217	14.895
4	1.407	111.407	3.441
6	0.382	50.990	25.490
6	0.935	74.725	11.813
6	1.785	113.225	-0.054
8	0.335	45.578	30.575
8	1.143	58.010	20.773
8	3.160	94.088	3.832

The results in Table 8 indicate with increasing significant wave height, the maximum loads increase, however, the minimum loads decrease to the point where slack events occur in the vertical stay. To eliminate this phenomenon, further design development would have to be performed to refine the heave plate and buoy dynamics.

10.5 Tow Testing

The final experiment performed in the tank was to simulate the proposed plan of towing the buoy out to the CORE site. The plan was to attach the heave plate directly to the bottom of the buoy; then upon arriving to the site, the heave plate would be lowered from the bottom of the buoy until the vertical stay was fully extended. In the tank tests, the 1/10 scale 8x8x6 heave plate was mounted directly to the bottom of the buoy in exactly in the configuration it would be deployed for tow out to the site. Measurement of tow force and visual observation of tow dynamic stability were of primary interest. The buoy was towed first at specified velocities in still water conditions. Since deploying in ideal field conditions was unlikely, it was important that experiments were also performed under a wave loading condition. The determined wave loading condition had a full scale wave period of 3.5 s with a wave height of 0.2 m.

A fixture was created so that the buoy could be towed using the tow carriage on the wave tank (see Figure 51). The fixture mounted on the carriage and extended down to a tow point level with the buoy so the buoy tow line was horizontal as in the planned field tow-out configuration. The fixture had two parallel lines, one with a 25 lb capacity load cell mounted in-line, which lead from the fixture base to two mooring line connection points at the bottom of the buoy.

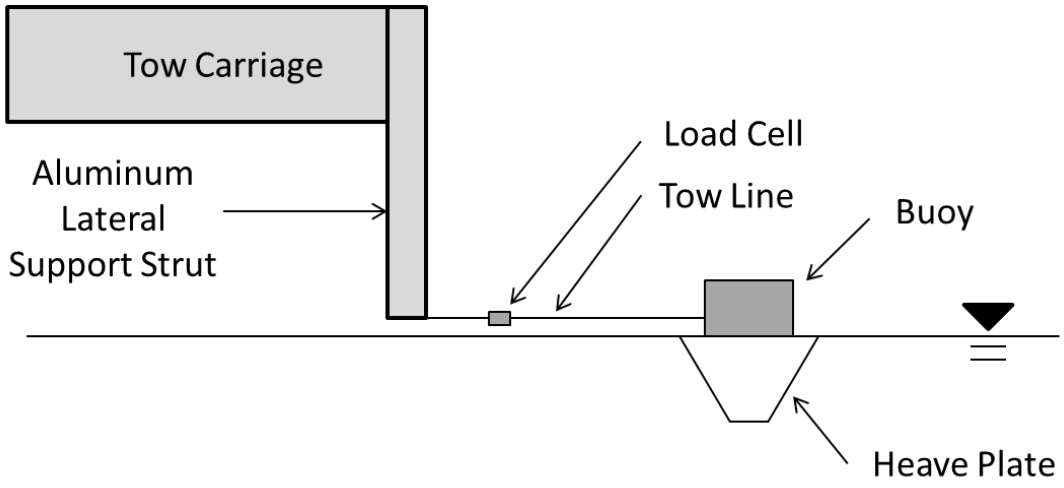

Figure 51: Tow fixture configuration while towing buoy with closely attached heave plate.

Tow tests were conducted at full scale towing velocities of 1,2, and 3 knots. A low acceleration to minimize any jerking effect on the load cell was used to eliminate any sudden loads. During tests, it was observed that the buoy moved slightly side to side. This motion was not restrained by the tow lines and was important to note for towing to the CORE site. The tow force results are shown in Figure 52. A surprising observation was that the mean, no-wave loading condition and the mean wave loading conditions were very similar. However, the maximum loads experienced between the two scenarios are very different as would be expected. These results show that deploying in small waves should be possible using Riverside and Pickering Marine's tug boat.

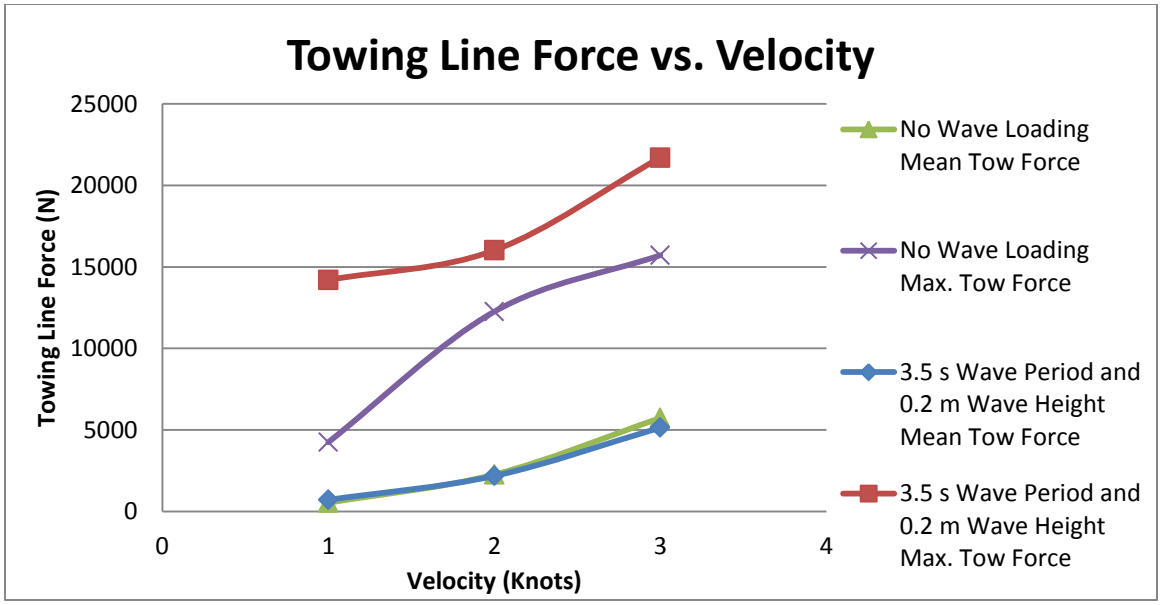

Figure 52: Tow force measurements from tow tank testing with the heave plate mounted directly to the bottom of the buoy.

CHAPTER 11-

SUMMER 2014 DEPLOYMENT

11.1 Buoy and Mooring Deployment

Full scale trials of the 2014 buoy-heave plate combination were conducted at UNH's CORE site south of the Isle of Shoals (see Figure 1). Since the 2014 buoy-heave plate combination size increased significantly compared to the summer 2013 system, larger anchors were needed. Staying with the three-point mooring configuration used in summer 2013(see Figure 7), two 2000 lb Jeyco anchors along with a 2000 lb Samson anchor were used due to their availability. To ensure the anchors would be loaded horizontally, a shot (90 ft) of 1 inch chain was added to each anchor. One leg of the three-leg configuration is shown in Figure 53.

To render the buoy/mooring system safer for all marine traffic, multiple changes were made to the mooring. The first change was adding navigation lights on the crown line buoys to further increase the system's visibility during the night. Another change was using 1.75 inch diameter nylon line which has a density greater than seawater preventing slack line from floating causing a navigation hazard. At the buoy connection end of the nylon line, 30 ft of wire rope was added to further reduce the possibility of the mooring line being cut. The crown lines consisted of 200 ft of 0.5 inch chain with a welded shackle connecting the chain to the crown line float.

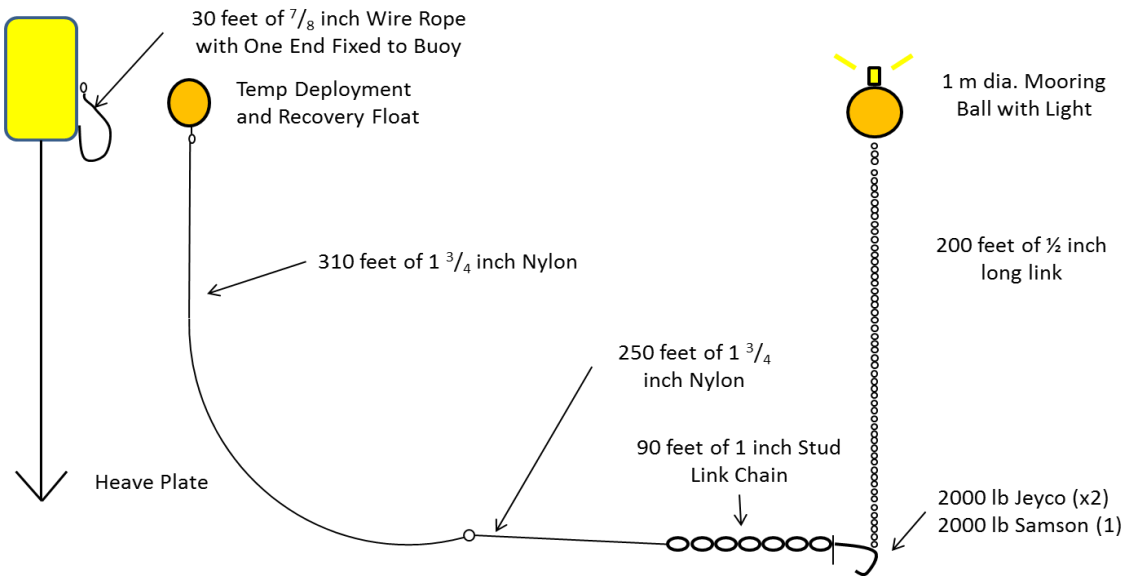

Figure 53: Summer 2014 deployment mooring configuration. In this figure, only one mooring line is shown, however, all three lines were configured the same with slight variation in anchors (either Jeyco or Samson).

The mooring line and anchors were deployed on July 11, 2014 prior to the arrival of the buoy, with the help of Pepperrell Cove Marine using a crane barge. The anchors were lowered into place using the crown line chain and set by pulling on the mooring line. Once the anchors were set, the buoyed ends of all three mooring lines were connected together (see Figure 54). These floats would later be replaced with the full scale buoy.

In addition to the anchors, a wave rider buoy was also deployed. The wave rider buoy recorded surface elevation by moving vertically with the waves while measuring vertical acceleration. The wave rider buoy data would then be compared to the tether loading data to get a direct correlation of wave events to tether loading.

Figure 54: Temporary floats terminating each of the three mooring lines connected together. These floats were removed and replaced with the full scale buoy for testing.

The buoy and heave plate connection and lowering/raising mechanism were tested in a lake in Seattle after receiving them from the fabrication company. After successful verification of operation sequence they were shipped on two separate trucks from Seattle. Upon arrival at the Port Authority in Portsmouth, NH on July 21, 2014, Moore's Crane Rental picked the heave plate off the truck and placed it upright on the pier to eliminate extra lifting steps prior to mating the buoy and heave plate. The same operation happened with the buoy, however, when rotating the buoy upright, the crane operator was instructed by OPI to orient the buoy vertically by pivoting on the bottom of the buoy. This resulted in bending the plating of the cone, lower end of the buoy, along with breaking some welds, as shown in Figure 55. After the plate was bent, gallons of water over a period of time leaked out of the buoy. This meant that during the preliminary testing in the lake, water leaked into the hull of the buoy. Water sump pumps were added to remedy this problem.

Figure 55: Damaged cone section on the bottom of the buoy after being pivoted on.

After the buoy lower end was damaged, it was decided by OPI to go ahead and mate the heave plate to the buoy. The mating process consisted of inserting a vertical pipe on the heave plate (see Figure 56) through a larger diameter pipe running vertically through the entire buoy. Once in place, the heave plate pipe was pinned at the top of the buoy. This step is shown in Figure 57. During the mating process, one of the heave plate connection points on the buoy was overloaded, pulling a bolt out of the threaded section into which it was screwed. This issue occurred because of the bent lower end of the buoy made the entire load of the buoy rest on that one bolt instead of the load being placed evenly on the internal heave plate frame. This problem was easily fixed by drilling out the threaded hole and adding a thread insert. This problem delayed the connection of the heave plate and buoy so the buoy was placed upright on the pier until the crane was available again.

Figure 56: Buoy being mated to the heave plate.

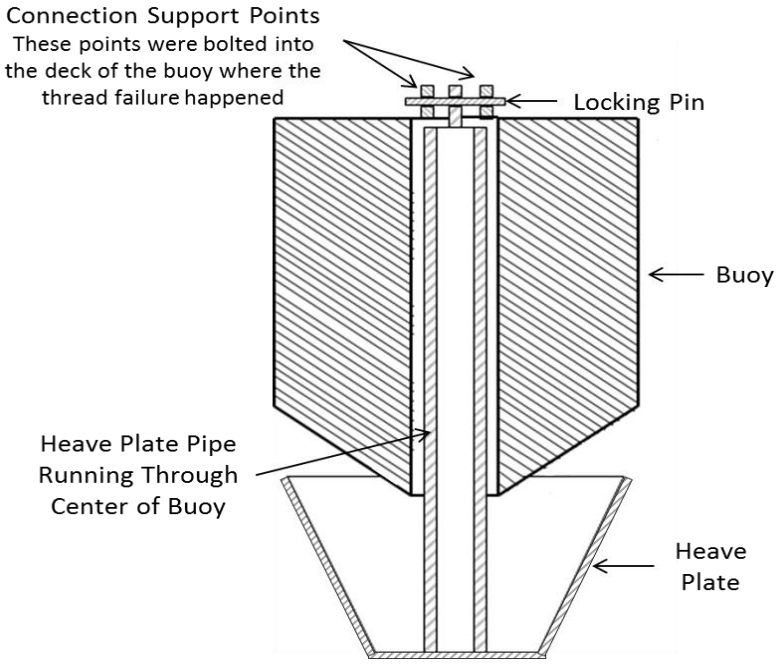

Figure 57: Heave plate connects to top of the buoy via a central pipe that runs through the center of the buoy. This pipe is then fixed to the buoy using a pin.

The next available crane day, July 29, 2014, the buoy was properly mated to the heave plate and both were lowered into the water where Riverside and Pickering Marine had a tug boat waiting. The tug boat then towed the buoy to Riverside and Pickering Marine's site on the Maine side of the Piscataqua River to enable OPI to make some last minute electronic corrections and wait for the next available weather window. On August 5, 2014, Riverside and Pickering Marine towed the buoy to the CORE site where the heave plate was lowered into place using an onboard winch. After the heave plate was lowered, the mooring lines were attached to the buoy. The deployed buoy can be seen in Figure 58.

Figure 58: Summer 2014 buoy deployed at the CORE site south of the Isle of Shoals.

11.2 Recovery

On September 5, 2014, the buoy was recovered and using Riverside and Pickering Marine's tug boat. The heave plate was lifted into place using the winch and secured to the buoy. To remove the buoy from the mooring lines, divers were used prior to recovery to attach temporary lines to the nylon end of the steel cable. This temporary line was then used to lift the steel cable section of the mooring lines out of the water. To do this, the tug boat pushed on the buoy to remove mooring line tension. Then, using the Galen J's pot hauler, the line was pulled up and the shackle mating the steel cable to the nylon was removed. Once the heave plate was secured and the mooring lines disconnected, the tug boat then towed the system to the Riverside and Pickering Marine site to be stored until the crane was available. On September 8, 2014, the buoy was towed to the Port Authority where Moore's Crane Rental and two trucks were waiting to remove the buoy and ship it back to Seattle.

CHAPTER 12-

CONCLUSION

12.1 Heave Plate

As an alternative to a taut moored system under investigation at the beginning of this study, the heave plate system allowed for power generation regardless of tide level while also reducing the anchor sizes required. To further optimize the heave plate concept, Froude scaled physical model testing, Aqua-FE testing, numerical models, and full scale tests were performed at the University of New Hampshire's Jere A. Chase Ocean Engineering Laboratory and at UNH's offshore CORE site south of the Isle of Shoals.

At the start of the UNH-Oscilla Power collaboration, taut, dead weight anchored mooring lines incorporating Oscilla PTOs were designed to provide the required oscillating tension amplitudes specified by Oscilla Power for their PTO to operate effectively. In preparation for the 2013 summer deployment, however, a suspended heave plate system in which the PTO was mounted in-line with the vertical stay was considered. To evaluate the concept, scaled physical models were tested in the wave tank. Experiments were conducted to ensure proper operation along with achieving the proper tether tension amplitudes. From the tank testing, the decision was made to use a vertical stay between the heave plate and buoy in the field experiments. Using a vertical motion dynamic numerical model, the sizing of the heave plate was determined between two different frame sizes. Once the system was specified, an Aqua-FE model was created to specify anchor size. The Aqua-FE model was also used to simulate extreme weather situations and predict vertical

stay tension amplitudes. Using the maximum tension and a factor of safety, the vertical stay line was specified along with the required mating hardware.

After the summer of 2013 system deployment, it was concluded that a larger system, to be designed by Oscilla Power with collaboration from UNH, was to be deployed in the summer of 2014. For this system, the main focus was to try to eliminate slack events experienced by the summer of 2013 system. To do this, four different asymmetrical heave plate designs were tested for their drag coefficient and added mass utilizing Froude scaled physical models. For these tests, a fixture was connected to the tow tank carriage where an in-line load cell connected to the heave plate recorded forces. Once the heave plates were tested for both minimum and maximum drag orientations, the best heave plate design, the 8x8x6 model, was chosen for further testing.

A Froude scaled physical model of the 2014 summer buoy was built and tested in the wave tank. The tests consisted of heave and pitch decay along with wave loading tests for both regular waves and random seas. Utilizing OPIE, the motion of the buoy was tracked and recorded for all testing. During the regular and random wave tests, the 8x8x6 heave plate was attached to the model buoy as well as having a load cell mounted in-line with the vertical stay. The OPIE and load cell data was given to Oscilla Power to be used to verify an Ocraflex model they created.

Upon completion of the summer of 2014 deployment, the heave plate solution was a successful option allowing power generation regardless of tide and storm surge and allowing the use of smaller anchors. The heave plate does induce slack events on the vertical stay under extreme weather events which is an issue that needs to be further

addressed. With the experience gained in both the deployments, the heave plate is a viable option to be used in other wave energy converters that require oscillating tension amplitudes.

12.2 Field Experiments

The first system was deployed in the summer of 2013 at the CORE site using UNH's research vessel the Gulf Challenger. During the deployment, the system experienced a combination of extreme storm events as well as fair weather events. These wave loading conditions provided ideal test parameters to fully test the system and the heave plate concept.

For the deployment in the summer of 2014 system, due to its size, the buoy and heave plate had to be towed out to the CORE site using a local marine contractor, Riverside and Pickering Marine. Also, with a more complex mooring system, another local marine contractor, Pepperrell Cove and Marine, was contracted to deployed and recover the mooring equipment. Due to the location of the CORE site, multiple contractors were available to help with the deployment efforts.

During the deployment, the system experienced some extreme weather events where the design was once again fully tested and verified. Also, unlike the last deployment, a wave rider buoy was deployed at the CORE site so a direct correlation of wave loading to tether tension amplitudes could be made. Along with the wave rider, a Global Positioning System (GPS) monitoring unit was mounted on the Oscilla Power buoy which required a base station with internet access. Since the CORE site is conveniently located near the Isle of Shoals, the base station was set up in the Shoals Marine Lab tower

on Appledore Island. This allowed data from the buoy to be streamed real-time back to Oscilla Power. In general, the UNH CORE site proved to be an inexpensive, accessible and well-supported site for testing and evaluating wave energy devices.

REFERENCES

Baldwin, K., M.R Swift, DeCew, J., and Byrne, J. (2012). *Oscilla Power Wave Energy Device Modeling*. Durham, NH: University of New Hampshire.

Berteaux, H. (1991). *Coastal and Oceanic Buoy Engineering*. Woods Hole, MA: H.O. Berteaux.

Chakrabarti, S. K. (1994) *Offshore Structure Modeling*, World Scientific, Singapore, 470 pp.

Dean, R. G., & Dalrymple, R.A. (1984). *Water Wave Mechanics for Engineers and Scientists* (Vol. 2). Englewood Cliffs, NJ: Prentice-Hall.

Fox, R., Pritchard, P., & McDonald, A. (2009). *Introduction to Fluid Mechanics* (7th ed., p. 280). Hoboken, N.J.: Wiley.

Gosz, M., Kestler, K., Swift, M.R., Celikkol, B., (1996). *Finite Element Modeling of Submerged Aquaculture Net-Pen Systems.* In: Polk, M (Ed), Open Ocean Aquaculture. Proceedings of an International Conference. May 8-10, 1996, Portland, Maine, New Hampshire/Maine Sea Grant College Program, Report UNHMP-CP-SG-96-9, 523-554.

Hart, Philip. (2007). Autonomous PowerBuoys Generate Power for Ocean Applications. *Sea Technology Magazine, 53*, 10-12. Retrieved from http://www.sea-technology.com/index.html.

iMEC Technology (2014, November, 11) Retrieved from http://oscillapower.com/imec-technology/.

Michelin, D. and S. Stott (1996) *Optical Positioning, Instrumentation and Evaluation*, Ocean Projects Course Final Report, Tech 797, Sea Grant, Kingman Farm, University of New Hampshire, Durham, NH, 85 p.

Muller, E., Celikkol, B. and Baldwin, K. (2002) *Open Aquaculture Engineering: Permitting an Offshore Aquaculture Site*, University of New Hampshire, Durham, NH.

Nair, B., Shendure, R. (2013). Harnessing Magnetostriction. *Marine Technology, July 2013*, 11-14.

Rocker, Karl. (1985). *Handbook for Marine Geotechnical Engineering*. Port Hueneme, California: Naval Civil Engineering Laboratory.

Tsukrov, I., Eroshkin, O. Fredriksson, D.W., Swift, M.R., Baldwin, K., and Celikkol, B., (2000). *Open Ocean Aquaculture Engineering: Numerical Modeling* Mar. Tech. Soc. J. 34(1), 29-40.

Tsukrov, I., Eroshkin, O., Fredriksson, D. W., Swift, M.R. and Celikkol, B., (2003) Finite Element Modeling of Net Panels Using Consistent Net Element. Ocean Eng. 30: pp. 251 – 270.

Turmelle, C. A. (2007). Development of a 20-ton Capacity Open Ocean Aquaculture Feed Buoy. Unpublished master's thesis, University of New Hampshire, Durham, NH.

APPENDICES

Appendix I – MathCAD Hydrostatics for Aqua-FE

Full Scale Deployment Buoy for 2014 with Taut Moored Mooring Lines

Constants

$\rho_{seawater} := 1025\frac{kg}{m^3}$ $\gamma_{seawater} := \rho_{seawater}\cdot g = 1.005\times 10^4\cdot\frac{N}{m^3}$

$\gamma_{concrete} := 144\frac{lbf}{ft^3} = 2.262\times 10^4\cdot\frac{N}{m^3}$ $\gamma_{steel} := 490\frac{lbf}{ft^3} = 7.697\times 10^4\cdot\frac{N}{m^3}$

Model Constants

$Number_{verticalelements} := 13$ $Number_{horizontalelements} := 12$

Buoy Sizing given Scaled Buoy Dimensions and Other Critical Information

Mass of the buoy

$m_{.scalebuoy} := 5176kg$ $m_{.scalebuoy} = 5.176\times 10^3\,kg$

Diameter of the buoy

$dia_{scalebuoy} := 1.842m$ $dia_{scalebuoy} = 6.043\,ft$

Calculating the Area of the buoy

$A_{scalebuoy} := \frac{\pi}{4}\cdot dia_{scalebuoy}^{\ 2}$ $A_{scalebuoy} = 2.665m^2$

Calculating the adjusted height from the required buoyancy

$B_{scalebuoy} := 1.22910^4 kg$

$H_{scalebuoy} := \frac{B_{scalebuoy}}{\left(\frac{\pi}{4}\cdot dia_{scalebuoy}^{\ 2}\right)\cdot\rho_{seawater}}$ $H_{scalebuoy} = 4.499m$

$H_{scalebuoy} = 14.762\,ft$

The buoyancy of the buoy if we drew it to exact stated dimensions

$F_{check} := B_{scalebuoy} - m_{.scalebuoy} = 7.114 \times 10^{3}\,kg$

$F_{prelim} := F_{check} \cdot g = 6.976 \times 10^{4}\,N$

Aqua-FE drawing height of the buoy

$H_{adjusted\_scalebuoy} := 4m$

This is the value that the model height is drawn at which needs to be adjusted for the real results to work properly

Tether Properties (1" Unitrex XS Mas Wear):

Diameter of the Tether

$D_{tether} := 1.15in$ $\qquad D_{tether} = 0.029m$

Maximum force the tether line can encounter

$F_{tether\_max} := 114kN$

Amount of Allowable stretch in the tether line

$Approx_{elongation\%} := .5\%$

$L_{tether\_temp} := 54.514m$ This information is based off the chart on the rope information sheet. L tether temp is calculated down below

$Stretch := L_{tether\_temp} \cdot Approx_{elongation\%} = 0.273m$

Calculating the area of a tether line

$$A_{tether} := \frac{\pi \cdot D_{tether}^{2}}{4} = 0.00067m^{2}$$

Calculating the maximum stress encountered by a tether

$$\sigma_{tether} := \frac{F_{tether\_max}}{A_{tether}} = 1.701 \times 10^{8}\,Pa$$

Calculating the maximum strain encountered by a tether

$$\varepsilon_{tether} := \frac{Stretch}{L_{tether\_temp}} = 5 \times 10^{-3}$$

Calculating the Young's Modulus of the tether line

$$E_{tether} := \frac{\sigma_{tether}}{\varepsilon_{tether}} = 3.402 \times 10^{10} \cdot Pa$$

Mass of tether per 100 m.

$$Mass_{tether\_per\_100\_m} := 63.1kg$$

Calculating the Volume of the tether per 100 m of line

$$Volume_{tether\_per\_100\_m} := A_{tether} \cdot 100m = 0.067m^3$$

Calculating the density of the tether along with the specific gravity of the tether

$$\rho_{tether} := \frac{Mass_{tether\_per\_100\_m}}{Volume_{tether\_per\_100\_m}} = 941.621\frac{kg}{m^3}$$

$$\gamma_{tether} := \rho_{tether} \cdot g = 9234.152\frac{N}{m^3}$$

Now accounting for an additional spring element in the tether to reduce snap load

New Spring Constant Tether Element

Goal: Generate and element equal in length to that of a previous model's tether element that will stretch one inch under the prescribed 19kN force.

$X\_One := -1.062504m$ $Y\_One := 48.8m$ $Z\_One := 0m$

$X\_Two := -1.308085m$ $Y\_Two := 48.082353m$ $Z\_Two := 0m$

$Xx := X\_Two - X\_One = -0.246m$

$Yy := Y\_Two - Y\_One = -0.718m$

$Zz := Z\_Two - Z\_One = 0$

$A_{tether\_temp} := 0.002027m^2$

$$L_{tether\_element} := \sqrt{Xx^2 + Yy^2 + Zz^2} = 0.759m$$

$$\sigma_{tether\_new} := \frac{19kN}{A_{tether\_temp}} = 9.373 \times 10^6 Pa$$

$$\varepsilon_{tether\_new} := \frac{1in}{L_{tether\_element}} = 0.033$$

$$E_{tether\_new} := \frac{\sigma_{tether\_new}}{\varepsilon_{tether\_new}} = 2.799 \times 10^{8}\,Pa$$

For Comparison,

$$E_{tether\_old} := 1.646 \times 10^{10}\,Pa$$

This new Young's Modulus will be applied to the top tether element.

$$k_{tether\_old} := \frac{F_{tether\_max}}{.03 L_{tether\_element}} = 5.01 \times 10^{6} \cdot \frac{N}{m}$$

$$k_{tether\_new} := \frac{19kN}{1in} = 7.48 \times 10^{5} \cdot \frac{N}{m}$$

Comparing the Differences between the Scaled buoy and the Full Scale Buoy Design

Given calculated maximum and average wave height that the system should experience

$H_{wave\_max} := 5.00m$ $H_{wave} := 4m$

Maximum loading that the system should encounter

$F_{amp\_tether} := 19000N$

Number of tethers along with the angle they are mounted onto the buoy

$N_{tethers} := 3$ $\Theta_{tether} := 20deg$

Amplitude of the waves the system will encounter

$$Amp_{wave} := \frac{H_{wave}}{2} = 2\,m$$

Draft of the system

$Draft := H_{scalebuoy} - 1.5m$ $Draft = 2.999m$

Water depth system will be deployed at

$Depth := 52m$

Force Amplitude experienced on the buoy

$$F_{amp\_scalebuoy} := \frac{A_{scalebuoy} \cdot Amp_{wave} \cdot \gamma_{seawater}}{\cos(\Theta_{tether}) \cdot N_{tethers}} \qquad F_{amp\_scalebuoy} = 1.9 \times 10^{4}\,N$$

Calculating the mass and weight of the tethers

$$Mass_{tethers} := \left[N_{tethers} \cdot \left(\frac{Depth}{\cos(\Theta_{tether})} \right) \right] \cdot A_{tether} \cdot \rho_{tether} = 104.753\,kg$$

$$Weight_{tethers} := Mass_{tethers} \cdot g = 1.027 \times 10^{3}\,N$$

Calculating the buoy system mass and weight as if the buoy was just floating there with the tethers attached.

$$Buoy\_and\_Tethers_{empty\_mass} := m_{.scalebuoy} + Mass_{tethers} = 5.281 \times 10^{3}\,kg$$

$$Buoy\_and\_Tethers_{empty\_weight} := Buoy\_and\_Tethers_{empty\_mass} \cdot g = 5.179 \times 10^{4}\,N$$

Calculating the Neutral buoyant line of the buoy from the bottom. This shows where the water line would be if the tether were not attached

$$Neutral\_Bouyant\_Line_{buoy} := \frac{4 \cdot Buoy\_and\_Tethers_{empty\_weight}}{\gamma_{seawater} \cdot \pi \cdot dia_{scalebuoy}^{2}} = 1.933\,m$$

Aqua-FE Model Design Using Above Buoy Parameters:

However the first thing to do will be to figure out the center of gravity / center of buoyancy. All distances are measured from the center of the bottom of the can.

Calculating the center of gravity assuming the center of gravity is in the center of the structure

$$cg_{buoy} := \frac{H_{scalebuoy}}{4.5} = 1\,m \qquad H_{scalebuoy} = 4.499\,m$$

Calculating the center of buoyancy for the buoy

$$cb_{buoy} := \frac{Draft}{2} \qquad cb_{buoy} = 1.5\,m$$

Calculating the Area of the Side of the buoy

$$A_{side.buoy} := H_{scalebuoy} \cdot dia_{scalebuoy}$$

$A_{side.buoy} = 8.288 m^2$ *Side view projected area of the buoy*

Calculating the Area of the Bottom of the buoy

$A_{bot.buoy} := A_{scalebuoy}$

$A_{bot.buoy} = 2.665 m^2$ *Bottom view projected area*

Calculating the total volume of the buoy

$V_{buoy} := A_{bot.buoy} \cdot H_{scalebuoy}$ $V_{buoy} = 11.99 m^3$

Calculating the volume of the buoy under the water

$V_{buoy\_sub} := A_{bot.buoy} \cdot Draft$ $V_{buoy\_sub} = 7.993 \times 10^3 L$

Calculating the density of the total buoy

$\rho_{buoy} := \frac{m_{.scalebuoy}}{V_{buoy}}$ $\rho_{buoy} = 431.684 \frac{kg}{m^3}$ Aqua-FE density of the buoy assuming that we use a single element.

Breaking the Buoy up into Multiple Elements

The buoy will be broken up into 9 pieces: a central spar and 8 pipes of equal volume. The bottom octagon will still be sized to provide the correct mass and volume.

$mass_{model.buoy} := m_{.scalebuoy}$ $mass_{model.buoy} = 5.176 \times 10^3 kg$

Given the length of the scaled buoy, the length of buoy side and the length of the buoy bottom elements can be calculated,

$L_{model.side.buoy} := H_{adjusted\_scalebuoy} = 4 m$

$L_{model.bot.buoy} := dia_{scalebuoy} \cdot \sin(15 deg) = 0.477 m$

Modify these values to ensure the volumes of the model in a wave are equal to the scaled buoy

$dia_{model.side.buoy} := .5109 m$ $dia_{model.bot.buoy} := .544 m$

Calculating the volume of the buoy that is 1m in a wave,

$$Wave_{buoydepth} := 1m$$

$$V_{model\_1m\_wave} := \frac{\pi \cdot \left(dia_{model.side.buoy}\right)^2}{4} \cdot Number_{verticalelements} \cdot Wave_{buoydepth} = 2.665\,m^3$$

$$V_{buoy\_1m\_wave} := A_{scalebuoy} \cdot Wave_{buoydepth} = 2.665\,m^3$$

Calculating the total side area of the model buoy to be broken down into single element densities

$$\begin{aligned} A_{model.side.buoy} := {} & Number_{verticalelements} \cdot L_{model.side.buoy} \cdot dia_{model.side.buoy} \ldots \\ & + 4 \cdot \left[L_{model.bot.buoy} \cdot dia_{model.bot.buoy} \cdot (\cos(75deg))\right] \ldots \\ & + 4 \cdot L_{model.bot.buoy} \cdot dia_{model.bot.buoy} \cdot \cos(45deg) \ldots \\ & + 4 \cdot \left[L_{model.bot.buoy} \cdot dia_{model.bot.buoy} \cdot (\cos(15deg))\right] \end{aligned}$$

Comparing the differences between the model side area and the actual side area

$$A_{model.side.buoy} = 28.571\,m^2 \qquad A_{side.buoy} = 8.288\,m^2$$

Comparing the difference between the model bottom area and the actual bottom area

$$A_{model.bot.buoy} := Number_{horizontalelements} \cdot L_{model.bot.buoy} \cdot dia_{model.bot.buoy}$$

$$A_{model.bot.buoy} = 3.112\,m^2 \qquad A_{bot.buoy} = 2.665\,m^2$$

Calculating the coefficient of drag on the buoys bottom to ensure similar results from model to the actual scale buoy

$$Cd_{flatplate} := 1.2$$

$$Cd_{bottom} := \frac{A_{bot.buoy}}{A_{model.bot.buoy}} \cdot Cd_{flatplate} = 1.028 \qquad Cd_{bottom} = 1.028$$

To compare the models, just take a Cd ratio of the two areas. then set the associated area in Jeff's model.

$$C_{d\_jeff} := 1.2$$

$$C_{d\_new} := C_{d\_jeff} \cdot \frac{A_{side.buoy}}{A_{model.side.buoy}} \qquad C_{d\_new} = 0.348$$

Calculating the Volume of the modeled buoy and comparing it to the actual volume. This is a check ensuring the values calculated above are correct. If the values highlighted in green are not the same, check prior calculations.

$$V_{model.buoy} := \left[Number_{horizontalelements} \cdot L_{model.bot.buoy} \cdot \pi \cdot \left(\frac{dia_{model.bot.buoy}}{2} \right)^2 \right] \ldots + \left[Number_{verticalelements} \cdot L_{model.side.buoy} \cdot \pi \cdot \left(\frac{dia_{model.side.buoy}}{2} \right)^2 \right]$$

$V_{model.buoy} = 11.99\,m^3$ $V_{buoy} = 11.99\,m^3$

Determining if the buoy drawn in Aqua-FE needs the vertical length elements to be 1 single line or if that lines needs to be split into to get the proper center of gravity

Now the properties for the numerical model can be determined. ASSUMING that the buoy side elements will be 1 element each and not subdivided.

$$A_{c.model.side.buoy} := \pi \cdot \left(\frac{dia_{model.side.buoy}}{2} \right)^2 \qquad A_{c.model.side.buoy} = 0.205\,m^2$$

$$A_{c.model.bot.buoy} := \pi \cdot \left(\frac{dia_{model.bot.buoy}}{2} \right)^2 \qquad A_{c.model.bot.buoy} = 0.232\,m^2$$

If only one density was used for the entire structure, the result would be the following:

$$\rho_{model.buoy} := \frac{mass_{model.buoy}}{V_{model.buoy}} \qquad \rho_{model.buoy} = 431.697\,\frac{kg}{m^3}$$

$$\rho_{buoy} = 431.684\,\frac{kg}{m^3}$$

Now, see if the model CG is equal to the real buoy CG.

$$mass_{model.buoy} \cdot cg_{model.buoy} = mass_{bot} \cdot cg_{bot} + mass_{side} \cdot cg_{side}$$

$cg_{bot} := 0 \cdot m$ centerline right at unit of measurement.

$$cg_{side} := \frac{L_{model.side.buoy}}{2} = 2\,m$$

Calculating the mass of the "bottom" of the model buoy

$$mass_{model.bot.buoy} := A_{c.model.bot.buoy} \cdot \rho_{model.buoy} \cdot \left(Number_{horizontalelements} \cdot L_{model.bot.buoy}\right)$$

$$mass_{model.bot.buoy} = 574.029\,kg$$

Calculating the mass of the "side" buoy elements

$$mass_{model.side.buoy} := A_{c.model.side.buoy} \cdot \rho_{model.buoy} \cdot \left(Number_{verticalelements} \cdot L_{model.side.buoy}\right)$$

$$mass_{model.side.buoy} = 4.602 \times 10^{3}\,kg$$

Check to insure the masses are equal

$$mass_{model.buoy} = 5.176 \times 10^{3}\,kg$$

$$mass_{model.side.buoy} + mass_{model.bot.buoy} = 5.176 \times 10^{3}\,kg$$

Calculating and comparing the modeled SOLID linear elements center of gravity

$$cg_{model.buoy} := \frac{mass_{model.bot.buoy} \cdot cg_{bot} + mass_{model.side.buoy} \cdot cg_{side}}{mass_{model.buoy}}$$

$cg_{model.buoy} = 1.778\,m$

$cg_{buoy} = 1\,m$

the Cg of the model is lower than the real buoy. therefore, need to split the "side" elements accordingly.

If this method works, the above highlighted values would match. If they match, the next section does not need to be looked at. If it doesn't work, proceed to the next section.

Splitting the Buoy vertical elements into 2 divisions instead of the 1 solid line element previously examined.

We will have to split to side buoy's into different densities to get correct cg.

$$L_{model.side.buoy\_split} := \frac{L_{model.side.buoy}}{2} \qquad L_{model.side.buoy\_split} = 2\,m$$

Calculating the center of gravity for the lower section of the split elements

$$cg_{side.bot} := \frac{L_{model.side.buoy}}{4} = 1\,m \qquad cg_{side.bot} = 1\,m$$

lower of the side elements CG

Calculating the center of gravity for the upper section of the split elements

$$cg_{side.top} := cg_{side.bot} + L_{model.side.buoy\_split} \qquad cg_{side.top} = 3\,m$$

upper of the side elements cg

As a result, the density of the top and bottom portions should be altered, however keep the same mass of the structure.

Initial guess for MathCad to calculate the proper mass for the system

$$mass_{model.bot.buoy} := 10\cdot kg \qquad mass_{model.side.buoy\_top} := 400\cdot kg$$

$$cg_{model.buoy} := cg_{buoy} \qquad mass_{model.side.buoy\_bot} := 250\cdot kg$$

Given

$$mass_{model.bot.buoy} + mass_{model.side.buoy\_top} + mass_{model.side.buoy\_bot} = mass_{model.buoy}$$

$$mass_{model.bot.buoy}\cdot cg_{bot} + mass_{model.side.buoy\_top}\cdot cg_{side.top} \cdots = mass_{model.buoy}\cdot cg_{model.buoy} + mass_{model.side.buoy\_bot}\cdot cg_{side.bot}$$

$$\begin{pmatrix} mass_{model.side.buoy\_top} \\ mass_{model.side.buoy\_bot} \end{pmatrix} = \begin{pmatrix} 4.68 \\ 5.161\times 10^{3} \end{pmatrix} kg$$

New total mass of the upper and lower side elements are shown in the highlighted region above.

Now the center of gravity can be calculated for the split element calculations

$$cg_{model.buoy2} := \frac{mass_{model.bot.buoy} \cdot cg_{bot} + mass_{model.side.buoy\_top} \cdot cg_{side.top} \cdots + mass_{model.side.buoy\_bot} \cdot cg_{side.bot}}{mass_{model.buoy}}$$

Checking to see if the center of gravity of the model is the same as the scale buoy to ensure the calculations were done properly

$$cg_{model.buoy2} = 1\,m$$

$$cg_{buoy} = 1\,m$$

Checking the mass of the system to ensure that the mass has not changed in the calculations

$$mass_{model.bot.buoy} + mass_{model.side.buoy\_top} + mass_{model.side.buoy\_bot} = 5.176 \times 10^3\,kg$$

$$mass_{model.buoy} = 5.176 \times 10^3\,kg$$

Now the volumes and property densities can be found.

Calculating the Volume of the upper side element

$$V_{model.side.buoy\_top} := L_{model.side.buoy\_split} \cdot A_{c.model.side.buoy}$$

$$V_{model.side.buoy\_top} = 0.41\,m^3$$

volume of 1 upper side element.

Calculating the volume of the bottom side element

$$V_{model.side.buoy\_bot} := L_{model.side.buoy\_split} \cdot A_{c.model.side.buoy}$$

$$V_{model.side.buoy\_bot} = 0.41\,m^3$$

volume of 1 lower side element.

Calculating the volume of the bottom of the buoy

$$V_{model.bot.buoy} := A_{c.model.bot.buoy} \cdot L_{model.bot.buoy}$$

$$V_{model.bot.buoy} = 0.111\,m^3$$

volume of 1 bottom element

Checking the total volume (bottom and the split top sections) to ensure the volume match.

$$V_{model.check} := Number_{horizontalelements} \cdot V_{model.bot.buoy} \dots + \left(Number_{verticalelements} \cdot V_{model.side.buoy\_bot}\right) \dots + Number_{verticalelements} \cdot V_{model.side.buoy\_top}$$

$$V_{model.check} = 11.99\,m^3 \qquad V_{buoy} = 11.99\,m^3$$

Now the densities can be calculated

$$\rho_{model.side.buoy\_top} := \frac{\frac{mass_{model.side.buoy\_top}}{Number_{verticalelements}}}{V_{model.side.buoy\_top}} \qquad \rho_{model.side.buoy\_top} = 0.878\,\frac{kg}{m^3}$$

$$\rho_{model.side.buoy\_bot} := \frac{\frac{mass_{model.side.buoy\_bot}}{Number_{verticalelements}}}{V_{model.side.buoy\_bot}} \qquad \rho_{model.side.buoy\_bot} = 968.335\,\frac{kg}{m^3}$$

$$\rho_{model.bot.buoy} := \frac{\frac{mass_{model.bot.buoy}}{Number_{horizontalelements}}}{V_{model.bot.buoy}} \qquad \rho_{model.bot.buoy} = 7.52\,\frac{kg}{m^3}$$

Checks to ensure the model is dimensioned properly

$$B_{final\_check} := V_{model.side.buoy\_top} \cdot Number_{verticalelements} \cdot \rho_{seawater} \dots + V_{model.side.buoy\_bot} \cdot Number_{verticalelements} \cdot \rho_{seawater} \dots + V_{model.bot.buoy} \cdot Number_{horizontalelements} \cdot \rho_{seawater}$$

$$M_{final\_check} := V_{model.side.buoy\_top} \cdot Number_{verticalelements} \cdot \rho_{model.side.buoy\_top} \cdots + V_{model.side.buoy\_bot} \cdot Number_{verticalelements} \cdot \rho_{model.side.buoy\_bot} \cdot + V_{model.bot.buoy} \cdot Number_{horizontalelements} \cdot \rho_{model.bot.buoy}$$

$$F_{final\_check} := \left(B_{final\_check} - M_{final\_check}\right) \cdot g = 6.976 \times 10^{4}\,N$$

These Values should equal each other if the model height, densities, volumes, masses are all right

$$F_{prelim} = 6.976 \times 10^{4}\,N$$

REMEMBER. We still have to check the proper waterline in this model as the bottom elements will add buoyancy. We can't have a large change in surface elevation get "underneath" the bottom of the buoy.

then, once you know the draft of this model buoy, we should check the projected area below the water to see how well those match (or don't).

Ballasting and Water Line Calculation

This calculation is for drawing the model. The L.tether is the height above zero where the bottom of the buoy must be drawn to account for the proper buoyancy.

This is where you have to draw the model bottom points below the water depth

For example if the water is 52m, then it would be 52-.774 instead of 52-.8

$$WaterLine_{model} := 2.5 \cdot m$$ <----- change this

$$L_{tether} := Depth - WaterLine_{model} = 49.5m$$

Comparing the submerged volume of the buoy to the model. Note these MUST match

$$SubmergedV_{buoy} := \frac{\pi}{4} \cdot \left(dia_{scalebuoy}\right)^2 \cdot Draft = 7.993 \times 10^{3}\,L$$ these must be matched...

$$SubmergedV_{model} := Number_{horizontalelements} \cdot V_{model.bot.buoy} \cdots + \left(Number_{verticalelements}\ A_{c.model.side.buoy} \cdot WaterLine_{model}\right)$$

$$SubmergedV_{model} = 7.992 \times 10^{3}\,L$$

$$ACTUAL\_LENGTH\_TETHER := \frac{L_{tether}}{\cos(20deg)} = 52.677m$$

$$A_{c.model.side.buoy} = 0.205m^2$$

$$A_{model.below.Waterline} := Number_{verticalelements} \cdot WaterLine_{model} \cdot dia_{model.side.buoy} \ldots = 17.856m^2$$
$$+ \left(2 \cdot L_{model.bot.buoy} \cdot dia_{model.bot.buoy}\right) \ldots$$
$$+ 4 \cdot L_{model.bot.buoy} \cdot dia_{model.bot.buoy} \cdot (\cos(45deg))$$

$$A_{buoy.below.Waterline} := dia_{scalebuoy} \cdot Draft = 5.525m^2$$

Calculating the Buoyant force change for 1 m of water. These values should match

$$Buoyant\_Force_{1m\_change\_.model} := Number_{verticalelements} \cdot 1m \cdot A_{c.model.side.buoy} \cdot \rho_{seawater} \cdot g$$

$$Buoyant\_Force_{1m\_change\_.model} = 2.679 \times 10^4 N$$

$$Buoyant\_Force_{1m\_change\_buoy} := \pi \cdot \left[\frac{\left(dia_{scalebuoy}\right)}{2}\right]^2 \cdot 1m \cdot \rho_{seawater} \cdot g = 2.679 \times 10^4 N$$

The following takes into account for the bottom of buoy when the flat does not touch the water. **DOES NOT APPLY FOR 2014 Taut Moored System**

$$dia_{model.bot.buoy} = 0.544m$$

$$R_{m\_b\_b} := \frac{dia_{model.bot.buoy}}{2} \qquad R_{m\_b\_b} = 0.272m$$

$$h_{water\_line} := .6075m$$ <----- change this

$$WaterLine_{model} - h_{water\_line} = 1.893m$$ This must to be **greater** than-> $\frac{H_{wave\_max}}{2} = 2.5m$

$$A_{sub\_bottom\_ring} := \left(R_{m\_b\_b}^2 \cdot \operatorname{acos}\left(\frac{R_{m\_b\_b} - h_{water\_line}}{R_{m\_b\_b}}\right)\right) \ldots$$
$$+ -\left[\left(R_{m\_b\_b} - h_{water\_line}\right) \cdot \sqrt{\left(2 \cdot R_{m\_b\_b} \cdot h_{water\_line}\right) - h_{water\_line}^2}\right]$$

$A_{sub\_bottom\_ring} = (0.232 + 0.016j)\,m^2$

$V_{sub\_bottom\_ring} := A_{sub\_bottom\_ring} \cdot 8 \cdot L_{model.bot.buoy} = (0.886 + 0.062j)\,m^3$

$V_{sub\_sides} := \frac{\pi \cdot dia_{model.side.buoy}^{2}}{4} \cdot 9 \cdot h_{water\_line} = 1.121\,m^3$

$V_{submerged\_at\_neutral} := V_{sub\_bottom\_ring} + V_{sub\_sides} = (2.007 + 0.062j)\,m^3$

These must be matched which will be very difficult or impossible for the current situations...

$Buoyant\_F := V_{submerged\_at\_neutral} \cdot \rho_{seawater} \cdot g = \left(2.018 \times 10^4 + 623.985j\right) N$

$Buoy\_and\_Tethers_{empty\_mass} \cdot g = 5.179 \times 10^4\,N$

Aqua-FE checks. These values should replicate the results of the buoy floating and the buoy submerged. If they do not, check to ensure the Aqua-FE model is setup correctly

$$F_{check\_submerged} := \frac{\left(F_{final\_check}\right)}{3\cos\left(\Theta_{tether}\right)} = 24.746kN$$

$$F_{check\_floating} := \frac{\left(SubmergedV_{buoy} \cdot \rho_{seawater}\right) \cdot g - \left(M_{final\_check}\right) \cdot g}{3 \cdot \cos\left(\Theta_{tether}\right)} = 10.495kN$$

Appendix II – Bearing Surface Calculations: Cohesionless Soils

Bearing Capacity for Anchor Footprint in Cohesionless Soils

Initial guess for anchor side length assuming a square anchor

$B := 9.25ft$ $B = 2.819m$

Intial guess on the depth of embedment for the anchor

$D_f := 1ft$ $D_f = 0.305m$

Entering soil parameters that will be required to the calculations for the bearing loads

$\mu_{soil} := .58$	Friction coefficient between the anchor bottom and the soil (pg 78)
$\phi_{soil} := 30deg$	Drained (effective) fiction angle for loose soil ranges from 28-30 deg
$D_r := 35\%$	Relative density (%) for loose soil ranges from 0-35%
$\gamma_b := 55pcf$	Buoyant unit weight for loose soil ranges from 45-55pcf
$\theta_{buoy} := 20deg$	Angle of the tethers coming off the buoy
$FOS := 1.5$	Factor of safety for the system
$Force_{max} := 114kN$	Maximum force the anchor is going to experience
$\beta_{downslope} := 5deg$	Angle the seafloor of which the anchor is placed on
$W_{bst} := 0N$	Effective or buoyant weight of the supported structure
$z_s := .5 \cdot B$	Shear keys depth if shear keys are applicable
$R_p := 0$	Passive soil resistance on leading edge of base
$\gamma_{b\_concrete} := 86pcf$	Buoyant unit weight for concrete
$\rho_{concrete} := 2420\frac{kg}{m^3}$	Density of concrete
$c_{bar} := 0\frac{lb}{ft^2}$	Effective soil cohesion
$d_\gamma := 1$	Removing any benefits of shear strength when the anchor is placed
$d_q := 1$	Removing any benefits of shear strength when the anchor is placed
$b_\gamma := 1$	Assuming the anchor is going to be placed fairly level on the seafloor
$b_q := 1$	Assuming the anchor is going to be placed fairly level on the seafloor

$g_\gamma := 1$ Assuming the anchor is placed in a near horizontal orientation

$g_q := 1$ Assuming the anchor is placed in a near horizontal orientation

$\phi := 30deg$ Soil Friction Angle

$N_q := \tan\left(45deg + \frac{\phi}{2}\right)^2 \cdot e^{\pi \tan(\phi)}$ $N_q = 18.401$

$N_c := (N_q - 1)\cot(\phi)$ $N_c = 30.14$

$N_\gamma := 2\cdot(N_q + 1)\cdot\tan(\phi)$ $N_\gamma = 22.402$

Calculating the forces acting on the anchor top

$Force_{horizontal} := Force_{max}\cdot\sin(\theta_{buoy}) = 3.899\times 10^4 N$

$Force_{vertical} := Force_{max}\cdot\cos(\theta_{buoy}) = 1.071\times 10^5 N$

Calculating the load component parallel to the slope of the seafloor

$F_{hp} := Force_{horizontal}\cdot\cos(\beta_{downslope}) - Force_{vertical}\cdot\sin(\beta_{downslope})$

$F_{hp} = 2.951\times 10^4 N$

$F_{downslop} := F_{hp}\cdot FOS = 4.426\times 10^4 N$

Calculating the effective or buoyant weight of the anchor

$$W_{bf} := \frac{(FOS + \mu_{soil}\cdot\tan(\beta_{downslope}))Force_{horizontal}}{\mu_{soil} - FOS\cdot\tan(\beta_{downslope})} + Force_{vertical} - W_{bst} - \gamma_b\cdot B^2\cdot z_s\cdot 0$$

Note: This calculation considers there to be no shear keys. In order for the calculation to be correct with shear keys, remove the zero on the last term

Calculating the anchors resistance to sliding in the short and long term lateral loading

$$Q_{ul} := \mu_{soil}\cdot\left[\begin{matrix}\left(W_{bf} + W_{bst} + \gamma_b\cdot B^2\cdot D_f - Force_{vertical}\right)\cdot\cos(\beta_{downslope}) \ldots \\ +(-1)Force_{horizontal}\cdot\sin(\beta_{downslope})\end{matrix}\right] + R_p$$

$Q_{ul} = 8.797\times 10^4 N$

Calculating the recommended height and the height based off of the width of the anchor

$H_{recommended} := .25 \cdot B = 2.313\,ft$ $\quad H_{recommended} = 0.705m$

$H_{calculated} := \dfrac{W_{bf}}{B^2 \cdot g \cdot \rho_{concrete}} = 4.206\,ft$ $\quad H_{calculated} = 1.282m$

Calculating the minimum width of the anchor to minimize overturning

$B_{minimum} := 6 \cdot \dfrac{Force_{horizontal} \cdot \left(H_{calculated} + D_f\right)}{W_{bf} + W_{bst} - Force_{vertical}} = 9.04\,ft$ $\quad B_{minimum} = 2.755m$

To maintain stability and feasibility, match the Bminimum value with the B value. If values cannot be match, ensure B value is larger than the B minimum

$B_{minimum} = 9.04\,ft$ $\quad B = 9.25\,ft$

Calculating the normal force of the anchor (acting perpendicular to the slope)

$F_n := W_{bf} \cdot \cos\left(\beta_{downslope}\right) + W_b \cdot \cos\left(\beta_{downslope}\right) - Force_{vertical} \cdot \cos\left(\beta_{downslope}\right) \cdots$
$\quad + (-1) Force_{horizontal} \cdot \sin\left(\beta_{downslope}\right)$

$F_n = 1.308 \times 10^5\,N$

Calculating the downslope eccentricity by summing the moments around the center of the shear key base

$M_o := W_b \cdot \left(\dfrac{z_s}{2}\right) \cdot \sin\left(\beta_{downslope}\right) + W_{bf} \cdot \left(z_s \cdot 0 + \dfrac{H_{calculated}}{2}\right) \cdot \sin\left(\beta_{downslope}\right) \cdots$
$\quad + (-1) Force_{vertical} \cdot \left(z_s \cdot 0 + H_{calculated}\right) \cdot \sin\left(\beta_{downslope}\right) \cdots$
$\quad + Force_{horizontal} \cdot \left(z_s \cdot 0 + H_{calculated}\right) \cdot \cos\left(\beta_{downslope}\right)$

$M_o = 5.134 \times 10^4\,J$ This calculation doesn't account for shear keys

$e_2 := \dfrac{M_o}{F_n} = 1.288\,ft$ $\quad e_2 = 0.392m$

Calculating the bearing area reduced for the eccentricity

$e_1 := 0$

This is due to the anchor having a square base

$L_{prime} := B - 2 \cdot e_1 = 9.25\,ft$ $\quad L_{prime} = 2.819m$

Newly calculated length of anchor bottom

$B_{prime} := B - 2 \cdot e_2 = 6.675\,ft$ $\quad B_{prime} = 2.035m$

$A_{prime} := B_{prime}^{2} = 44.554\,ft^{2}$ $A_{prime} = 4.139\,m^{2}$ Newly calculated bottom area accounting for extreme conditions

Calculating the total of all vertical loads

$Force_{vertical\_total} := W_{bf} + W_{b} - Force_{vertical} = 3.029 \times 10^{4}\,lbf$

$Force_{vertical\_total} = 1.347 \times 10^{5}\,N$

Calculating the correction factors for the inclination of the resultant load

$\theta_{line} := 0deg$ Angle between the line of action of F.horizontal and the long axis of the foundation

$$m := \left[\frac{\left(2 + \frac{L_{prime}}{B_{prime}}\right)}{\left(1 + \frac{L_{prime}}{B_{prime}}\right)}\right] \cdot \cos\left(\theta_{line}^{2}\right) + \left[\frac{\left(2 + \frac{B_{prime}}{L_{prime}}\right)}{\left(1 + \frac{B_{prime}}{L_{prime}}\right)}\right] \cdot \sin\left(\theta_{line}^{2}\right) = 1.419$$

$$i_{q} := \left(1 - \frac{Force_{horizontal}}{Force_{vertical\_total} + B_{prime}^{2} \cdot c_{bar} \cdot \cot(30deg)}\right)^{m} = 0.616$$

$$i_{\gamma} := \left(1 - \frac{Force_{horizontal}}{Force_{vertical\_total} + B_{prime}^{2} \cdot c_{bar} \cdot \cot(30deg)}\right)^{m+1} = 0.438$$

$$s_{q} := 1 + \left(\frac{B_{prime}}{L_{prime}}\right) \cdot \tan(\phi) = 1.417$$

$$s_{\gamma} := 1 - .4\left(\frac{B_{prime}}{L_{prime}}\right) = 0.711$$

Calculating the correction factors for the bearing capacity equation

$K_{\gamma} := i_{\gamma} \cdot s_{\gamma} \cdot d_{\gamma} \cdot b_{\gamma} \cdot g_{\gamma} = 0.311$

$K_{q} := i_{q} \cdot s_{q} \cdot d_{q} \cdot b_{q} \cdot g_{q} = 0.872$

Calculating the bearing capacity

$$Q_u := A_{prime}\cdot\left(\gamma_b\cdot D_f\cdot N_q\cdot K_q + .5\cdot\gamma_b\cdot B_{prime}\cdot N_\gamma\cdot K_\gamma\right) = 4.287\times 10^5\,N$$

Check that Qu is higher than the total normal forces of the anchor with the safety factor included. If not, there is insufficient bearing capacity

$Q_u = 4.287\times 10^5\,N$ < is greater than > $F_n\cdot FOS = 1.962\times 10^5\,N$

If not, recalculate anchor designs. This anchor could require shear keys

$$K_p := \tan\left[45deg + \left(\frac{\phi}{2}\right)\right]^2$$

$$z_s := .5\cdot B$$

$$R_p := \frac{K_p\cdot\gamma_b\cdot z_s^{\,2}\cdot B}{2} = 7.261\times 10^4\,N$$

$$n := \frac{FOS\cdot F_{hp} + \left(W_{bf} + W_{bst}\right)\cdot\sin\left(\beta_{downslope}\right)}{R_p} + 1 \qquad n = 1.9$$

$$Shear_{key\_spacing} := \frac{B}{n-1} = 10.28ft$$

Stability against over turn sufficiency check

$$e_{maximum} := \frac{B}{6} = 0.47m$$

$$e_2 = 0.392m$$

$e_2 = 0.392m$ < is less than > $e_{maximum} = 0.47m$

Calculating the initial displacement of the anchor in the sea floor when it is first put on the sea floor

$$R_w := \frac{B}{2} = 1.41m$$

$E_{tsf} := 100$

$E := E_{tsf} \cdot 95760.3\,Pa$ From chart on internet
http://www.geotechnicalinfo.com/youngs_modulus.html

$\nu := .35$

$G := \frac{E}{2} \cdot (1 - \nu) = 3.112 \times 10^{6}\,Pa$ $R = 1.41m$

$\delta_i := \frac{(1 - \nu)}{4 \cdot G \cdot R} \cdot Force_{vertical\_total} = 0.016ft$ $\delta_i = 4.99 \times 10^{-3}\,m$

Calculating shallow penetration of anchor when Z.penetration is less than .25*B

$z_{penetration} := 1ft$ Initial guess for the depth at which the anchor will penetrate

$z_{penetration} = 0.305m$

$\frac{z_{penetration}}{B} = 0.108$ Ratio to use on chart to obtain bearing capacity factor

$\lambda := 1$ Shape function for specific depth and angle (pg 187)

$N_{\gamma q} := .00175 10^{3}$ Bearing capacity factor

$Q_{u\_penetration} := .5 \cdot B^2 \cdot \left(B \cdot \gamma_b \cdot N_{\gamma q}\right) \lambda$ Penetration resistance

$Q_{u\_penetration} = 1.694 \times 10^{5}\,N$ < greater than > $Force_{vertical\_total} = 1.347 \times 10^{5}\,N$

$Q_{ufg} := \left(1.3 c_{bar} \cdot N_c + .4 \gamma_b \cdot B \cdot N_\gamma\right) \cdot B^2 = 1.735 \times 10^{6}\,N$

$Q_u = 4.287 \times 10^{5}\,N$

Appendix III – Bearing Surface Calculations: Cohesive Soils

Bearing Capacity for Anchor Footprint

Initial Guess for anchor side length

$B := 9.25ft$ $B = 2.819m$

Calculating D.f using the shear keys of depth z.s and placing the anchor parallel to the downslope direction. Df is just stating how far into the ground the anchor will go ideally.

$z_s := 0$

$D_f := 1ft$ $\theta_{buoy} := 20deg$

Calculating the load component parallel to the slope (beta downslope) from existing force. A factor of safety will also be added to ensure the proper calculation.

$F_{max} := 114kN$

$F_{vertical} := F_{max} \cdot \cos(\theta_{buoy}) = 1.071 \times 10^5 N$

$F_{horizontal} := F_{max} \cdot \sin(\theta_{buoy}) = 3.899 \times 10^4 N$

$\beta_{downslope} := 5deg$

$F_{hp} := F_{horizontal} \cdot \cos(\beta_{downslope}) - F_{vertical} \cdot \sin(\beta_{downslope}) = 2.951 \times 10^4 N$

$FOS_{force} := 1.5$

$FOS_{force} \cdot F_{hp} = 4.426 \times 10^4 N$

Calculate the anchor resistance to sliding for a short deployment.

s.uz is the undrained shear strength of the soil at depth z.s

$s_{uz} := 144psf + (45pcf) \cdot z_s = 6.895 \times 10^3 Pa$

This is the equation given in the manual. This will need to be found for our specific sediments

$s_{uz} := 75kPa$

$s_u := s_{uz}$

$Area_{footprint} := B^2 = 85.563\,ft^2$ $Area_{footprint} = 7.949\,m^2$

s.ua is the average undrained shear strength between the seafloor and depth d.f

$s_{ua} := 144psf + (45pcf)\cdot\frac{D_f}{2} = 7.972\times 10^3\,Pa$

This is the equation given in the manual. This will need to be found for our specific sediments

$s_{uz} := s_u$

Calculating the resistance

$Q_{u1} := s_{uz}\cdot Area_{footprint} + 2\cdot s_{ua}\cdot D_f\cdot B = 7.251\times 10^5\,N$ $Q_{u1} = 1.63\times 10^5\cdot lbf$

Calculate minimum foundation weight required to resist sliding

$\mu_{soil} := .58$

This can be looked up on page 4-12 in the manual. This also varies for soil and material properties

$\beta_{downslope} = 5\cdot deg$

$c_{bar} := 0$ effective soil cohesion

$W_{bst} := 0$ buoyant weight of bottom-supported structure

$\gamma_b := 55pcf$ buoyant weight of the soil

$$W_{bf} := \frac{\left(FOS_{force} + \mu_{soil}\cdot\tan\left(\beta_{downslope}\right)\right)\cdot F_{horizontal} - \frac{c_{bar}\cdot Area_{footprint}}{\cos\left(\beta_{downslope}\right)}}{\mu_{soil} - FOS_{force}\cdot\tan\left(\beta_{downslope}\right)} \ldots + F_{vertical} - W_{bst} - \gamma_b\cdot Area_{footprint}\cdot 0$$

$W_{bf} = 5.437\times 10^4\cdot lbf$ $W_{bf} = 2.419\times 10^5\,N$

$W_b := \gamma_b\cdot Area_{footprint}\cdot z_s = 0\cdot lbf$

Check to see if the foundation resistance to sliding is less than the forces driving it downslope

$Forces_{downslope} := FOS_{force}\cdot\left[F_{hp} + \left(W_{bf} + W_{bst} + W_b\right)\sin\left(\beta_{downslope}\right)\right] = 7.588\times 10^4\,N$

If the design is good, Qul >= Forces down slope

$Q_{u1} = 7.251\times 10^5\,N$ Must be >= $Forces_{downslope} = 7.588\times 10^4\,N$

Calculating the height of a concrete trial foundation

$\rho_{concrete} := 2420\frac{kg}{m^3}$

$Height := \frac{W_{bf}}{\rho_{concrete} \cdot g \cdot Area_{footprint}}$ $Height = 4.206ft$

Is height less than .25B?

$Height = 1.282m$ less than ? $B \cdot .25 = 0.705m$

$Height_{new} := B \cdot .25$

If height is greater than B*.25, the anchor may tip over so changes to the buoyant density of the anchor need to be calculated

Basically the buoyancy of the anchor has to be taken into account for the rotation force. If the anchor is too buoyant, it will flip. To help reduce that, the anchor must be heavier.

$\gamma_{recommended} := \frac{W_{bf}}{Area_{footprint} \cdot Height_{new}} = 274.796pcf$ Recommended material buoyancy density based off the recommended maximum height of anchor

Check to ensure the anchors mass is large enough with given dimensions

$Volume\_anchor := B^2 \cdot Height = 10.191m^3$

$Mass\_anchor := Volume\_anchor \cdot \rho_{concrete} = 2.466 \times 10^4 kg$

$Mass\_anchor\_in\_water := Mass\_anchor \cdot .57 = 1.406 \times 10^4 kg$

$Underwater\_mass\_required := \frac{F_{max}}{g} = 1.162 \times 10^4 kg$

Is mass_anchor_in_water > underwater_mass_required?

Calculating the trial foundations resultant normal force acting perpendicular to the slope

$F_n := W_{bf} \cdot \cos(\beta_{downslope}) \ldots$
$+ W_b \cdot \cos(\beta_{downslope}) - F_{vertical} \cdot \cos(\beta_{downslope}) - F_{horizontal} \cdot \sin(\beta_{downslope})$

$F_n = 1.308 \times 10^5 N$

Calculating the down slope eccentricity by summing the moments around the center of the shear key base. This will account for the odd forces experienced by the anchor

$$SumM_o := W_b \cdot \left(\frac{z_s}{2}\right) \cdot \sin\left(\beta_{downslope}\right) \cdots + W_{bf} \cdot \left(z_s + \frac{Height}{2}\right) \cdot \sin\left(\beta_{downslope}\right) - F_{vertical} \cdot \left(z_s + Height\right) \cdot \sin\left(\beta_{downslope}\right) \cdots + F_{horizontal} \cdot \left(z_s + Height\right) \cdot \cos\left(\beta_{downslope}\right)$$

$$e_2 := \frac{SumM_o}{F_n} = 0.392m \qquad e_2 = 1.288ft$$

Calculate the breaing area reduced for the eccentricity

$$e_1 := 0 \qquad B = 2.819m$$

$$L_{prime} := B - 2 \cdot e_1 = 2.819m$$

$$B_{prime} := B - 2 \cdot e_2 = 2.035m$$

$$A_{prime} := B_{prime}^{2} = 4.139m^2$$

This is the new bottom footprint of the anchor to account for the loading the anchor will experience

Calculating the s.u for the bearing capacity equation (average s.u over the depth B below the shear keys)

$$s_u = 1.566 \times 10^3 \cdot psf$$

From Su @ z.s+B

$$s_{u\_zsplusB} := 144psf + (45pcf) \cdot \left(L_{prime} + z_s\right) = 560.25psf$$

$$s_{uavg} := \frac{s_u + s_{u\_zsplusB}}{2} = 1.566 \times 10^3 \cdot psf$$

Calculating the correction factors K.c and K.q for the bearing capacity

$\phi := 1deg$ Soil Friction Angle

$$N_q := \tan\left(45deg + \frac{\phi}{2}\right)^2 \cdot e^{\pi \tan(\phi)} \qquad N_q = 1.094$$

$$N_c := \left(N_q - 1\right)\cot(\phi) \qquad N_c = 5.379$$

$N_\gamma := 2\cdot\left(N_q + 1\right)\cdot\tan(\phi)$ $\quad N_\gamma = 0.073$

$\theta_{line} := 0deg$

Angle between the line of action of F.horizontal and the long axis of the foundation

$$m := \left[\frac{\left(2 + \frac{L_{prime}}{B_{prime}}\right)}{\left(1 + \frac{L_{prime}}{B_{prime}}\right)}\right]\cdot\cos\left(\theta_{line}^{2}\right) + \left[\frac{\left(2 + \frac{B_{prime}}{L_{prime}}\right)}{\left(1 + \frac{B_{prime}}{L_{prime}}\right)}\right]\cdot\sin\left(\theta_{line}^{2}\right) = 1.419$$

$$i_c := 1 - \frac{m\cdot F_{horizontal}}{B_{prime}\cdot L_{prime}\cdot s_{uavg}\cdot N_c} = 0.976$$

$F_{vnew} := W_{bf} + W_b - F_{vertical} = 3.029\times 10^{4}\cdot lbf$

$$i_q := \left(1 - \frac{F_{horizontal}}{F_{vnew} + B_{prime}\cdot L_{prime}\cdot c_{bar}\cdot\cot(30deg)}\right)^{m} = 0.616$$

$$s_c := 1 + \left(\frac{B_{prime}}{L_{prime}}\right)\cdot\left(\frac{N_q}{N_c}\right) = 1.147$$

$$s_q := 1 + \left(\frac{B_{prime}}{L_{prime}}\right)\cdot\tan(30deg) = 1.417$$

$d_q := 1$

$b_q := d_q$

$g_q := d_q$

This accounts for the disruption to the soil when the anchor is dropped into place. It also assumes that the floor is nearly level.

$d_c := 1$

$b_c := d_c$

$g_c := d_c$

$K_c := i_c\cdot s_c\cdot d_c\cdot b_c\cdot g_c = 1.119$

$K_q := i_q\cdot s_q\cdot d_q\cdot b_q\cdot g_q = 0.872$

Calculated the short term bearing capacity

$$Q_{ushortterm} := A_{prime}\cdot\left(s_{uavg}\cdot N_c\cdot K_c + \gamma_b\cdot D_f\cdot K_q\right) = 4.224\times 10^5\cdot lbf$$

is Q.ushortterm > FOS.force*Fn. If it is, then there is enough bearing capacity. If not, redo the calculations to ensure the bottom of the anchor is large enough

$Q_{ushortterm} = 4.224\times 10^5\cdot lbf$ is > than ? $F_n\cdot FOS_{force} = 4.412\times 10^4\cdot lbf$

Calculating the short term bearing capacity for the foundation when the mooring line load is not applied. Once again compare this to the bearing surface capacity to see if there is enough bearing capacity

$$F_{nnomooringlineload} := W_{bf}\cdot\cos\left(\beta_{downslope}\right) + W_b\cdot\cos\left(\beta_{downslope}\right) = 2.409\times 10^5\,N$$

Is Qu > F.nnomooringlineload*FOS.force?

$Q_{ushortterm} = 1.879\times 10^6\,N$ is > than ? $F_{nnomooringlineload}\cdot FOS_{force} = 3.614\times 10^5\,N$

Is the stability against over turning sufficient?

$$max_e := \frac{B}{6} = 1.542ft$$

Is e.2 < Max e?

$e_2 = 0.392m$ is < than ? $max_e = 0.47m$

Appendix IV – Finite Element Modeling: Taut Moored LW Buoy

For completeness and to have design values available for comparison, the LW buoy employing a taut-moored system was created in Aqua-FE using the buoy and mooring line physical properties which were previously determined. Also, the previous dead-weight anchor designs were to be used. The front mooring line, of the 3 legged taut-moored system, was located parallel with the wave loading with a 120 degree angle separating all mooring lines. The mooring lines ran at a 20 degree angle off of the bottom of the buoy to the sea floor.

The taut moored system was then tested in in two different wave regimes. These wave regimes consisted of random waves with a significant wave height of 1.5 m and a period of 5.34 s and regular waves with a height of 1 m and a period of 6 s. Along with wave events, currents of 0.1 m/s and 1 m/s were also tested. The final aspect that was tested was the water line of the buoy. Since the taut-moored system would be fully submerged approximately twice a day, it was important to examine how various water depths would affect the system so the Aqua-FE model was run with water depths of 52 m, 53 m, and 53.5 m. It is important to note that the CORE site water depth is approximately 52 m so at 53.5 m, the buoy is fully submerged. In Figure 59, a water depth of 52 m was simulated to see how the buoy and mooring would react in the ideal water depth while Figure 60 shows the buoy full submerged. In these figures, the top plot shows the front mooring line tension while the bottom two plots show the tension on the rear mooring lines.

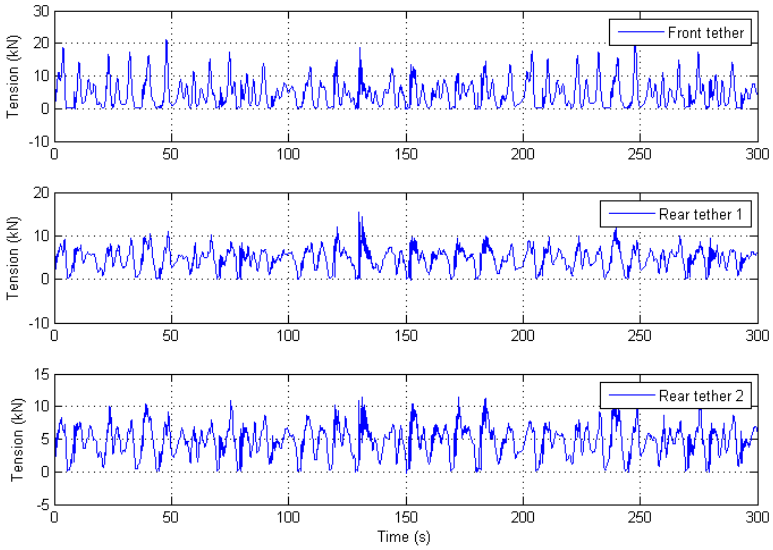

Figure 59: 20 degree angled mooring line system analyzed at a 52m water depth with no current with a random wave loading of 1.5m significant wave height and a period of 5.34s. The maximum tension recorded was 21.5kN in the front tether while the mean tensions were 4.5kN in the front tether and 4.7kN in the rear tethers.

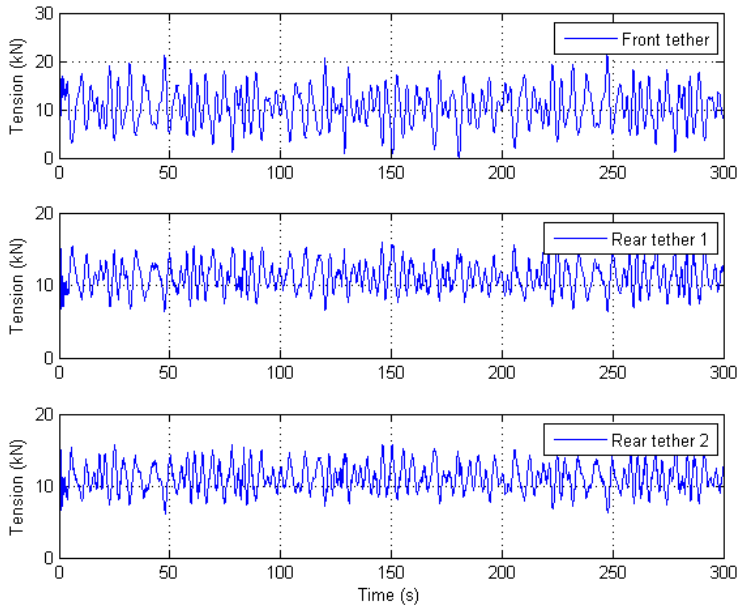

Figure 60: 20 degree angled mooring line system analyzed at a 53.5m water depth with no current with a random wave loading of 1.5m significant wave height and a period of 5.34s. The maximum tension recorded was 21.2kN in the front tether while the mean tensions were 10.48kN in the front tether and 11.2kN in the rear tethers.

Additional tests were performed using a vertical mooring line configuration. The concept behind the vertical mooring lines was that the change in tensions would be greater due to the buoy moving up and down in a vertical motion without being laterally constrained like in the angled mooring line configuration. This vertical motion would then be directly transferred to the PTOs creating the optimum power. To be consistent in testing, the same tests were simulated using the same system as above just using vertical mooring lines instead of angled mooring lines. In Figure 61, it can be seen that the vertical mooring lines produced similar results to the same test as the angled mooring lines at a water depth of 52 m. In Figure 62, the vertical mooring line configuration at a water depth of 53.5 m has substantially lower tension amplitudes than the angled mooring line configuration at the same water depth.

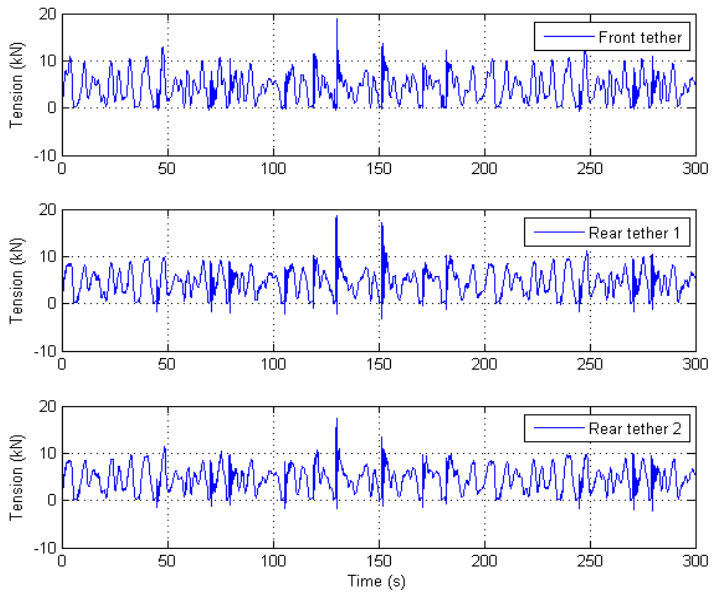

Figure 61: Vertical mooring line system analyzed at a 52m water depth with no current with a random wave loading of 1.5m significant wave height and a period of 5.34s. The maximum tension recorded was 18.9kN in the front tether while the mean tensions were 4.3kN in the front tether and 4.5kN in the rear tethers.

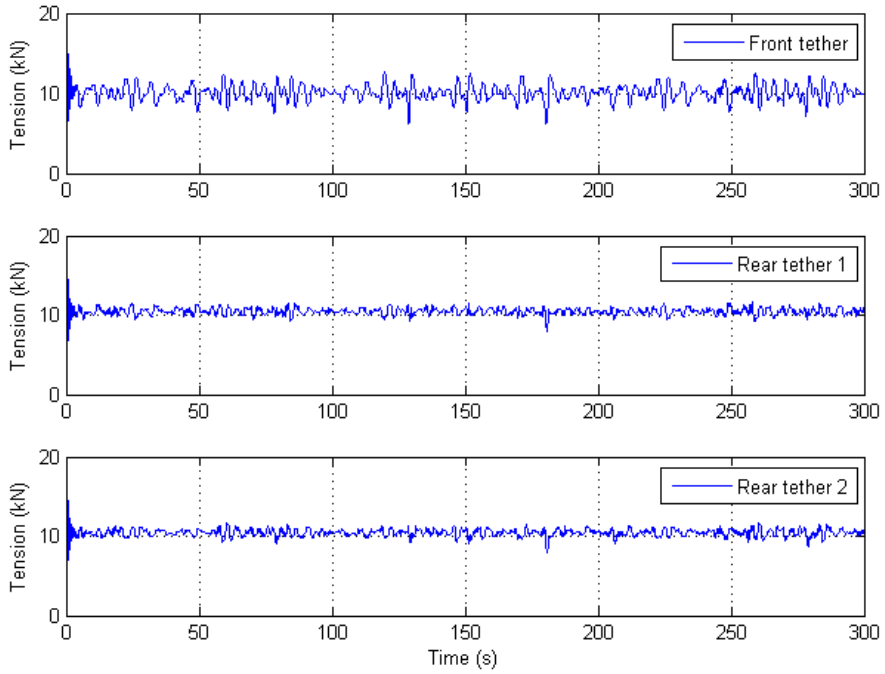

Figure 62: Vertical mooring line system analyzed at a 53.5m water depth with no current with a random wave loading of 1.5m significant wave height and a period of 5.34s. The maximum tension recorded was 17.0kN in the front tether while the mean tensions were 10.0kN in the front tether and 10.4kN in the rear tethers.

After the testing, it was observed that the vertical line mooring system did not provide the change in tensions that the PTOs required to generate power. The reason why the tension fluctuations were not achieved was, instead of moving only in the vertical direction, the buoy moved an equal or greater amount in the horizontal direction. The angled mooring line configuration would only allow the buoy to move slightly in the horizontal direction due to the angled line setup. Once the buoy was fully submerged, the only tensions the vertical mooring line configuration experienced was the buoys buoyancy force. This is because the buoy would move with the underwater wave motion, allowing it to move primarily in the horizontal direction, which was not ideal.

Comparing the angled mooring line configuration to the vertical mooring line configuration, it was obvious that the vertical mooring line concept would not generate the desired tension fluctuations the PTOs require. If a taut-moored system were to be selected for the summer 2013 deployment, the angled mooring lines configuration would be further pursued.